IOWA STATE UNIVERSITY
Digital Repository

Retrospective Theses and Dissertations

Iowa State University Capstones, Theses and Dissertations

1979

The methanation reaction on ruthenium thin films: a mechanistic investigation

Michael Dwayne Slaughter
Iowa State University

Follow this and additional works at: https://lib.dr.iastate.edu/rtd

 Part of the Physical Chemistry Commons

Recommended Citation
Slaughter, Michael Dwayne, "The methanation reaction on ruthenium thin films: a mechanistic investigation" (1979). *Retrospective Theses and Dissertations*. 6674.
https://lib.dr.iastate.edu/rtd/6674

This Dissertation is brought to you for free and open access by the Iowa State University Capstones, Theses and Dissertations at Iowa State University Digital Repository. It has been accepted for inclusion in Retrospective Theses and Dissertations by an authorized administrator of Iowa State University Digital Repository. For more information, please contact digirep@iastate.edu.

www.manaraa.com

INFORMATION TO USERS

This was produced from a copy of a document sent to us for microfilming. While the most advanced technological means to photograph and reproduce this document have been used, the quality is heavily dependent upon the quality of the material submitted.

The following explanation of techniques is provided to help you understand markings or notations which may appear on this reproduction.

1. The sign or "target" for pages apparently lacking from the document photographed is "Missing Page(s)". If it was possible to obtain the missing page(s) or section, they are spliced into the film along with adjacent pages. This may have necessitated cutting through an image and duplicating adjacent pages to assure you of complete continuity.

2. When an image on the film is obliterated with a round black mark it is an indication that the film inspector noticed either blurred copy because of movement during exposure, or duplicate copy. Unless we meant to delete copyrighted materials that should not have been filmed, you will find a good image of the page in the adjacent frame.

3. When a map, drawing or chart, etc., is part of the material being photographed the photographer has followed a definite method in "sectioning" the material. It is customary to begin filming at the upper left hand corner of a large sheet and to continue from left to right in equal sections with small overlaps. If necessary, sectioning is continued again—beginning below the first row and continuing on until complete.

4. For any illustrations that cannot be reproduced satisfactorily by xerography, photographic prints can be purchased at additional cost and tipped into your xerographic copy. Requests can be made to our Dissertations Customer Services Department.

5. Some pages in any document may have indistinct print. In all cases we have filmed the best available copy.

University Microfilms International

300 N. ZEEB ROAD, ANN ARBOR, MI 48106
18 BEDFORD ROW, LONDON WC1R 4EJ, ENGLAND

7924272

SLAUGHTER, MICHAEL DWAYNE
THE METHANATION REACTION ON RUTHENIUM THIN FILMS: A MECHANISTIC INVESTIGATION.

IOWA STATE UNIVERSITY, PH.D., 1979

University Microfilms International 300 N. ZEEB ROAD, ANN ARBOR, MI 48106

PLEASE NOTE:

In all cases this material has been filmed in the best possible way from the available copy. Problems encountered with this document have been identified here with a check mark ✓.

1. Glossy photographs ✓
2. Colored illustrations _____
3. Photographs with dark background ✓
4. Illustrations are poor copy _____
5. Print shows through as there is text on both sides of page _____
6. Indistinct, broken or small print on several pages _____ throughout _____
7. Tightly bound copy with print lost in spine _____
8. Computer printout pages with indistinct print _____
9. Page(s) _____ lacking when material received, and not available from school or author _____
10. Page(s) _____ seem to be missing in numbering only as text follows _____
11. Poor carbon copy _____
12. Not original copy, several pages with blurred type _____
13. Appendix pages are poor copy _____
14. Original copy with light type _____
15. Curling and wrinkled pages _____
16. Other _____

University Microfilms International

300 N. ZEEB RD., ANN ARBOR, MI 48106 (313) 761-4700

The methanation reaction on ruthenium thin films: A mechanistic investigation

by

Michael Dwayne Slaughter

A Dissertation Submitted to the

Graduate Faculty in Partial Fulfillment of

The Requirements for the Degree of

DOCTOR OF PHILOSOPHY

Department: Chemistry
Major: Physical Chemistry

Approved:

Signature was redacted for privacy.

In Charge of Major Work

Signature was redacted for privacy.

For the Major Department

Signature was redacted for privacy.

For the Graduate College

Iowa State University
Ames, Iowa
1979

TABLE OF CONTENTS

INTRODUCTION

Processes which involve the conversion of relatively low Btu substances to useful fuels and chemical feedstocks are assuming ever increasing roles as potential substitutes for those that involve the conversion of petroleum. One such process which has been in commercial operation for many years is the Fischer-Tropsch synthesis involving the reduction of carbon monoxide by hydrogen. The Fischer-Tropsch synthesis yields a wide variety of saturated and unsaturated hydrocarbons and oxygen-containing compounds. A judicious choice of reaction conditions and catalyst will generally result in the selective production of the desired product distribution. The special case of the Fischer-Tropsch synthesis in which methane is the only carbon-containing product is referred to as methanation. Both the Fischer-Tropsch synthesis and methanation are heterogeneous catalytic processes which are known to occur on certain group VIII metals and their oxides. Although a fairly large number of studies have been performed in an effort to understand the reaction mechanisms of the Fischer-Tropsch and methanation processes, no thorough understanding of either process has been developed. The purpose of this study is to seek a mechanistic understanding of the methanation reaction on unsupported ruthenium. Since the Fischer-Tropsch and methanation processes are so directly related, a brief discussion of the Fischer-Tropsch synthesis will precede a more detailed discussion of the methanation process. Excellent reviews of both the Fischer-Tropsch and methanation processes have been published [1-7].

The general reactions for the hydrogenation of carbon monoxide to paraffins, olefins and alcohols are as follows:

$$(2n+1)H_2 + nCO \rightleftarrows C_nH_{2n+2} + nH_2O \quad (1)$$

$$2nH_2 + nCO \rightleftarrows C_nH_{2n} + nH_2O \quad (2)$$

$$2nH_2 + nCO \rightleftarrows C_nH_{2n+1}OH + (n-1)H_2O \quad (3)$$

The special case of reaction (1) in which n = 1 is the methanation reaction:

$$3H_2 + CO \rightleftarrows CH_4 + H_2O \quad (4)$$

Other reactions which are thermodynamically favored include the formation of aldehydes, ketones, aromatics and organic acids. It should be noted that when feedstocks rich in hydrogen are used, paraffins are produced, whereas low hydrogen content feedstocks are required for the production of olefins and alcohols.

A number of potentially complicating reactions can occur under the same conditions as the Fischer-Tropsch and methanation syntheses. The water-gas shift reaction (5) has the rather insignificant effect

$$CO + H_2O \rightleftarrows CO_2 + H_2 \quad (5)$$

of converting the water by-product to carbon dioxide. However, the undesirable effect of the water-gas shift reaction is to change the hydrogen to carbon monoxide ratio during the reaction process. This could alter the product distribution in some cases. Both the Boudouard reaction (6) and coke deposition (7) can occur on most of these catalyst surfaces. Both reactions have the effect of producing a carbon

$$2CO \rightleftarrows C + CO_2 \quad (6)$$

$$H_2 + CO \rightleftarrows C + H_2O \quad (7)$$

overlayer on the surface. This frequently leads to catalyst fouling and often decreases the lifetime of the catalyst significantly. These reactions are generally reversible and the catalyst activity can be regenerated by high temperature reduction. Metal carbide formation (8)

$$xM + C \rightarrow M_xC \qquad (8)$$

is generally irreversible and leads to permanent deactivation of the catalyst.

A summary of the significant discoveries in Fischer-Tropsch chemistry is shown in Appendix I. The first catalytic hydrogenation of carbon monoxide was reported in 1902 [8,9] and involved the production of methane at atmospheric pressure over supported nickel and cobalt catalysts. Although these scientists observed carbon monoxide conversion, they were quite disappointed that methane was the sole carbon containing product. Until about the middle of this century, cheap natural gas was readily available in most parts of the world and alternate methane sources were neither being looked for nor were they being commercialized when discovered. The real hope among scientists was that carbon monoxide could be hydrogenated to produce higher molecular weight hydrocarbons and oxygenated compounds--especially gasoline and alcohols. The Badische Anilin-und-Soda-Fabrik A. G. was successful in producing a fairly wide range of hydrocarbons and chemicals at high pressure over a range of catalysts. In 1913 they were granted a German patent [10] for this process and in 1923 they received two French patents [11,12] for a similar high pressure process which produced only methanol from carbon monoxide and hydrogen.

The fundamental understanding of the carbon monoxide-hydrogen interaction and the early commercialization of the process came about as a result of Franz Fischer and the members of his group at the Kaiser Wilhelm Institut für Kohlenforschung at Mülheim Ruhr. Fischer worked with Hans Tropsch during the period from 1922 until 1928, conducting basic research into the carbon monoxide-hydrogen interaction at atmospheric pressure. Their first publications on the conversion at atmospheric pressure were in 1926 [13-15] and contained the fundamental observations that became the basis for the early understanding of the process:

1) Iron, cobalt and nickel are active catalysts for the reaction. Cobalt tends to produce higher hydrocarbons and nickel tends to favor methane production.

2) Oxides that are difficult to reduce, such as ZnO and Cr_2O_3, have increased catalytic activity and are more resistant to sintering than the metals.

3) Small doses of alkali favor the formation of larger hydrocarbon molecules.

4) Copper-iron mixtures are more active than iron alone.

5) Sulfur poisons the catalysts.

It was as a result of this work that the reaction became known as the Fischer-Tropsch synthesis. In general, all the studies made during this period were at atmospheric pressure with a few at 15 atmospheres. The catalysts were generally some form of cobalt or iron and the temperatures fell in the 523-673K range.

Tropsch left Mülheim in 1928 to become director of a coal research institute in Czechoslovakia. From 1928 until 1934 Fischer, Meyer, Koch and Roelen continued to study the Fischer-Tropsch synthesis with

emphasis on catalyst preparation and its effect upon product distribution. They worked primarily with kieselguhr-supported nickel and cobalt catalysts. The development of more active catalysts made it possible to run the reaction at 450K. This resulted in a substantial lowering of the amount of methane formed (30 per cent of the synthetic hydrocarbons consisted of methane at 450K compared to 90 per cent at 525K). The cobalt catalyst led to lower conversion to methane and became known as the "standard cobalt catalyst". The findings of the catalyst development work with cobalt may be summarized as follows [16]:

1) Increasing catalyst age and increasing temperatures cause lower molecular weight products.

2) Increasing amounts of ThO_2, increasing amounts of unreduced cobalt and traces of alkali increase the yield of higher hydrocarbons.

3) Higher carbon monoxide to hydrogen ratios increase the yield of olefins.

4) The percentage of olefins decreases with increasing molecular weight of the hydrocarbon products.

5) The reaction products are mainly straight chain hydrocarbons with small amounts of oxygenated products.

During the period 1935 to 1937, Fischer and Pichler continued the research on the Fischer-Tropsch synthesis. They modified the atmospheric pressure process to consist of several steps with immediate removal of liquid reaction products [17]. This increased the product yield by 10-20 per cent without modifying the catalyst or the reaction temperature. Although most of the early work from Fischer's group was carried out at atmospheric pressure producing primarily hydrocarbons, it was known that by increasing the pressure a larger yield of

oxygenated products could be achieved. Fisher and Pichler developed a "medium pressure" process which operated at 5 to 20 atmospheres and used the same cobalt-thorium-kieselguhr catalyst as in the atmospheric pressure process. The medium pressure process had these advantages:

1) The yield of solid paraffins increased tenfold.

2) The yield of C_3+ hydrocarbons (those with more than three carbons per molecule) increased by 20 per cent.

3) Catalyst regeneration, required in the atmospheric pressure process, was not needed.

4) The reaction products were in general more saturated. This is an advantage for production of paraffins and diesel oil, but a disadvantage for gasoline production.

Until early 1935, iron had not been used in the Fischer-Tropsch synthesis because the yields of C_5+ hydrocarbons had been too low. Fischer and Meyer in [2] and Meyer and Bahr in [2] made some studies to improve the yields of higher hydrocarbons on iron, but the results had not been promising. However, with the development of the medium pressure process, the yield of these higher molecular weight hydrocarbons over iron catalysts was significantly increased. During the period from 1938 to 1945, Fischer and Pichler developed iron catalysts which had 1.0 per cent copper and 0.25 per cent alkali and were quite satisfactory Fischer-Tropsch catalysts. Their work involved the development of precipitated iron catalysts (which generally contained both copper and alkali), decomposition iron catalysts, fused iron catalysts and pretreated iron ores. Unlike cobalt, iron catalysts are useful under a wide range of synthesis conditions. Different preparation techniques were found to yield catalysts with different properties.

Pichler [18] obtained some very interesting results using a ruthenium catalyst at 413K and very high pressure (~150 atmospheres). He observed the formation of paraffins with molecular weights and melting points higher than were known before. Indeed, compounds with molecular weights as high as 400,000 can be produced over ruthenium. Pichler's ruthenium catalyst was found to be very stable for long periods of time. Pichler extended the Fischer-Tropsch work to high pressures using thoria and other catalysts and found that branched hydrocarbons were produced [19].

Since the late forties there has been little change in the fundamental understanding of the Fischer-Tropsch synthesis and of the fundamental processes to produce hydrocarbons from carbon monoxide and hydrogen. Research has continued and has resulted primarily in the improvement of already existing catalysts and processes. One significant contribution has recently come from Pruett and Walker [20] who have developed a homogeneous rhodium catalyst that catalyzes the conversion of carbon monoxide and hydrogen to ethylene glycol at 523K and 1360 to 3400 atmospheres total pressure. This discovery has opened a new frontier of Fischer-Tropsch research involving the novel approach of homogeneous catalysis instead of the traditional heterogeneous catalytic approach. Table 1 lists the catalysts, along with their applications, that have been found to be most useful in Fischer-Tropsch synthetic processes. In general metal catalysts favor the production of normal paraffins and olefins whereas metal oxides such as ThO_2/Al_2O_3 can produce isomerized hydrocarbons. Metal oxides and doped metal

Table 1. Catalysts frequently used in the Fischer-Tropsch synthesis

Nickel	Used primarily in methanation
Cobalt	Promoted with ThO_2/MgO and supported on kieselguhr Used primarily in the atmospheric pressure process for making higher hydrocarbons and in the medium pressure process for synthesizing paraffins
Iron	Most important medium pressure catalyst in use today--generally promoted by alkali
Ruthenium	Unique for the production of high molecular weight hydrocarbons
Metal Oxides	Used in the production of oxygenated products

oxides are generally required for the production of alcohols from carbon monoxide and hydrogen.

In order to use the Fischer-Tropsch synthesis to produce chemicals and fuels, large quantities of carbon monoxide and hydrogen must be available relatively cheaply. One process which involves the gasification of coal to supply the carbon monoxide and hydrogen is shown in Figure 1. Coal plus either steam or oxygen is introduced into a gasification chamber where the coal is oxidized yielding primarily carbon monoxide and hydrogen, with slight amounts of carbon dioxide, methane and sulfur-containing compounds. The methane is removed at this stage and the remaining feedstream is passed into a desulfurization-purification chamber to remove the carbon dioxide and sulfur-containing compounds which would foul the catalysts downstream. The remaining feedstream is passed into the water-gas shift reactor to catalytically adjust the hydrogen to carbon monoxide ratio to the desired value (usually between 2 and 3). Finally, the feedstream passes over the

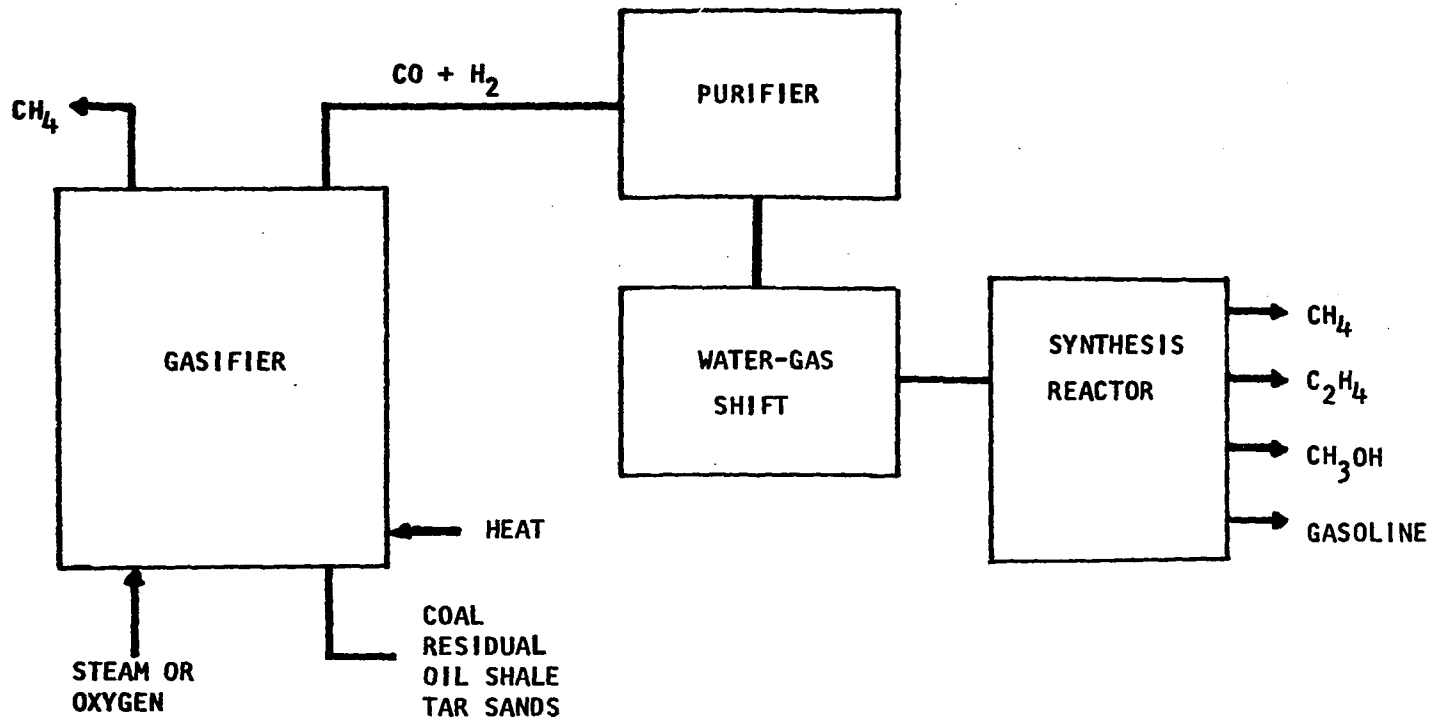

Figure 1. Schematic of process for the conversion of hydrogen deficient materials to useful chemicals and fuels

Fischer-Tropsch catalyst and the products are produced. Only one commercial plant utilizing this technology is in operation today. This is SASOL in South Africa where large coal reserves combined with essentially no petroleum reserves led to an early development of such a process.

The mechanism for the Fischer-Tropsch synthesis is obviously dependent upon the choice of products. Many scientists believe, however, that most, if not all, of the products have identical reaction intermediates. In 1926, Fischer and Tropsch proposed the "carbide theory" [21] in which a reactive metal carbide intermediate exists on the surface. This theory was refined by Craxford and Rideal [22,23] but was subsequently rejected as a result of work discussed by Pichler [2] and Kini and Lahiri [24].

The first proposal that oxygen containing surface intermediates are involved came from Elvins and Nash [25], also in 1926. Today, two forms of this proposal are believed most likely to describe the reaction sequence. A theory proposed by Storch and co-workers [26] postulates that carbon monoxide and hydrogen interact on a metal surface to produce an intermediate of the type $M\text{-}CH_2O$. They propose that ch in growth occurs *via* the interaction of these intermediates to form longer chain oxygen containing complexes of the general form $M\text{-}CH_2(CH_2)_xOH$. A theory by Pichler and Schulz [27] postulates the same $M\text{-}CH_2O$ intermediate but requires that chain growth occur *via* the interaction of this intermediate with an adsorbed carbon monoxide molecule. Recently, tracer studies by Emmett, *et al.* [28], Sanstri, *et al.* [29] and Kölbel

and Hanus [30] tend to support the Anderson model. whereas work by Blyholder and Goodsel [31] tends to support Pichler's model. Although there seems to be agreement as to the structure of one of the reaction intermediates, the details of the mechanism are still not understood.

The methanation reaction has, over the past 70 years, received quite a bit of attention, although not nearly so much as the more industrially significant Fischer-Tropsch synthesis. There are essentially three reasons for studying the methanation reaction:

1) to form a high Btu methane rich fuel with low carbon monoxide content

2) to eliminate carbon monoxide present in small amounts in hydrogen rich gases by conversion to methane

3) to avoid methane formation in the manufacture of higher hydrocarbons and oxygenated chemicals from synthesis gas *via* the Fischer-Tropsch reaction

Early research was concerned primarily with learning enough about the methanation process to avoid methane formation in manufacturing higher hydrocarbons and alcohols *via* the Fischer-Tropsch synthesis. Later work has been concerned with the conversion of the small carbon monoxide impurity present in a lot of natural gas so that it will meet federal requirements for introduction into transcontinental pipelines (0.1 ppm max.). Also, with the growing world shortage of petroleum and natural gas supplies, the formation of large quantities of methane from alternate fuel sources is becoming increasingly feasible.

The thermodynamics of the methanation reaction are summarized in Table 2. The free energy values indicate that the reaction is thermodynamically favored at lower temperatures. This requires the operation

Table 2. Methanation Thermodynamics[a] [32]

T (K)	ΔG^{o} (kcal/mole)	ΔH^{o} (kcal/mole)
300	-33.9	-49.3
400	-28.6	-50.4
500	-23.0	-51.3
600	-17.3	-52.1
700	-11.4	-53.2
800	- 5.5	-52.7
900	0.5	-53.6
1000	6.5	-53.9

[a]All reactants and products have a gaseous standard state.

of the reaction process at the lowest possible temperature in order to increase the thermodynamic yield. As is the case with all activated processes, lower temperatures reduce the kinetic rate of the overall process. Therefore, a situation exists in which two opposing factors must be simultaneously satisfied--the temperature must be kept low enough for a favorable thermodynamic equilibrium and to prevent sintering of the catalyst, but high enough to achieve an appreciable rate of conversion to products. Generally the methanation reaction is run at a temperature of 525 to 725K. Fairly high reactant pressures are used to achieve rapid conversion and higher product yields. Once a reaction temperature is chosen for a process, special precautions must be taken to prevent the highly exothermic reaction from causing catalyst overheating.

Wide varieties of catalysts and conditions have been used to study the methanation reaction. The work reported has included studies that measured the kinetics of the reaction process as well as spectroscopic

and thermal desorption studies designed to yield information about the bonding and interaction of the carbon monoxide and hydrogen to the surface.

During the past few decades many studies have been made to determine the kinetics of the methanation reaction on a variety of catalysts. Because of its economic availability as well as its high reactivity and selectivity toward methane formation, nickel has been used in most of these studies. Work by Vannice [33] in 1975 produced a turning point in the reporting of methanation kinetic results. The vast majority of the kinetic data taken prior to 1975 did not include measurement of the surface areas of the catalysts used. Although the information obtained from each of these early studies was useful, comparisons between laboratories or even between studies with a given lab were impossible since the rates were dependent upon catalyst surface areas. Vannice introduced the specific activity (molecules of methane produced per site per second) which is generally independent of the catalyst surface area. Most of the data since Vannice's work have been in the form of specific activities and comparisons are much more informative. Subsequent studies by Vannice [34-36] have demonstrated that, because of catalyst support interactions, the specific activities of metals supported on different materials are not necessarily the same.

Several reviews have discussed the kinetics of the methanation reaction, therefore, no detailed comparison of kinetic results will be presented here. Instead, a brief summary of these results on the group VIII metals will be followed by a more detailed discussion of

the mechanisms that have been proposed for the methanation process in recent years.

One fact that is immediately evident from the earlier methanation studies is that great diversity exists among the results. Much of the variation is likely due to differences in reaction parameters as well as differences in catalyst support materials and methods of pretreatment. If one choses to compare results with similar hydrogen to carbon monoxide ratios, say between 1 and 3, then some useful generalizations can be made. Usually the data are fit to a rate law of the form:

$$r_{CH_4} = k\, P_{H_2}^{m}\, P_{CO}^{n} \qquad (9)$$

The kinetic order in hydrogen, m, is usually between 0.5 and 1.5 and the order in carbon monoxide, n, falls in the 0 to -1.0 range. The interaction of the products with the catalyst is usually quite weak and yields a zero order dependence in the rate law. The kinetic studies have led to a general belief that under the conditions of the methanation reaction, the surface is nearly completely covered with strongly adsorbed carbon monoxide with the more weakly bound hydrogen competing for the remaining sites.

Vannice was the first to determine the specific activities of all the group VIII metals, except osmium, toward the methanation reaction [33]. His experiments were conducted at atmospheric pressure and 558K on alumina supported catalysts. The specific activities of these metals toward the methanation reaction are as follows:

$$Ru > Fe > Ni > Co > Rh > Pd > Pt > Ir$$

It is quite surprising that only two orders of magnitude separare the specific activities of ruthenium and iridium. Sinfelt's work with the hydrogenation of ethane demonstrated a difference of eight orders of magnitude between the specific activities of the most active and least active metals [37]. Vannice fit the kinetic data from his study to the same rate expression used in earlier studies (9). He found that for all the metals studied the kinetic order in hydrogen was between 0.77 and 1.6 and that for carbon monoxide was between 0.10 and -0.60, in general agreement with earlier results.

In a subsequent paper [38] Vannice demonstrated that there is an inverse trend between the heat of adsorption of carbon monoxide on a group VIII metal and the methanation activity of that metal. An opposite trend exists when the rates are compared to the heats of adsorption of hydrogen on the metals studied. A fairly large compensation effect exists for the methanation reaction on these metals.

Spectroscopic studies have generally led to the conclusion that carbon monoxide adsorbs on the group VIII metals in such a fashion that one of the following structures is an intermediate in the methanation reaction:

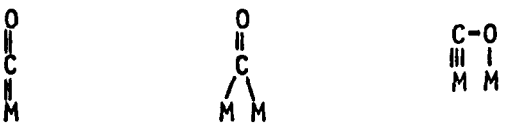

Another intermediate in the methanation reaction is believed to be identical to one of the ones postulated for the Fischer-Tropsch synthesis, $M\text{-}CH_2O$. This results from studies that establish a carbon monoxide to hydrogen ratio of 1:1 in this surface intermediate.

Although the structure of this surface complex is the subject of ongoing investigations, many believe that it can be adequately represented as follows:

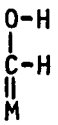

Several mechanisms have been postulated to describe the methanation reaction. All except two have been fit to data taken over nickel catalysts. The first mechanism for the methanation reaction was reported in 1965 by Kozub, Rosov and Vlasenko [39]. They performed work function measurements on a nickel-chromium catalyst and established that the mechanism should involve the interaction of charged species; adsorbed hydrogen increased the work function whereas adsorbed carbon monoxide decreased the work function. When a carbon monoxide dose was followed by a hydrogen dose the work function dropped, suggesting a positively charged surface complex. The proposed mechanism which is consistent with these work function changes is as follows (M=metal surface site):

$$M + e^- + H_2 \rightarrow MH_2^- \quad (10)$$

$$M + MH_2^- + e^- \rightleftarrows 2MH^- \quad (11)$$

$$M + CO \rightarrow MCO^+ + e^- \quad (12)$$

$$MCO^+ + 2MH^- \rightarrow MHCOH^+ + 2e^- + 2M \quad (13)$$

$$MHCOH^+ + MH_2^- \rightarrow MCH_2 + H_2O + M \quad (14)$$

$$MCH_2 + H_2 \rightarrow CH_4 + M \quad (15)$$

The intermediates in this mechanism seem quite reasonable. The authors did not specify the structure of the adsorbed MH_2^- complex, however it

is assumed that the hydrogen is dissociatively adsorbed. The postulation that hydrogen is molecularly adsorbed at the elevated temperatures used in the methanation process is difficult to believe. In a subsequent paper, Vlasenko and Yuzefovich [6] modified the mechanism to involve only one type of adsorbed hydrogen:

$$M + e^- + H_2 \rightarrow MH_2^- \quad (16)$$

$$M + CO \rightarrow MCO^+ + e^- \quad (17)$$

$$MCO^+ + MH_2^- \rightarrow MHCOH^+ + e^- + M \quad (18)$$

$$MHCOH^+ + MH_2^- \rightarrow MCH_2 + H_2O + M \quad (19)$$

$$MCH_2 + MH_2^- \rightarrow CH_4 + e^- + 2M \quad (20)$$

It was postulated that the step denoted by (18) is the rate determining step.

The second methanation mechanism was proposed in 1969 by Schoubye [40] who made a kinetic study on several nickel catalysts. Schoubye found that his data, which were collected between 443 and 623K and 1 to 15 atmospheres total pressure, could be fit by a rate law of the following form:

$$r_{CH_4} = \frac{AP_{H_2}^{0.15}}{\left[1+\left(\frac{BP_{CO}}{P_{H_2}}\right)\right]^{0.5}}$$

By assuming that the major surface species were adsorbed carbon monoxide and adsorbed hydrogen, the following simple mechanism was found to fit the data:

$$CO + 2M \rightleftarrows M_2CO \quad (21)$$

$$H_2 + 2M \rightleftarrows 2MH' \quad (22)$$

and/or $$H_2 + 2M \rightleftarrows M_2H_2 \rightleftarrows 2MH \rightarrow 2MH'' \quad (23)$$

where only MH' and MH'' (which are probably identical) can react with adsorbed carbon monoxide. The author postulates that the dissociation of the hydrogen molecule is the rate limiting step in the methanation reaction and that the dissociation of carbon monoxide is a poisoning side reaction which can occur.

In 1972 Bousquet, Gravelle and Teichner [41] proposed a mechanism to describe the methanation reaction over a nickel-alumina catalyst at 573K and with total pressures between 0.1 and 1 atmosphere. The kinetic results did not allow this group to distinguish between a Langmuir-Hinshelwood model and a Rideal-Eley model (see Appendix II) for those steps leading to the formation of the MH_2CO surface complex. Therefore, the authors developed a Langmuir-Hinshelwood mechanism in which adsorbed carbon monoxide is involved in the reaction:

$$H_2 + 2M \rightleftarrows 2MH \quad (24)$$

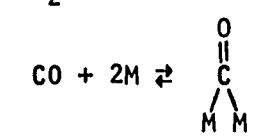

(25)

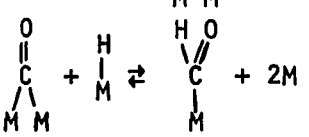

(26)

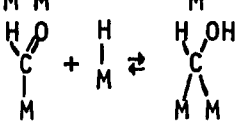
(27)

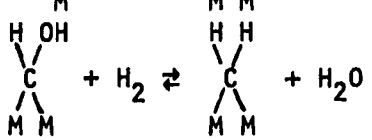

(28)

(29)

and a Rideal-Eley mechanism in which adsorbed carbon monoxide is an inhibitor:

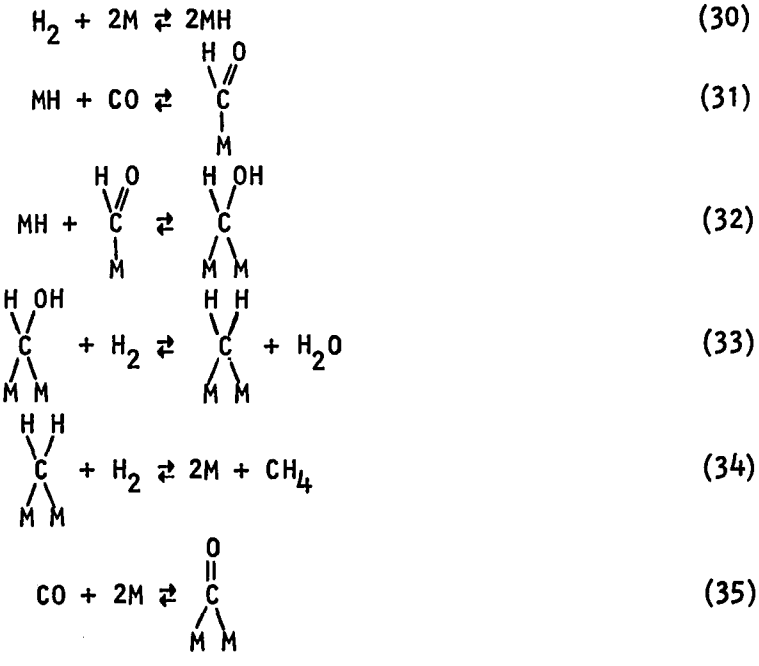

(30)

(31)

(32)

(33)

(34)

(35)

Both of these mechanisms are quite reasonable. Each involves the reaction of adsorbed hydrogen atoms and hydrogen gas with adsorbed carbonaceous intermediates to produce methane and water. It is interesting to note that, according to these models, the water is at no time bound to the surface of the catalyst.

Van Herwijnen, Van Doesburg and De Jong [42] in 1973 developed a mechanism for the methanation reaction in the 443 to 483K range and at atmospheric pressure. The reaction was found to have a variable CO

order from +1.0 to -1.0. No attempt was made to obtain a hydrogen order. The data were fit by the following expression (constant hydrogen pressure):

$$r_{CH_4} = \frac{AP_{CO}}{(1+BP_{CO})^2}$$

It was assumed that the rate determining step involved the interaction of two adsorbed species--one of which is carbon monoxide or a complex formed by carbon monoxide. The authors proposed the following interaction, involving an adsorbed enol complex and adsorbed hydrogen, as the rate determining elementary step:

$$MH_2CO + MH_2 \rightarrow MH_2O + MCH_2 \qquad (36)$$

This is a fairly incomplete description of the methanation process since it does not specify the steps preceding the rate determining step, nor does it specify the modes of bonding of any of the intermediates to the surface.

At about the same time as Van Herwijnen's model was proposed, Fontaine [43] developed a different model of the methanation process, once again on nickel. For pressures greater than 0.1 atmospheres, the following four steps were proposed:

$$CO + M \rightleftarrows M\text{-}CO \qquad (37)$$

$$H_2 + 2M \rightleftarrows 2M\text{-}H \qquad (38)$$

$$M\text{-}H + M\text{-}CO \rightleftarrows MHCO + M \qquad (39)$$

$$M\text{-}H + MHCO \rightleftarrows MH_2CO + M \qquad (40)$$

The last step was found to be the rate determining process. For pressures less than 0.1 atmosphere, it was determined that two more

reaction steps were needed to describe completely the methanation process:

$$M\text{-}H + MH_2CO \rightleftarrows MH_3CO + M \quad (41)$$

$$MH_3CO + M\text{-}H \rightarrow \text{Products} \quad (42)$$

As in the case of Van Herwijnen's model, Fontaine proposed that the H_2CO surface complex was formed <u>via</u> an irreversible reaction step. In the low pressure case, the last step (producing products) would be rate determining. The relative rates of these two irreversible steps would govern the concentration of the adsorbed H_2CO intermediate.

In 1975 McGill and Richardson [44] proposed a mechanism to describe their data taken between 423 and 673K over a commercial nickel-kieselguhr catalyst. The total pressure was 1 atmosphere. The mechanism that was proposed is as follows:

$$H_2 + 2M \rightleftarrows 2MH \quad (43)$$

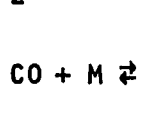

(44)

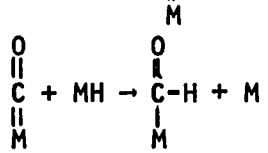

(45)

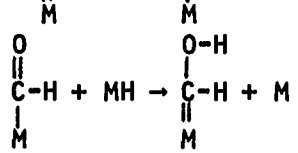

(46)

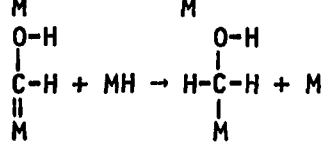

(47)

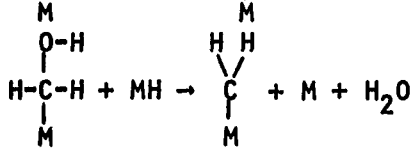

(48)

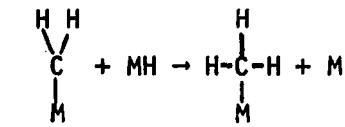

(49)

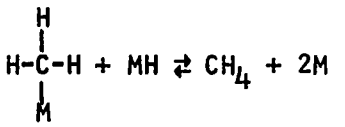

(50)

This mechanism proposes that atomic hydrogen is the adsorbed form of hydrogen. The atomic hydrogen in a stepwise fashion attacks the carbon-containing intermediate. McGill and Richardson found that at temperatures below 473K the step designated by (48) is rate determining. Between 473 and 573K step (45) is rate determining and at temperatures above 573K it was found that the adsorption of carbon monoxide (44) is the rate determining step.

In the same year Vannice [33] reported the results of a study that established an order for methanation activity of the group VIII metals based upon their specific activities. In a subsequent study [38] the kinetics of the methanation reaction were measured over the same metals. The studies were performed at atmospheric pressure and 548K on supported catalysts. Two mechanisms were proposed to describe the methanation process. The first was postulated for uniform surfaces:

$$CO + M \rightleftarrows MCO \tag{51}$$

$$H_2 + M \rightleftarrows MH_2 \tag{52}$$

$$MCO + MH_2 \rightleftarrows MCHOH \tag{53}$$

$$MCHOH + \frac{Y}{2}MH_2 \rightarrow MCH_y + H_2O \tag{54}$$

$$MCH_y + (\frac{4-Y}{2})MH_2 \rightarrow CH_4 \tag{55}$$

In this mechanism the step designated by (54) is the rate determining

process and the surface is believed to be predominantly covered with the MCHOH complex. For non-uniform surfaces with two types of sites, the following mechanism was proposed:

$$H_2 + * \rightleftarrows *H_2 \tag{56}$$

$$M + CO + H_2 \rightarrow MCHOH \tag{57}$$

$$MCHOH + (\tfrac{y}{2})*H_2 \rightarrow MCH_y + * + H_2O \tag{58}$$

$$MCH_y + (\tfrac{4-y}{2})H_2 \rightarrow CH_4 + M \tag{59}$$

The two non-equivalent surface sites are represented by M and *. In order to obtain a fit with this mechanism it was assumed that the step designated by (58) is the rate determining step. Sites designated by M adsorb only carbon monoxide and cover the greater portion of the surface. Sites designated by * adsorb only hydrogen. The intermediates in both mechanisms are reasonable, however the suggestion that one half (y=1) or three halves (y=3) of an adsorbed molecule could be involved in the reaction is unacceptable. This is the only mechanism known that attempts to describe the methanation process on all metals studied (the value of y depends upon the metal) and it is one of only two mechanisms that have been proposed to describe the reaction on ruthenium catalysts.

About a year later, Vannice's mechanism was modified by Bond and Turnham [45] to involve a different form of hydrogen bonding to the catalyst. A Ru-Cu supported bimetallic catalyst was used to collect kinetic data between 533 and 673K at pressures of about 0.1 atmosphere. The modified mechanism for uniform surfaces is as follows:

$$H_2 + 2M. \rightleftarrows 2MH \tag{60}$$

$$CO + M \rightleftarrows MCO \quad (61)$$

$$2MH + MCO \rightleftarrows MCHOH + 2M \quad (62)$$

$$MCHOH + aMH \rightarrow MCH_a + H_2O \quad (63)$$

$$MCH_a + (4-a)MH \overset{rapid}{\rightarrow} CH_4 + (5-a)M \quad (64)$$

The step designated as (63) is the rate determining step, as in Vannice's proposal. This mechanism, although it only describes work on the Ru-Cu alloy, is more acceptable than Vannice's proposal because the hydrogen is explicitly adsorbed in the atomic form and the problem concerning fractional adsorbed molecules is eliminated. This, of course, assumes that Vannice intended that $*H_2$ represent an adsorbed hydrogen molecule. His paper did not specify the sort of hydrogen bonding involved.

Also in 1976, Araki and Ponec [46] performed some methanation studies on nickel and nickel-copper alloys. They found that at 573K and 0.48 torr, the carbon monoxide disproportionation reaction (6) occurs. This led to a mechanism involving dissociated carbon monoxide:

$$H_2 + 2M \rightleftarrows 2MH \quad (65)$$

$$CO + 2M \rightleftarrows MC + MO \quad (66)$$

$$MC + MH \rightarrow MCH + M \quad (67)$$

$$MO + MH \rightarrow MOH + M \quad (68)$$

$$MOH + MH \rightarrow H_2O + 2M \quad (69)$$

The step designated as (67) was postulated as being the rate determining step. One situation not addressed by the authors concerns the observation that nickel catalysts tend to coke quite rapidly in Fischer-Tropsch processes. This coking reduces the catalyst activity

tremendously. If surface carbon is the active intermediate then it would seem that coking would not decrease the rate so rapidly and significantly.

Finally, a recent study by Ekerdt and Bell [47] has reported a mechanism for the methanation reaction on silica supported ruthenium catalysts. The study combined infrared and kinetic techniques. A temperature range of 464 to 548K was employed. The pressure was in the 0.1 to 1.0 atmosphere range. The following mechanism was proposed:

$$CO + M \rightleftarrows MCO \tag{70}$$

$$MCO + M \rightleftarrows MC + MO \tag{71}$$

$$MO + H_2 \rightarrow H_2O + M \tag{72}$$

$$H_2 + 2M \rightleftarrows 2MH \tag{73}$$

$$MC + MH \rightleftarrows MCH + M \tag{74}$$

$$MCH + MH \rightleftarrows MCH_2 + M \tag{75}$$

$$MCH_2 + H_2 \rightleftarrows CH_4 + M \tag{76}$$

In order to have this mechanism fit the kinetic data it was assumed that step (76) was the rate limiting step and that the coverage of adsorbed carbon monoxide molecules was much larger than that of any other intermediate.

Although some very significant differences exist among these mechanisms, some general trends seem to be apparent:

1) Each mechanism involves the interaction of one or more forms of adsorbed hydrogen.

2) All involved adsorbed molecular carbon monoxide except that proposed by Araki and Ponec. The mechanism by Ekerdt and Bell involves adsorbed molecular carbon monoxide which dissociates to form adsorbed carbon and adsorbed oxygen atoms.

3) All involve a H_2CO type adsorbed complex except those of Schoubye, Akari[2] and Ponec and Ekerdt and Bell. It is very likely that a H_2CO type complex is involved in Schoubye's mechanism, but he does not explicitly state so.

4) No mechanism except those of Araki and Ponec and Ekerdt and Bell involves the direct bonding of oxygen to the surface.

Work currently in progress will hopefully increase our understanding of the mechanism involved in the methanation reaction on a variety of catalysts.

Ruthenium has been found to be unique among the group VIII metals with respect to the catalysis of the hydrogen-carbon monoxide conversion. While it is the most active catalyst known for the methanation reaction, it is one of the least selective for methane formation, with about 60 per cent methane selectivity under moderate conditions. The remainder of the products are higher hydrocarbons, and it is these higher hydrocarbons that contribute to ruthenium's uniqueness. Ruthenium produces the highest C_5^+ fraction of all group VIII metals even at atmospheric pressure. Under conditions of high pressure and low temperature ruthenium will catalyze the formation of high molecular weight (up to 400,000) paraffinic waxes from carbon monoxide and hydrogen. No other catalyst is known to do this. The products of the reduction of carbon monoxide over ruthenium are generally a wide variety of saturated hydrocarbons. Essentially no oxygen containing compounds are produced (other than H_2O and CO_2). This unique ability to form high molecular weight compounds coupled with the high activity of the catalyst has resulted in several investigations that focused on

a fundamental understanding of the reaction processes that occur on ruthenium. One of the major drawbacks to the widespread use of ruthenium catalysts in Fischer-Tropsch/methanation processes has been its relatively rapid deactivation under rigorous industrial conditions. If this lifetime could be improved and the selectivity of product formation adequately controlled, then the use of ruthenium in processes that produce saturated hydrocarbons might be possible.

Although ruthenium primarily catalyzes the production of higher molecular weight paraffins the selective formation of methane can be caused to occur by modifying the reaction conditions. Relatively few kinetic studies of the methanation reaction have been made using ruthenium catalysts. The results of these studies have been fit to the same rate expression as those studies on other group VIII metals (equation (9)). A summary of these results is presented in Table 3.

A wide variety of spectroscopic studies has been performed on carbon monoxide and hydrogen adsorbed on ruthenium. Carbon monoxide is believed to adsorb in the undissociated form at low pressures. Higher pressure pulsed kinetic studies suggest that both undissociated and dissociated carbon monoxide exist in equilibrium at temperatures above 373K. It is generally believed that hydrogen adsorbs in the dissociated form.

If the two mechanisms that have been proposed to describe the methanation reaction on ruthenium are examined closer it is evident that each involves steps that are somewhat difficult to justify. For ruthenium, Vannice found that $y=4$. This leads to the following rate

Table 3. Kinetics of methanation studies on ruthenium

Catalyst	Temperature (K)	Pressures (atm)			Rate expression	Reference
		H_2	CO	Total		
0.5% Ru/Al_2O_3	493-533	16.1	5.3	21.4	$r_{(3H_2+CO)}=kP_{H_2}^{1.33}P_{CO}^{-0.13}$	48
Ru metal	293-433	0.02-0.05	0.013-0.13	0.01-0.16	$r_{CH_4}=kP_{H_2}^{2}$	49
1.5% Ru/Al_2O_3	473-613	0.55	0.18	0.73	$r_{CH_4}=kP_{H_2}^{1.8}P_{CO}^{-1.1}$	50
5% Ru/Al_2O_3	478-503	0.75	0.25	1.0	$r_{CH_4}=kP_{H_2}^{1.6}P_{CO}^{-0.6}$	33
0.5% Ru/Al_2O_3	448-548	1.0	0.0005	1.0	$r_{CH_4}=kP_{CO}$	51

determining step for his mechanism (determined by substituting y=4 into equation (54)):

$$MCHOH + 2MH_2 \rightarrow CH_4 + H_2O \qquad (77)$$

This step involves a three body collision which simultaneously adds four hydrogen atoms to the intermediate while the carbon-oxygen bond is being cleaved. So many bonds are being broken and formed during the rate determining step that it does not even resemble an elementary process.

The mechanism by Ekerdt and Bell proposes that the carbon monoxide molecule dissociates prior to being attacked by hydrogen in the methanation process. This is in disagreement with not only Vannice but also a considerable amount of spectroscopic and flash desorption evidence which suggests that carbon monoxide adsorbs on ruthenium in a non-dissociated manner. Also, the authors postulate a rate determining step which involves the attack of an adsorbed methylene group by gas phase hydrogen to form methane. They comment that they have no basis for expecting this to actually occur, but that it does cause the mechanism to fit the kinetic data.

Two recent studies have probed the effects of temperature, pressure and space velocity [52] and catalyst support [53] upon the hydrogenation of carbon monoxide on ruthenium. Catalyst activity and product selectivity were studied as functions of these variables. The results may be summarized as follows:

1) Low temperatures decrease the methane selectivity and increase the olefin to paraffin ratio in the higher hydrocarbons.

2) The tendency to form higher hydrocarbons increases with pressure as does the tendency to produce carbonaceous deposits.

3) Feedstocks with low mole percent carbon monoxide are selective to methanation.

4) Low space velocity increases methane production.

5) Both Fischer-Tropsch and methanation activities vary by an order of magnitude depending upon the catalyst dispersion and support.

6) The fraction of olefins may be increased by having low carbon monoxide conversions or by using Cr_2O_3 or ThO_2 to support the ruthenium.

7) Methane selectivity is independent of support.

8) Isomerization occurs subsequent to and downstream from straight chain production (probably occurs on the support).

These results provide guidelines that may be important in future attempts to produce ruthenium catalysts and processes to selectively convert carbon monoxide and hydrogen to methane and other hydrocarbons. Recent evidence suggests that carbon dioxide may be hydrogenated to methane on ruthenium catalysts [54,55] and that in a mixture of carbon monoxide and carbon dioxide, the carbon monoxide can be selectively hydrogenated [56].

It has been suggested that similar intermediates exist for both the methanation and Fischer-Tropsch reactions. The relative concentrations of these surface complexes likely determine which reaction will occur. The purpose of this study is to develop a mechanistic understanding of the methanation reaction on unsupported ruthenium catalysts. An attempt will be made to correlate these results with other methanation studies as well as with results obtained under

conditions that favored the formation of higher hydrocarbons. The role of the carbonaceous overlayer present on most Fischer-Tropsch/ methanation catalysts under reaction conditions will also be discussed.

EXPERIMENTAL

The methanation reaction on ruthenium thin films was studied using a variety of experimental techniques. The kinetics of the reaction were studied over a wide pressure range and under different catalyst pretreatment conditions. Isotopic exchange studies, as well as studies involving the flash desorption of carbon monoxide from ruthenium, were conducted. The catalyst surface was characterized before and after exposure to carbon monoxide and hydrogen under reaction conditions by Auger electron spectroscopy (AES), electron spectroscopy for chemical analysis (ESCA) and low energy electron diffraction (LEED). All kinetic and related studies were conducted in an ultra-high vacuum system designed and constructed specifically for this work. The LEED/Auger and ESCA studies were performed in commercial surface analysis systems built by Varian Associates (Palo Alto, California) and AEI Scientific Apparatus, Inc. (Elmsford, New York) respectively. Since each of these systems required the attainment and maintenance of ultra-high vacuum (10^{-9} to 10^{-10} torr range), UHV techniques were used extensively in the collection of these data. Several excellent reviews of the theory and attainment of ultra-high vacuum are available [57,58], therefore this discussion will be limited to the systems and procedures used specifically in this work.

Vacuum System Design

A diagram of the ultra-high vacuum system used in the kinetic and flash desorption studies is shown in Figure 2. Functionally the system

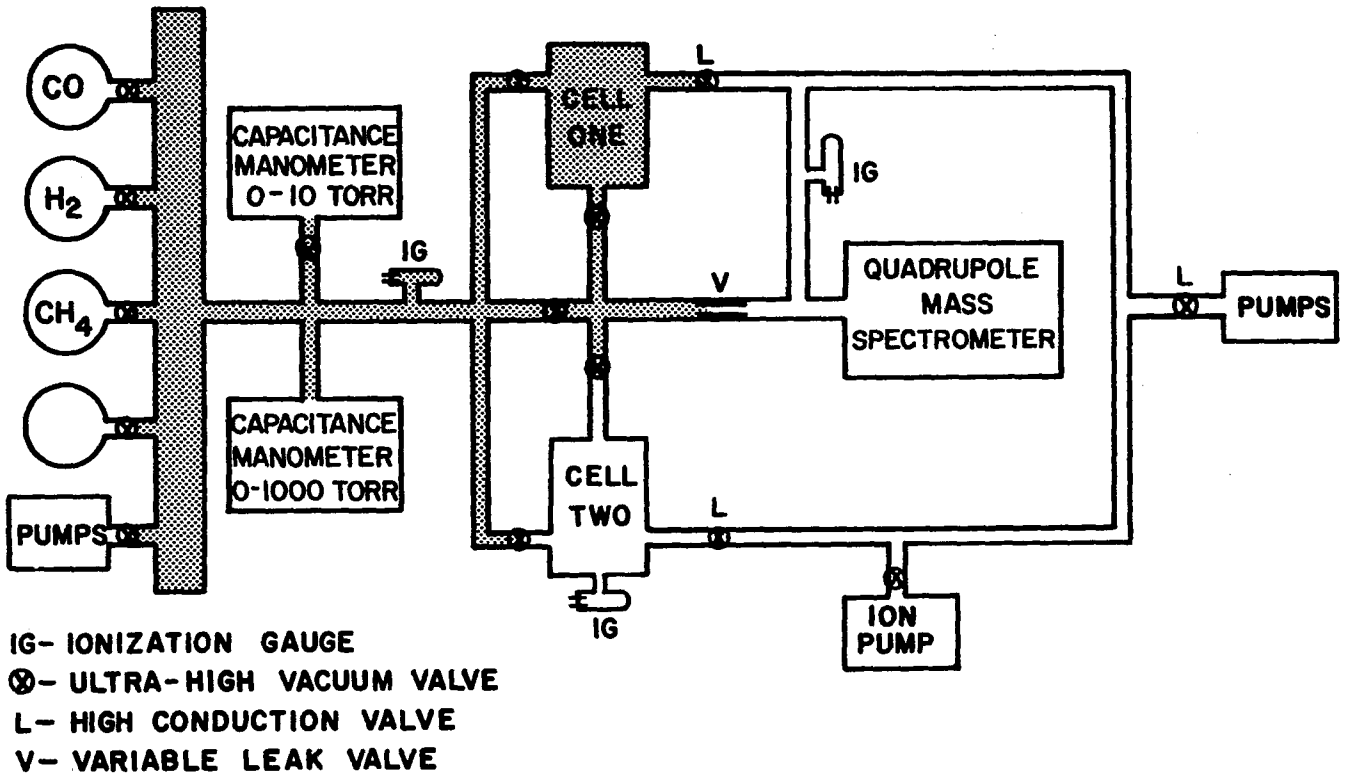

Figure 2. Diagram of ultra-high vacuum system used in kinetic and flash desorption experiments. (Shaded area = reaction volume ≅ 2.0 liters).

consisted of three portions. A gas manifold was used to premix the desired amounts of reactant gases. The reaction cell contained the catalyst which was maintained at an elevated temperature during the kinetic studies. The mass spectrometer was connected to the reaction cell via a leak valve to permit continual sampling of the gas mixture.

The gas manifold was constructed of 14 mm. (o.d.) pyrex tubulation. It was pumped by a two stage mercury diffusion pump to a base pressure of about 1×10^{-7} torr. The pressure in the empty manifold was measured by a conventional Bayard-Alpert ionization gauge. Connected to the manifold were several glass bulbs of high purity gases used in this study. These gases were generally predosed into the manifold prior to dosing onto the catalyst. The gas pressure in the manifold was measured by one of two capacitance manometers attached to the manifold. A low pressure capacitance manometer (Granville Phillips Co., series 212, Boulder, Colorado) was used to measure gas pressures between 1 μ and 10 torr. The reference side of this manometer was continually pumped to 10^{-6} to 10^{-7} torr to provide a stable baseline. The sensor head was water thermostated at 305.4K to prevent drift due to changes in the ambient temperature. The manometer was calibrated against a McLeod gauge (Consolidated Vacuum Corp., Rochester, New York) using argon. Pressure changes were recorded as a meter deflection on the manometer control unit. Five ranges were used with maximum pressures of approximately 100 μm, 300 μm, 1 torr, 3 torr and 10 torr (1 μm = 10^{-3} torr). Each range yielded a linear calibration of the form:

$$\text{Pressure } (\mu m) = A \times \text{Scale deflection} + B$$

The calibration was repeated periodically and never varied by more than 10 per cent from the initial calibration.

A high pressure capacitance manometer (MKS Instruments, type 107M, Burlington, Mass.) was used to measure gas pressures greater than 10 torr. The reference side of the manometer was pumped to 10^{-6} to 10^{-7} torr by the same pump used on the low pressure manometer. The higher pressure manometer had five ranges with maximum pressures of 10, 30, 100, 300 and 1000 torr. This manometer was factory calibrated such that the actual pressure could be read directly from the instrument meter. The factory calibration was checked twice during the course of this work and did not change by more than 2 per cent. In conjunction these capacitance manometers gave an effective manifold pressure range of 0.1 μm to 1000 torr (seven orders of magnitude). The manifold volume was measured by argon expansion from a standard volume attached to one of the gas inlet valves and was found to be 1087.1 cm^3.

The system had two reaction cells which were connected to the gas manifold. Initially, each cell consisted of a 500 ml. round bottom flask with three feedthroughs for electrical contact to a ruthenium crystal and a thoria coated iridium filament placed in the center of the bulb. Since no procedure for the deposition of ruthenium thin films was available when this project was begun, one of the early goals was to develop such a procedure. This necessitated the deposition of many films under slightly different conditions and the comparison of their activities and stabilities. After use the film was removed and a new round bottom flask was glass blown onto the system. A bakeout

was required before the reattainment of UHV conditions and the deposition of another ruthenium thin film. Having two cells allowed the deposition of two films between bakeouts resulting in more rapid data collection since half of the time lost during bakeouts was eliminated. The procedure developed for film deposition will be discussed in another section.

During the experiments a tube furnace (S. B. Lindberg, type SP, Watertown, Wis.) was placed around the reaction bulbs. The bottom of the vertical furnace was sealed and the top was covered to prevent air conduction through the furnace. In this manner, the bulbs could be conveniently heated to any temperature between room temperature and 775K (the approximate softening point of pyrex). The temperature was monitored by a chromel-alumel thermocouple which was inside the furnace and in direct thermal contact with the glass bulb. Once thermal equilibrium was reached, the temperature was stable to within $\pm 2^{o}$. The vertical temperature variation over the 12 inch long furnace was about 3^{o}.

After the procedure for film deposition had been developed, cell two was changed from a reaction cell to a flash desorption cell. This added versatility to the system in that both kinetic studies and flash desorption studies could be conducted without modification of the system. A description of the flash cell will be made in a subsequent section. The volume of the reaction cell and connecting tubulation was measured by argon expansion from the manifold and was found to be 889.4 cm^3. The total reaction volume was 1976.5 cm^3.

A variable leak valve (Granville Phillips Co., series 203, Boulder, Colorado) was used to control the flow of gases from the reaction cell (several torr) to the mass spectrometer (10^{-5} torr). The valve was set such that during the duration of an experiment (up to 30 minutes) no detectable pressure drop due to the leak occurred. The pressure in the mass spectrometer chamber was at all times maintained at 10^{-5} torr or below. This volume was pumped by a 20 l/s differential ion pump (Ultek, model 203-2000, Palo Alto, Ca.) and by two 2-stage mercury diffusion pumps attached in series. High conductance valves connected each cell to these pumps so that they could be pumped to a base pressure of 10^{-9} torr before film deposition. These high conductance valves were closed at all other times (except when flash desorption studies were performed in cell two).

A Finnigan Spectrascan 400 quadrupole mass spectrometer (Finnigan Corp., Sunnyvale, Ca.) was used to analyze the gas composition. A range of 1 to 60u was normally scanned once every 3.5 seconds. Periodically the range was widened to scan from 1 to 200u to check for changes in high mass peaks which might be suggestive of higher hydrocarbon formation. No changes past (m/z)=44 were ever detected. The output of the mass spectrometer was directed onto either a 2-channel strip chart recorder (Hewlett-Packard, model 7402A, Palo Alto, Ca.) or an oscilloscope (Tektronix, Inc., type R.M. 503, Portland, Oregon).

The entire system, with the exception of the mercury diffusion pumps, could be baked to 623K. The minimum base pressure was 3×10^{-10} torr. All valves were ultra-high vacuum valves (Granville Phillips,

Co., series 202, 203 and 204, Boulder, Co.). All glass was Corning 7740 borosilicate glass.

Thin Film Deposition Techniques

The usual procedure for deposition of thin metal films is to resistively heat a thin wire of the metal until a film is deposited. Unfortunately, ruthenium wires are not commercially available. The metal is so brittle that when thin wires are drawn they tend to break very easily. Three procedures for the production of ruthenium thin films were considered, "in house" production of ruthenium wires, argon ion bombardment of polycrystalline ruthenium and electron bombardment of polycrystalline ruthenium. The electron bombardment technique was ultimately chosen to produce the films used in this work. Since several discussions of thin film techniques are available [59,60], only those procedures used to produce these ruthenium thin films will be mentioned.

An attempt was made to produce ruthenium thin wires so that the more traditional procedure for the production of thin films could be used. A 3.0 gram sample of 99.95% ruthenium powder (Engelhard Industries, Inc., Carteret, N. J.) was melted in vacuum to produce two ruthenium rods (0.7 cm. x 10 cm.). One of the rods was sliced lengthwise several times to produce 20 mil thick slabs of ruthenium metal (1 mil = 0.001 inch). The slabs were sliced lengthwise to produce 20 mil "wires" of ruthenium. The cutting was done on a diamond wheel cutter (Buehler, Ltd., model 11-1180, Evanston, Ill.).

Many of the "wires" were broken in the cutting procedure. Some were ruined during efforts to spotweld them to the support rods in the reaction cell. Of the two or three that were actually put into the system and heated resistively, none resulted in a thin film. The "wires" would repeatedly fracture (presumably along grain boundaries). This procedure was eliminated as a feasible method of producing ruthenium thin films.

Figure 3 shows a diagram of the cell used for production of ruthenium thin films by electron bombardment. A ruthenium polycrystalline disc (Materials Research Corp., Orangeburg, N. Y.) was spotwelded to a tungsten support rod in the center of the glass bulb. The geometric surface area of the sample was approximately 1 cm^2. Auger as well as x-ray fluorescence spectroscopies indicated that the sample was pure ruthenium with no detectable impurities. Located adjacent to the ruthenium sample was a thoria coated iridium filament.

During electron bombardment the ruthenium disc was maintained at +400V with a regulated high voltage power supply (Heath Company, model SP-17A, Benton Harbor, Mi.). Current from a modified dc power supply (Hewlett-Packard, model 6286A, Palo Alto, California) was passed through the throia coated iridium filament. The dc power supply was modified to regulate the electron emission from the filament to the ruthenium sample. The electrons impacting the ruthenium disc caused it to be heated. The background pressure was maintained in the low 10^{-8} torr range. The temperature of the disc was maintained at 2223K for 3 hours while a fairly even ruthenium film was deposited.

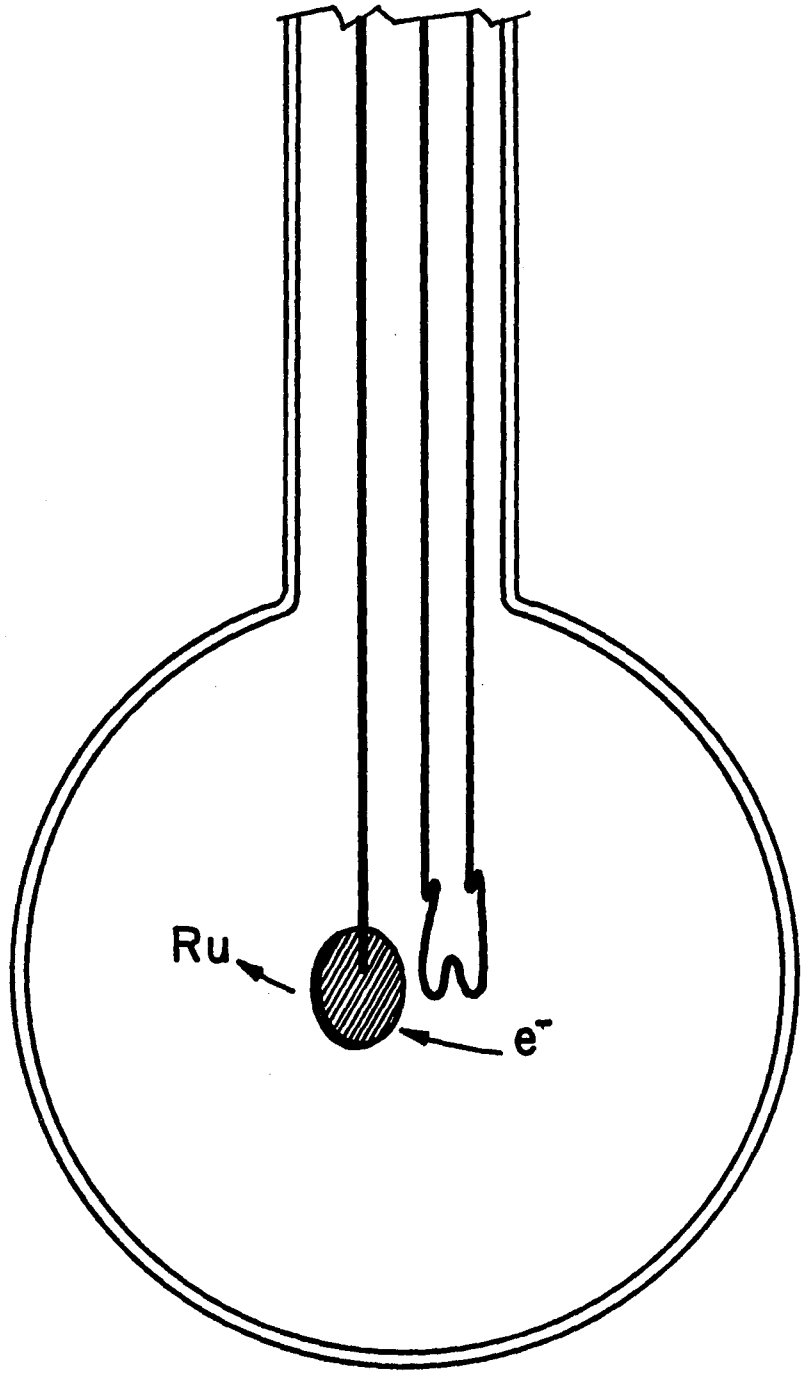

Figure 3. Diagram of the cell used for the production of ruthenium thin films on glass by electron bombardment.

During this entire process, the pyrex bulb was submerged in a large beaker of water. Sufficient heat was transmitted radiatively to the bulb to cause the water to boil. Therefore, the film was deposited with the glass at 373K. The film was then sintered at 673K for 1 hour. Films deposited in this manner were found to be fairly active and quite stable.

It was thought that argon ion bombardment might be a better technique for depositing the film in that deposition would occur without heating the disc quite so hot. This would allow deposition at a lower background pressure and with the glass bulb at a temperature less than 373K. The set-up for this work was essentially the same as with the electron bombardment study except that an additional electrode was located near the disc. The filament was heated while the extra electrode was maintained at +400V. The disc was at a -600V potential. Argon was dosed into the system to a pressure of 2×10^{-4} torr. Argon ions were produced between the filament and the electrode. They were attracted by the -600V potential to the disc. The ion emission to the ruthenium disc was monitored. After a couple of hours at an ion emission of 80 mA a fairly thin, uneven film was produced. The electron bombardment technique produced higher quality films as judged by activity, stability and appearance. All films used in the collection of the data presented were deposited by electron bombardment of a ruthenium disc.

Kinetics Procedure

The kinetic studies were conducted in the temperature range 548 to 623K. Most of the data were collected at 573 to 583K. Mixtures of carbon monoxide and hydrogen were prepared in the manifold. Hydrogen was always present in excess. The initial pressure of each gas was measured using the capacitance manometer. The final pressures (after expansion into the reaction cell) were calculated from the initial pressures and the known volume ratio of the manifold and the reaction cell. At very low carbon monoxide pressures (manifold pressure under 200 μm) a substantial portion of the gas adsorbed onto the film upon exposure. Corrections for this pressure change were made using the data from Figure 4. In this figure an r, which is a factor that converts the pressure of carbon monoxide in the manifold to the pressure of carbon monoxide in the reaction cell, is plotted against the manifold carbon monoxide pressure. Deviations from constancy are due to carbon monoxide adsorption on the film.

The reaction rate was always determined from the change in the methane concentration in the mass spectral chamber as a function of time. Equilibration of the methane across the leak usually occurred quite rapidly (5 seconds or less). It was observed that water did not equilibrate across the leak rapidly enough to give reliable rate information. With each set of data collected, a calibration of the mass spectrometer with respect to methane was made. A known pressure of methane was dosed into the reaction cell and the intensity of the $(m/z)=15$ peak was monitored. This peak was used to measure the methane

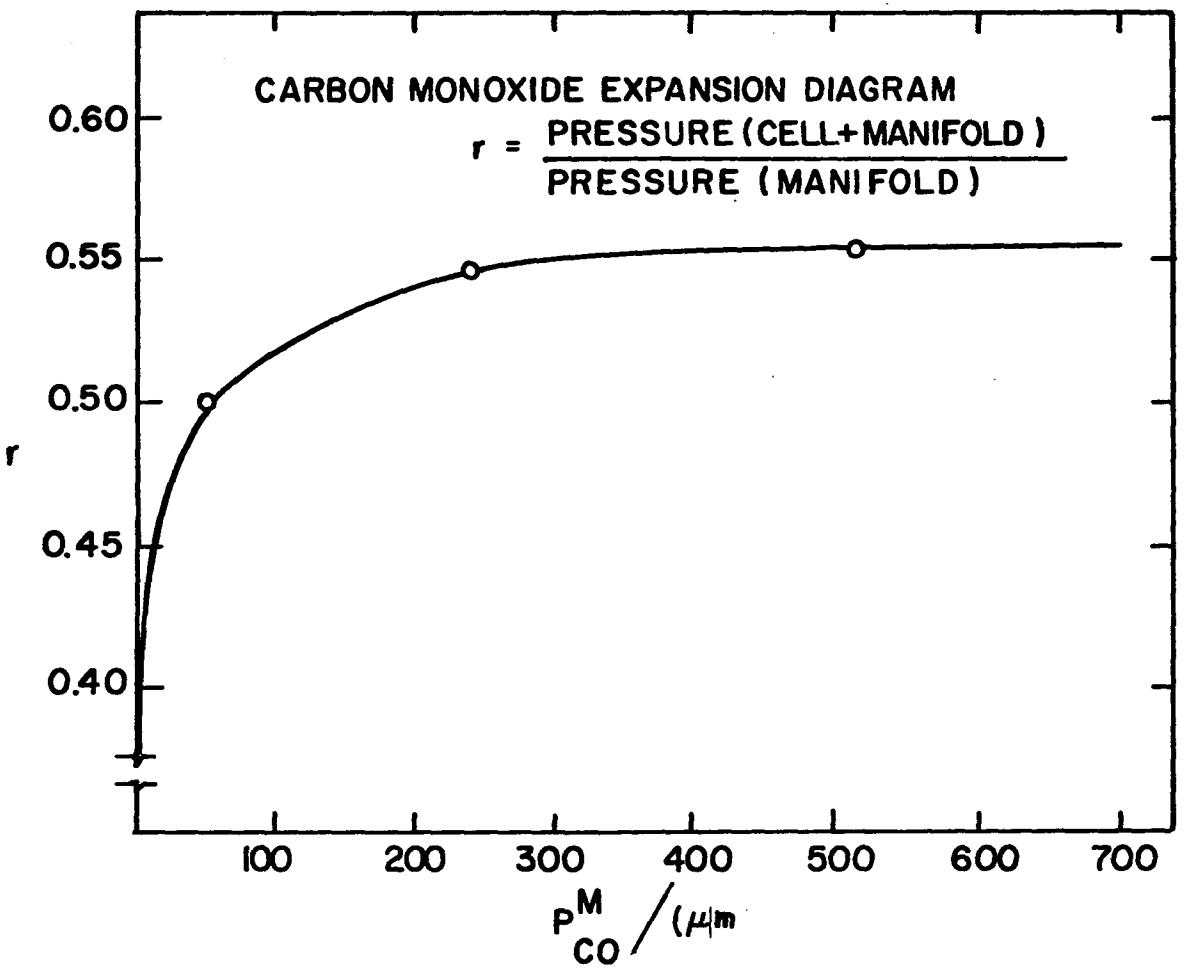

Figure 4. The variation of the carbon monoxide pressure conversion factor as a function of the pressure of carbon monoxide in the manifold.

produced rather than the (m/z)=16 because of oxygen interference from carbon monoxide and water. It was found that the mass spectrometer sensitivity to methane varied with the amount of hydrogen present in the reaction cell. As the hydrogen pressure was increased the intensity of the methane peaks in the mass spectrum also increased at constant methane pressure. The change in mass spectrometer response expressed as μm of methane per mv ((m/z)=15) is shown in Figure 5 as a function of hydrogen pressure in the cell. The quantity s, which is inversely proportional to the mass spectrometer sensitivity, is observed to decrease with increased hydrogen pressure. This sensitivity change is routinely seen in systems which have a high pressure volume connected to the mass spectrometer via a leak or capillary tube. The cause of this effect has been discussed by Masterson [61]. Ion/molecule interactions might also be involved.

Initial rates were measured in all cases. In general all rates were determined within the first 60 seconds after the initiation of the reaction. After a rate was determined, the reaction cell was pumped through the manifold. When the pressure dropped below 10^{-4} torr as measured by the more sensitive capacitance manometer, 3.5 torr of hydrogen (standard hydrogen dose) was dosed into the reaction cell which was at the reaction temperature, usually 573K. This hydrogen dose had the effect of removing any reactive carbon left on the surface from the previous run so that the initial catalyst surface was regenerated for the next run. It was observed that the amount of methane produced during this standard hydrogen dose depended upon not

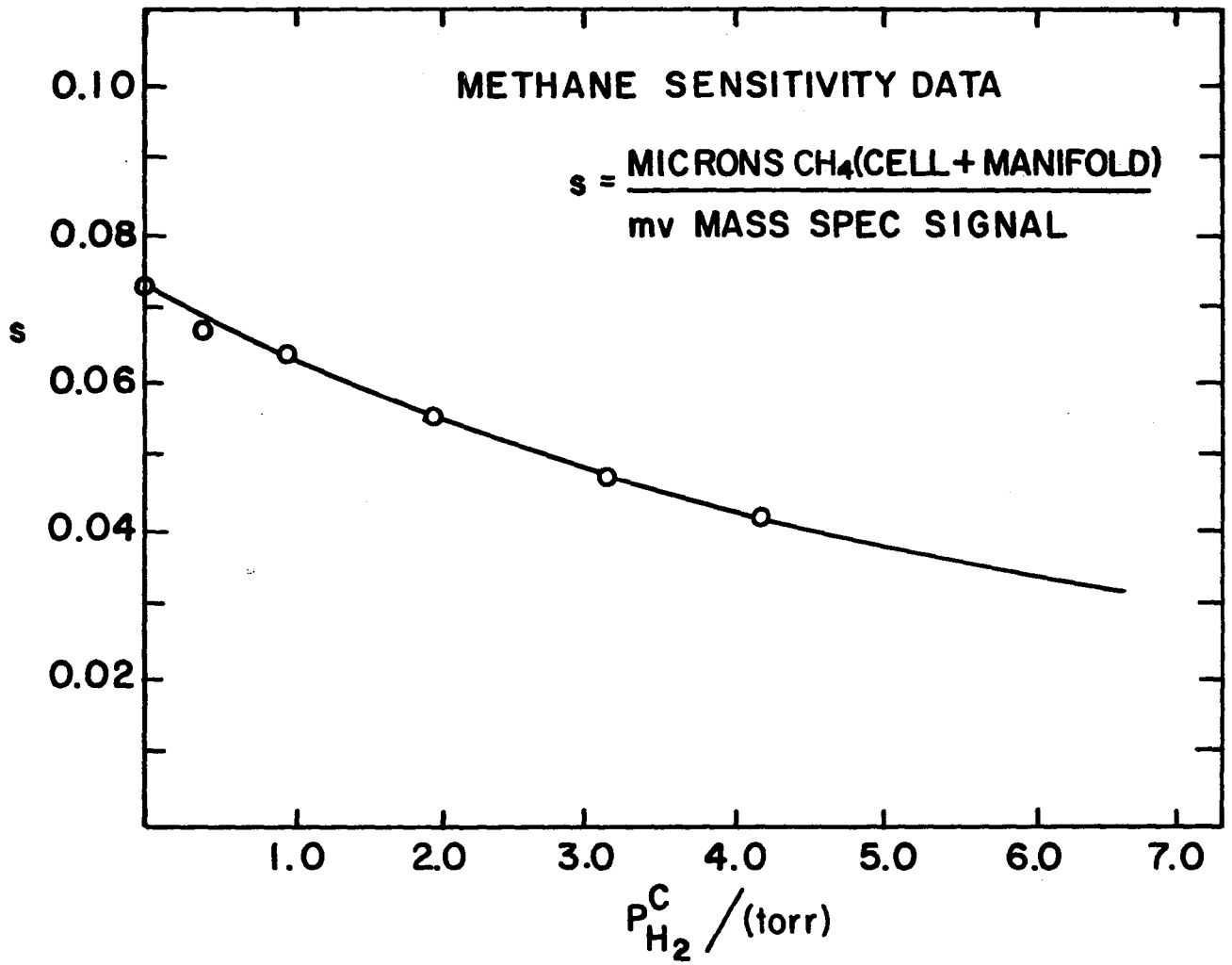

Figure 5. Variation in mass spectrometer response ((m/z)=15) as a function of the pressure of hydrogen in the reaction cell.

only the amounts of carbon monoxide and hydrogen present in the previous kinetic run but also upon the length of time that the reaction cell had been pumped prior to the standard hydrogen dose. This observation will be discussed in more detail in a subsequent section.

Experiments were performed to measure the reaction order with respect to carbon monoxide, hydrogen, water and methane. All of these studies were conducted using the techniques summarized earlier. Calibration rates were always run with each set of data to allow the absolute comparison of data from day to day. When not in use the films were stored in 3.5 torr of hydrogen at room temperature. All rates are reported as turnover numbers (molecules of methane/site·s). This rate is explicitly independent of the catalyst surface area and allows a more direct comparison of the data to literature values obtained under similar conditions.

Studies of the exchange rates of $^{13}C^{18}O$ and $^{12}C^{16}O$ as well as hydrogen and deuterium were performed on the ruthenium thin films at 573K.

Surface Pretreatment Studies

Several experiments were performed to determine the dependence of rate on several kinds of surface pretreatment. Prior to a kinetic run, the surface was predosed with carbon monoxide. The disproportionation reaction (6) occurred, leaving a carbon deposit on the surface. The disproportionation reaction was allowed to proceed for different lengths of time producing different fractional coverages by

carbon. The effect of this carbon overlayer upon the kinetics of the methanation reaction was then determined. Studies were also made to attempt to establish the effect of predosing the catalyst with $^{13}C^{18}O$. The mass spectrum was carefully analyzed to see if $^{13}CH_4$ or $^{12}CH_4$ was produced first when the isotopic predose was followed by a kinetic run. The effect of removing the standard hydrogen dose from the kinetic studies was also determined.

Flash Desorption Studies

A few flash desorption experiments were conducted to elucidate the bonding of carbon monoxide to a polycrystalline ruthenium surface. A flash desorption cell was mounted in the position of cell two on the system. A diagram of the flash cell is shown in Figure 6. The cell was constructed entirely of pyrex. A polycrystalline ruthenium disc was spotwelded to a 40 mil support rod. The geometric surface area of the disc was approximately 1 cm^2. A nearby thoria coated iridium filament supplied electrons so that the sample could be heated by electron bombardment. A thermocouple was spotwelded to the disc for temperature measurement. The thermocouple wires were 3 mil W/5%Re, W/26%Re (Hoskins Manufacturing Co., Detroit, Michigan). Two pyrex faceplates were positioned parallel to the faces of the ruthenium disc. This enabled the disc to be heated using a well-focused light beam. Heating by light was chosen over heating by electron bombardment for the flash studies because the latter technique would very likely produce results indicative of the adsorbate-electron interaction rather

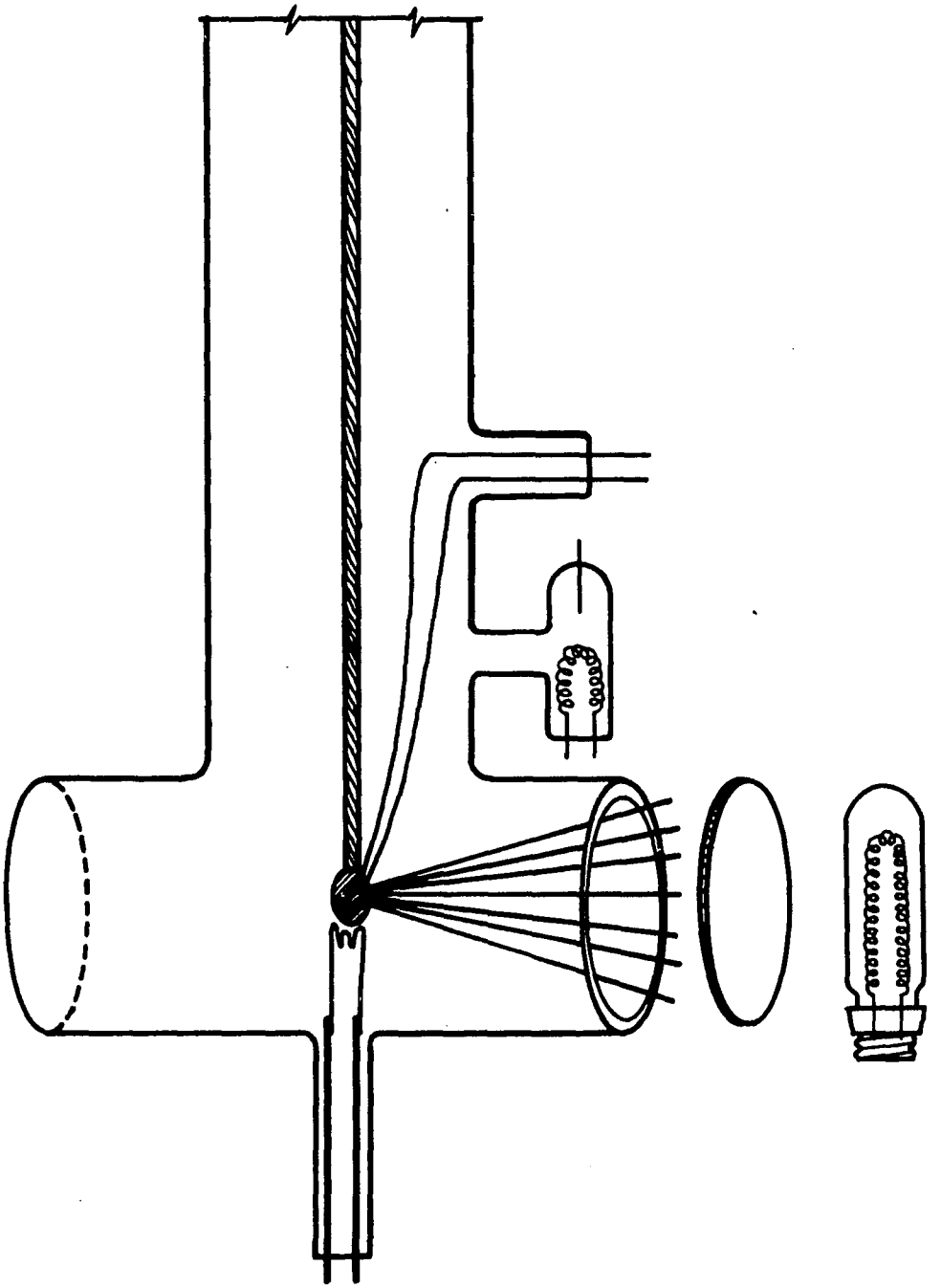

Figure 6. Diagram of the flash desorption cell showing the disc being heated by a well-focused beam of light.

than the adsorbate-substrate interaction. A 1000 watt projector bulb was used to produce a well-focused light beam which could heat the crystal linearly from room temperature to 723K in 30 seconds. The light could be used to heat the crystal to a maximum temperature of 973K.

The disc was cleaned by heating for several days at 1173K using electron bombardment. Several $1x10^{-6}$ torr oxygen and hydrogen cleaning cycles followed. The oxygen was effective in removing phosphorus and sulfur. The hydrogen removed any remaining oxygen. Flashing to 1773K removed any remaining surface carbon. The experiments were performed by dosing carbon monoxide into the pumped cell with the disc at room temperature (300K). The dose was measured with an gauge attached to the cell and was expressed as Langmuirs (1 Langmuir= $1x10^{-6}$ torr·s). The dose was stopped and the remaining carbon monoxide was pumped out. The flash was begun by turning on the light. The desorbed gas was monitored on the ion gauge and the mass spectrometer. The output of both the ion gauge and the thermocouple were directed onto two X-Y recorders (Hewlett-Packard, model 7044A, Palo Alto, Ca.) so that a temperature could be assigned to the peak maximum.

Surface Characterization Studies

LEED, Auger and ESCA studies were performed under a variety of conditions to characterize the ruthenium surface before, during and after the methanation reaction had occurred. LEED can be used to predict the symmetry of any ordered adlayer relative to the symmetry

of the substrate. Auger electron spectroscopy establishes which atoms are present on the surface and in the first five or so layers of the bulk. ESCA is useful in predicting the sorts of bonding involved between the metal and the adsorbed species. Excellent reviews of the theory and application of LEED [62], Auger [63] and ESCA [64-68] are available.

The LEED/Auger experiments were performed in a Varian 981-2000 vacuum system with 4 grid LEED optics and cylindrical mirror Auger electronics. The system was bakeable to 623K and operated at a base pressure of 2×10^{-10} torr. A circular polycrystalline ruthenium disc was used for the Auger work. The disc had a diameter of 0.6 cm. and a thickness of 0.1 cm. The disc was polished with silicon carbide covered paper. A polished ruthenium $(10\bar{1}2)$ crystal was used for the LEED study. The crystals were mounted to an offset manipulator with movement in the x, y and z directions. A W/5%Re, W/26%Re thermocouple was spotwelded to the face of the disc to permit temperature measurement. The sample was heated by an indirect heater block. The maximum temperature was 1500K. The discs could be flashed to 1400K in 60 seconds. All Auger spectra were run with 10 μa. emission to the sample at a beam energy of 2000 eV. It is predicted that with this fairly low emission only 5 to 10 layers were being sampled. A scan width of 50 to 550 eV was usually used with a 1.67 $eV \cdot s^{-1}$ scan speed. Studies were made to develop an understanding of the interaction of ruthenium with carbon monoxide and hydrogen as well as to characterize the catalyst before and after methanation.

Gases were dosed into the Auger system from a gas handling system through a Granville Phillips leak valve. When carbon monoxide-hydrogen mixtures were dosed, the mixing was done in the gas manifold prior to actual dosing. The manifold pressure was measured with a mercury manometer which could be valved off when not in use. During all doses the poppet valve was closed to prevent flooding of the ion pumps. At the end of each experiment the gases were roughed out with the VacSorb pumps. High vacuum (10^{-8} torr range) was restored in 3 to 5 minutes by opening the poppet valve to the ion pumps. All Auger studies were performed with the catalyst at 573K unless otherwise noted. The Auger spectrometer was also used routinely to characterize the purity of thin films that were removed form the kinetic system.

One result that was immediately evident from the Auger work was that a ruthenium catalyst exposed to carbon monoxide and hydrogen always had carbon associated with it under the conditions of the kinetic studies. An attempt was made to use ESCA and LEED to characterize further this carbon. After the Auger studies were completed the polycrystalline ruthenium sample was placed in an AEI model ES 100B XPS/UPS spectrometer (Associated Electronics Industries, Westwood, New Jersey). The Al K_{α} line (1486.6 eV) was used as an energy source for the XPS work. An attempt was made to determine whether the carbon had formed graphite. Some XPS studies were also made to further characterize the interaction of polycrystalline ruthenium with carbon monoxide and with methanol. These studies involved low pressure doses of each adsorbate onto clean ruthenium.

A LEED study was undertaken to see if the carbon left on the catalyst surface after methanation formed an ordered overlayer with respect to the ruthenium substrate. A ruthenium (10$\bar{1}$2) crystal was used in this study. The crystal was cleaned and then exposed to carbon monoxide and hydrogen at 573K so that methanation would occur. LEED patterns were taken before and after methanation. Presumably, if graphite had formed, the LEED pattern should show a hexagonal structure characteristic of graphite.

Materials

Most of the gases used in the kinetic and isotopic studies were research grade ultra-high purity gases. The hydrogen (99.9995%), carbon monoxide (99.97%), methane (99.99%), argon (99.9995%) and carbon dioxide (99.998%) were purchased from the Linde division of Union Carbide (Chicago, Ill.) The deuterium (99.99%) was purchased from Air Products and Chemicals, Inc. (Los Angeles, Ca.). The $^{13}C^{18}O$ (90% C, 95% O) was purchased from Prochem Isotopes (Summit, New Jersey). All of these gases were purchased in pyrex bulbs with breakable seals. The water was doubly distilled tap water which was further distilled several times under vacuum. The water was boiled while under vacuum to remove any dissolved gases. A mass spectral analysis indicated that there were no detectable impurities in the water.

The hydrogen used in the LEED/Auger studies was taken from a cylinder and purified by passing through a Pd/25% Ag diffuser. The methanol used in the XPS study was spectral quality distilled in glass

(Burdick & Jackson Laboratories, Inc., Muskegon, Mi.). This was distilled in vacuum several times before using. All other gases used in the LEED/Auger and ESCA studies were identical to those used in the kinetic studies.

RESULTS AND DISCUSSION

Thin Film Characterization

As has been previously mentioned, all rates determined in this study are expressed as turnover numbers (molecules/site·s) This rate is functionally dependent upon the change in methane pressure with time, the reactor volume, the catalyst temperature and the number of active catalyst sites. Chemisorption techniques for the measurement of the number of surface sites of several ruthenium catalysts have been reported using hydrogen [69-73], carbon monoxide [73-75] and oxygen [70,76] as adsorbing gases. In all cases the quantity of a particular gas adsorbing on a clean ruthenium catalyst at some temperature (usually room temperature) is measured. A BET surface area of the catalyst is obtained using either argon or nitrogen adsorption. By assuming the surface area of a typical surface atom, the number of ruthenium surface sites may be calculated. The results of the hydrogen, carbon monoxide and oxygen studies can be used to predict the number of adsorbed atoms (or molecules) per ruthenium surface site. Although this technique is used quite extensively, there is no direct correlation between the number of sites obtained using the adsorption technique and the actual number of catalytically active ruthenium sites. It is quite conceivable that some sites which adsorb hydrogen, for example, might not be active for a particular reaction for which the ruthenium catalyst is used. For example, the activity of the group VIII metals for the methanation reaction has been found to decrease as the heat of adsorption of carbon

monoxide on metals increases [5]. What appears to happen is that in some cases, the carbon monoxide bonds to the catalyst so strongly that the desorption of either the carbon monoxide or the reaction product is difficult to achieve under reaction conditions. Also, with catalyst surfaces which are atomically rough, some sites are uncoordinated relative to the others. This variation in coordination of individual surface sites of a metal is believed to have a drastic effect upon the activity of those sites toward certain reactions [77]. These differences in bond strengths to the sites are not properly reflected in the chemisorption techniques mentioned above. Also, the assumptions made to calculate the surface area of a typical surface atom are sometimes difficult to justify.

In this work eight ruthenium thin films were used. Initially, the procedure was to deposit a thin film using electron bombardment and then to do kinetic runs on the film. The first films were used for one day only. After being used the film was removed and a new film was deposited before any more data were collected. This was a very time consuming process. It was decided that an attempt would be made to use one film for several sets of data if the activity of the film would remain reproducible from day to day. A film was deposited and it was used for fifteen months. The stability of this film was found to be excellent. The data were reproducible to ± 10% during this entire period. All data reported in this thesis were taken over this film. Comparison of the large quantity of data taken over this film to the rather small amount taken over previous films indicates that there was no appreciable

variation in the results obtained among the films. None of the data presented have been adjusted to improve the correlation of results taken on different days.

An actual determination of the number of ruthenium surface sites active in the methanation reaction has been made in this study. The ruthenium thin film was reduced with hydrogen at 573K to remove any reactive carbonaceous material. The hydrogen was pumped from the reaction cell and a 35.9 μm carbon monoxide dose was made. The carbon monoxide disproportionation reaction (6) proceeded yielding adsorbed carbon atoms and carbon dioxide. The reaction was allowed to proceed for various lengths of time to produce different fractional coverages of carbon. The amount of carbon dioxide produced was used to count the number of adsorbed carbon atoms. Following the completion of the carbon monoxide dose the cell was pumped for 300 seconds. A 3.5 torr hydrogen dose was made to remove the adsorbed carbon as methane. The results of this study are shown in Figure 7. At each time the quantities of both carbon dioxide and methane produced were determined. For some points the number of molecules of the two gases were equal. Those entries are represented in the figure as a single solid point. One observation that is immediately evident from this figure is the excellent agreement between the carbon dioxide and methane results. No point exists in which these two values differ by more than 2%. As the time of exposure of the film to carbon monoxide is increased, the quantity of reactive carbon on the surface also increases up to a time of about 300 seconds. After that the amount of carbon on the surface

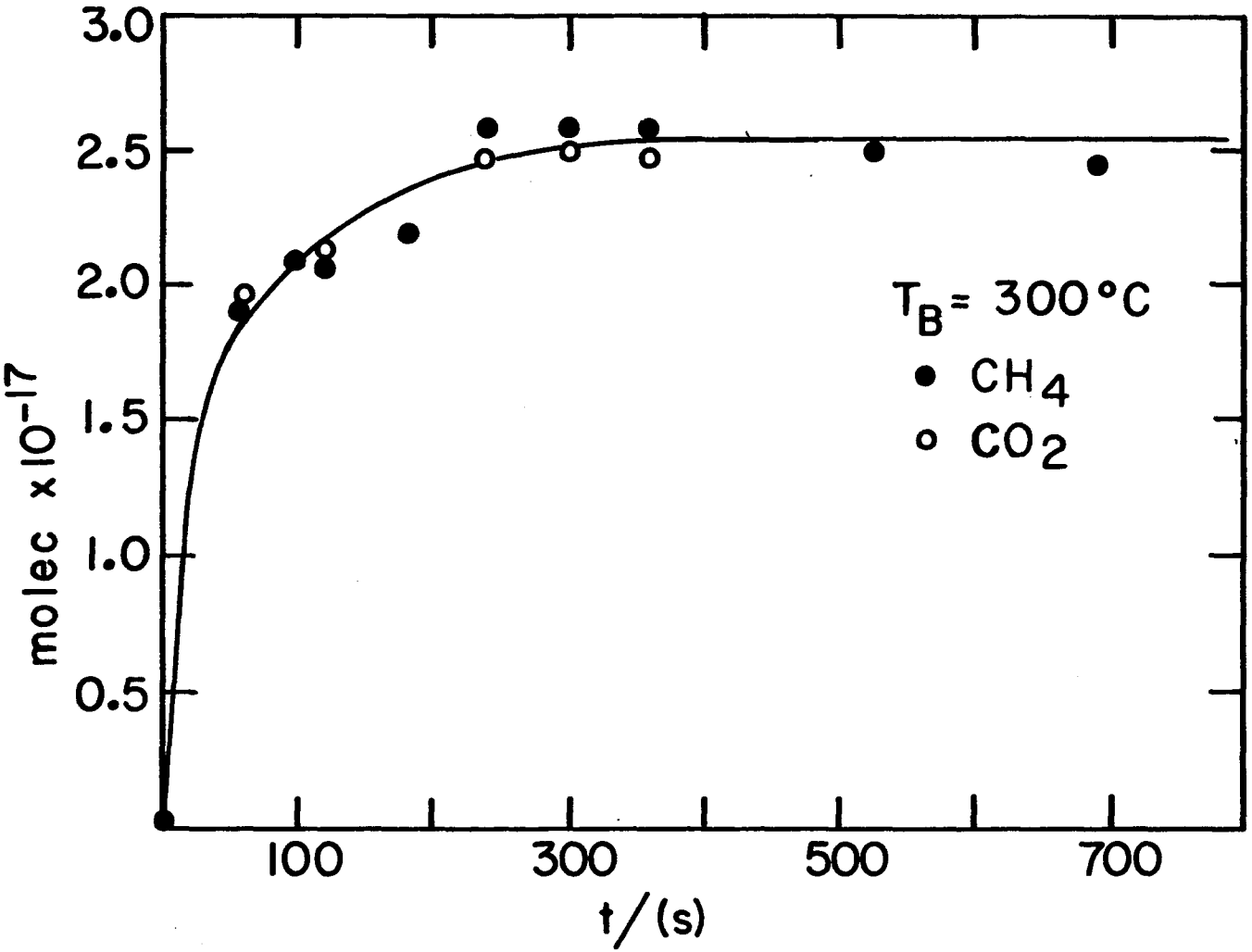

Figure 7. Catalyst surface area determination: the open circles represent the amount of CO_2 produced during a CO disproportionation study; the closed circles represent the amount of CH_4 that resulted when the surface was flushed with H_2.

levels off. This suggests that under the conditions of this study a monolayer coverage of carbon is achieved and further exposure to carbon monoxide does not increase the quantity of surface carbon. This in itself is an interesting result since the amount of surface carbon on some methanation catalysts seems to increase for periods of up to four hours under methanation conditions [78].

The amount of methane and carbon dioxide produced due to a monolayer of surface carbon is shown in Figure 7 to be 2.54×10^{17} molecules. This is also the number of active catalyst sites for methanation since there is by definition a 1:1 correlation between the amount of methane produced from a saturation carbon coverage and the number of active sites. In this context the term site is not used to designate a single ruthenium atom. It is used to designate a place where carbon monoxide can bond and upon exposure to hydrogen produce methane. In this context a site might be a single ruthenium atom, it might be a pair or a group of atoms, or there might be more than one site per atom. This method does not count ruthenium atoms that are at the surface but are inactive in the methanation reaction. Since using this procedure to measure the number of surface sites does not involve an assumption of either the mode of bonding of the carbon to the surface or of the surface area of a typical ruthenium atom, it is believed to be more accurate than previously mentioned methods that involve one or both of these assumptions.

The structure of the thin film was studied using electron diffraction techniques. A sample of the thin film was removed from the glass by treatment with 20% hydrofluoric acid. After about 1 minute in the

acid solution the film peeled off the glass and floated to the top of the solution. The film was mounted on an electron microscope grid and placed in a Hitachi electron microscope (model HU125). An electron diffraction pattern was obtained of the thin film. This is shown in Figure 8(a). The pattern is a series of concentric circles made up of diffraction spots. An electron micrograph of the film is shown in Figure 8(b). The micrograph was taken at a magnification of x38,000. The picture indicates a grainy nature to the catalyst. Each little spot is a crystallite with a maximum diameter of about 500 Å. Each crystallite diffracts as a single crystal producing a series of diffracted electron beams. Since these beams interfere both constructively and destructively the pattern shown in Figure 8(a) results with regions of high intensity and regions of low intensity. The analysis indicates that this film, which was used in all the kinetic studies to be discussed, consisted of a very large number of small single crystal planes interconnected by grain boundaries. This suggests that certain areas are fairly smooth while the interconnecting grain boundary areas are quite likely very rough. The fact that the film had a quite stable and reproducible activity for many months indicates that it was well-sintered. Frequently, the crystallites of well-sintered films are the low index (fairly smooth) planes of the crystal.

The thickness of the film was approximated using the theory of evaporation rates. The rate of evaporation in number of ruthenium atoms per square centimeter per second (γ) can be expressed in the

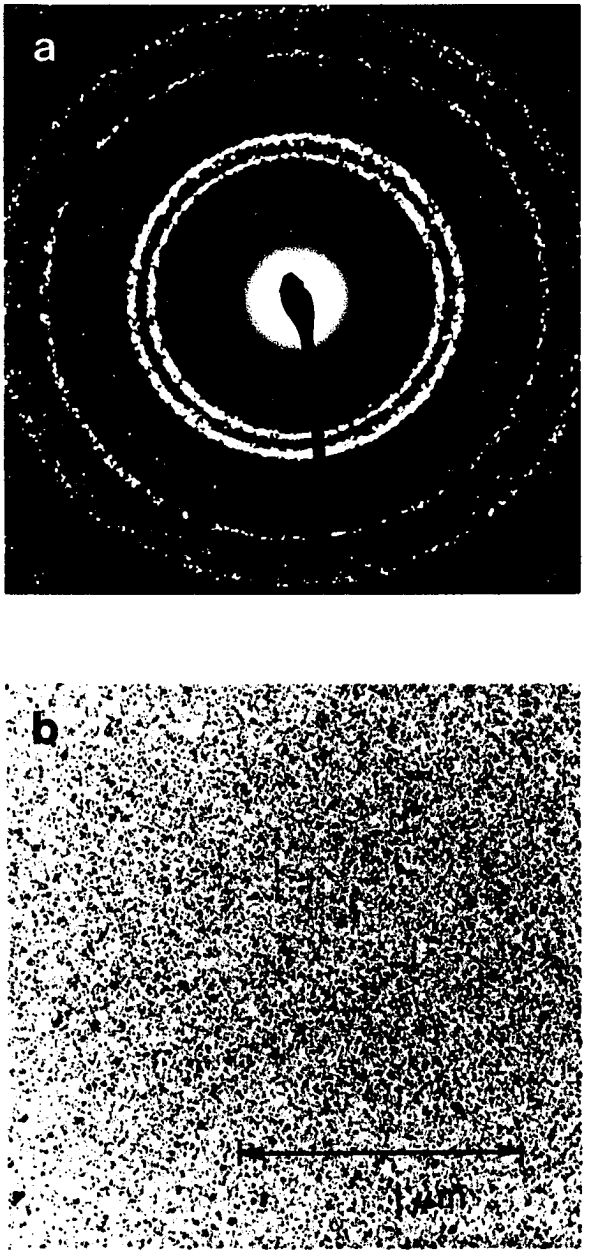

Figure 8. Electron microscope analysis of the ruthenium thin film: (a) electron diffraction pattern, (b) electron micrograph taken at a magnification of x38,000.

following manner [58]:

$$\log \gamma = 32.41 - 0.5 \log T - \frac{33800}{T} \qquad (78)$$

Since the film was deposited at 2223K over a period of 3 hours from a ruthenium sample of 1 cm^2 it is evident that 3.68×10^{19} atoms (2.69×10^{-3} grams) of ruthenium were evaporated. Using a ruthenium bulk density of 12.30 g/cm^3 [79] and assuming that the film was deposited evenly over the approximately 250 cm^2 of interior surface area of the pyrex bulb a film thickness of 87 Å is obtained.

Surface Characterization Studies

A series of Auger experiments was performed in an effort to characterize the state of the catalyst surface before, during and after methanation had occurred. Interpretation of these experiments required a method for converting Auger intensity data into amounts of carbon and oxygen present on the ruthenium sample. The principal peaks in the ruthenium Auger spectrum occur at 150 eV, 200 eV, 231 eV and 273 eV. The oxygen spectrum has peaks at 468 eV, 483 eV and 503 eV. This suggests that there should be no problem determining the amount of oxygen present in a ruthenium sample from Auger results. Carbon, however, is more difficult to measure. The only peak in the carbon Auger spectrum is at 272 eV. This overlaps the major ruthenium peak and complicates the analysis. It should be noted that the ruthenium peak is a fairly symmetric peak whereas almost all of the carbon peak lies below the baseline. Therefore, it would be expected

that as carbon is deposited on a ruthenium surface the asymmetry of the 273 eV peak would increase. In this study the change in the symmetry of the 273 eV peak was used to estimate qualitatively the amount of carbon present on the ruthenium sample. The ratio, Q, of the intensity above the baseline to that below the baseline was used as a measure of the amount of carbon present in the sample. Spectra of clean ruthenium taken from the literature yield Q values of approximately 0.75 to 0.80. Lower Q values suggest increased amounts of carbon associated with the sample. All Auger transition energies are from a book by Davis, et al. [80].

After loading the ruthenium sample the system was baked at 523K. The ruthenium disc was then outgassed at 1373K for 72 hours and cooled to room temperature. The Auger spectrum shown in Figure 9(a) was taken at this point. The sample was fairly dirty. The peak at 117 eV indicates the presence of phosphorus. The peak at 150 eV is due to both ruthenium and sulfur. Ruthenium is responsible for the peaks at 178 eV, 200 eV and 230 eV. The 274 eV peak indicates that there is some carbon on the ruthenium sample. In this instance Q = 0.61, indicating a fairly large carbon contamination. The peak at 510 eV is due to oxygen. The carbon and sulfur are common impurities in ruthenium samples.

Several cleaning procedures exist for ruthenium. One begins with an argon ion bombardment and follows with a hydrogen treatment and a high temperature (1500K) flash [81]. Others omit the argon bombardment and use an oxygen treatment followed by a high temperature flash

[82-86]. The sample used in this work was bombarded with argon ions (5 minutes, 1 ma, 2.3 keV). This treatment removed the phosphorus, sulfur and most of the oxygen as shown in Figure 9(b). The carbon contamination was still quite bad, Q = 0.59. An oxygen dose of $1x10^{-6}$ torr for 300 seconds at 783K was followed by a hydrogen dose of $3x10^{-6}$ torr for 300 seconds at the same temperature. The Auger spectrum shown in Figure 9(c) demonstrates that the sample was clean after this treatment. This spectrum is qualitatively identical to that reported for ruthenium in several recent studies [86-89]. This cleaning procedure is similar to several of the methods reported by other groups. In general an initial argon ion bombardment removes most of the impurities with the exception of carbon. This is quite likely the result of a relatively high carbon impurity in the bulk. Since the carbon is dispersed throughout the sample removal of a few surface layers does not clean the sample. A mild oxygen treatment is generally quite effective in removing the surface carbon. A hydrogen treatment is then used to reduce the sample. An exception to the carbon reactivity towards oxygen has been reported by Grant and Haas [87]. They observed that the carbon contaminant in their Ru (0001) single crystal was unreactive to an oxygen dose ($1x10^{-7}$ torr at 1273K for 30 minutes). Subsequent studies indicated that this carbon was in the form of graphite. The reactivity of the carbon to the oxygen dose in the present study suggests that the carbon is probably not graphitic in nature. During a series of experiments in which carbon monoxide was dosed onto the clean sample, it was discovered that the carbon could be

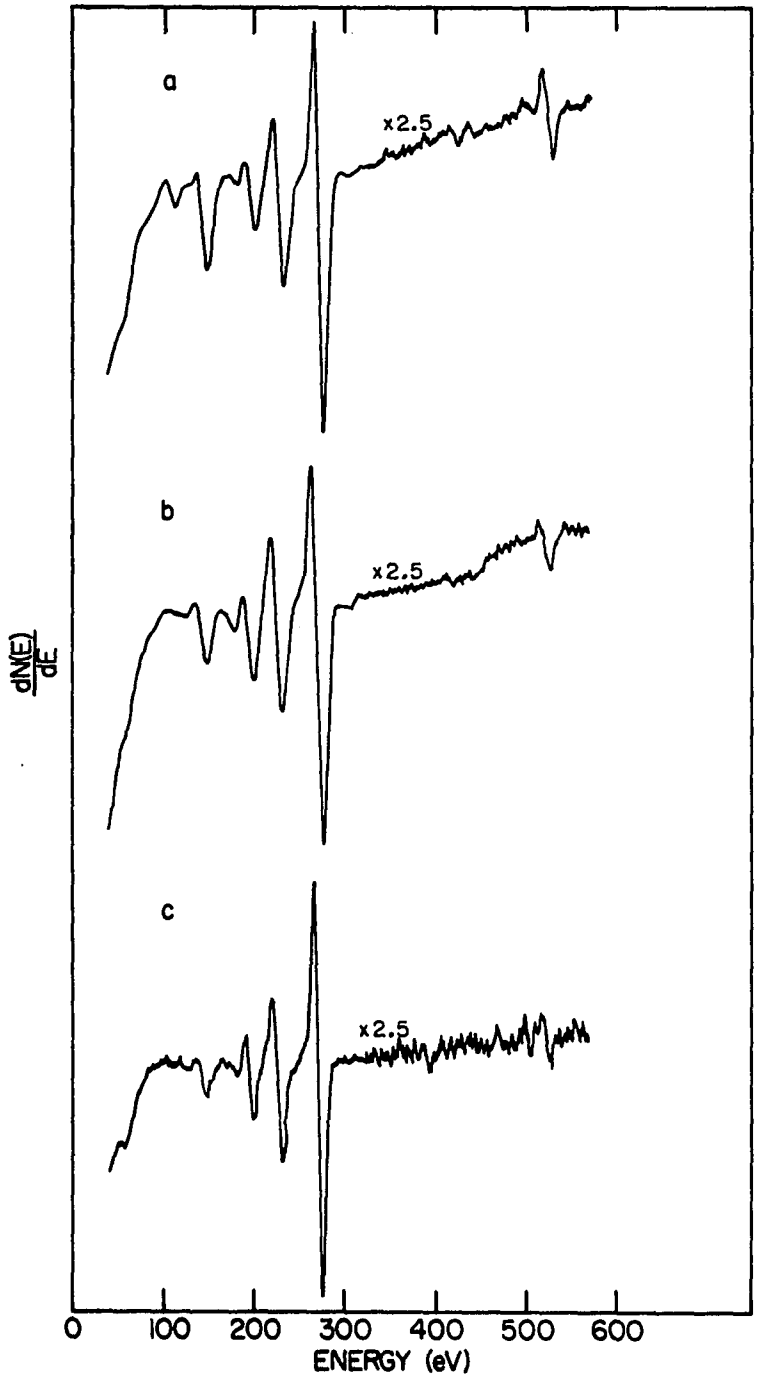

Figure 9. The sequential preparation of a clean ruthenium sample: (a) after heating at 1373K for 72 hours, (b) after argon ion bombardment, (c) after oxygen and hydrogen treatment.

removed by flashing the sample to 1373K. Prolonged treatment at this temperature would result in the diffusion of sulfur and phosphorus from the bulk necessitating the more rigorous cleaning procedure outlined above. Most experiments resulted in the deposition of some sort of carbonaceous intermediate without any associated oxygen. Indeed, the carbon monoxide disproportionation reaction (6) deposited a monolayer of carbon atoms. This carbon could be removed by flashing. It is believed that the carbon merely diffused into the bulk.

Since the cleaning procedure suggested that diffusion of carbon into and possibly out of the bulk could occur, it had to be established that these processes do not occur at 573K during the time frame in which experiments were performed. To establish that diffusion from the bulk did not occur at 573K the crystal was cleaned by flashing to 1373K and cooled to 573K. The change in the carbon coverage, ΔQ, was measured as a function of time beginning when the sample cooled to 573K. The results are shown in Table 4 in which $\Delta Q = Q_t - Q_{t=0}$:

Table 4. Carbon coverage as a function of time on a clean ruthenium sample

time (min.)	ΔQ
5	0.00
15	0.01
20	0.01
42	0.00

These results establish conclusively that no diffusion of bulk carbon to the surface occurs in a 42 minute period with the catalyst at 573K.

A similar study was performed in which the diffusion of carbon from the surface into the bulk was monitored as a function of time at 573K. A 175 μ carbon monoxide dose was made and the disproportionation reaction proceeded for about 5 minutes building up a monolayer of surface carbon. Once again, ΔQ was monitored as a function of time after the background carbon monoxide was evacuated. The results are shown in Table 5:

Table 5. Carbon coverage as a function of time on a carbon covered ruthenium sample

time (min.)	ΔQ
1	0.00
10	0.00
20	0.00

No diffusion of the surface carbon occurred after the gas phase carbon monoxide was removed. It is quite possible, however, that some carbon did diffuse into the subsurface bulk when the surface carbon deposition began. The equilibrium between surface and subsurface bulk carbon is apparently established rapidly compared to the length of time required to do an experiment (several minutes).

In an effort to understand more about the state of the catalyst surface during and after methanation the following study was made. Experiments were conducted to determine if a carbonaceous material is left on the surface of the ruthenium catalyst after the methanation reaction has occurred. If so, an understanding of the reactivity of this material toward the "standard hydrogen dose" (3.5 torr) could yield

information concerning the structure of the active sites of the catalyst. Recall that the normal sequence of steps in a kinetic run was to dose carbon monoxide and hydrogen and monitor the methane production. This gas mixture was then pumped out and followed by a hydrogen dose (3.5 torr) to regenerate the reactive surface and remove any reactive carbonaceous material left from the previous run.

Figure 10(a) shows the Auger spectrum of the clean ruthenium catalyst (Q = 0.80). Note that a small oxygen impurity is evident. This oxygen could be removed as was established earlier. However, it reappeared rather quickly when the sample was maintained at 573K. The oxygen reached the level shown in Figure 10(a) in a time frame that was short relative to the length of time required to measure the surface species present after a methanation run. It then remained at this level for long periods of time, being unreactive to any gas used in this study. All experiments were therefore conducted on a surface that had a constant oxygen contaminant. By conducting the experiments in this manner changes in the surface oxygen coverage caused by the reaction could be unambiguously measured. It is believed that this background oxygen is due to a relatively small amount of bulk oxygen. Previous work done in this group on an identical ruthenium sample indicated that the oxygen could be totally removed only after cycling the cleaning procedure for 2 to 3 months [90]. The fact that this oxygen reaches a rapid equilibrium and does not increase upon exposure to the background gases suggests strongly that the adsorption of gas phase oxygen or carbon monoxide is not the source.

The sample was exposed to 138 μm of carbon monoxide and 8.63 torr of hydrogen at 573K and the methanation reaction occurred. After 300 seconds the ambient gases were evacuated and the spectrum shown in Figure 10(b) was taken. At this point Q = 0.62 indicating the presence of a fairly large amount of carbon on the catalyst surface. Of course the structure of this carbon cannot be deduced directly from these data. The sample was then exposed to 3.5 torr of hydrogen at 573K for 300 seconds and the hydrogen was then evacuated. The Auger spectrum shown in Figure 10(c) was obtained with Q = 0.70. This increase in Q suggests that some of the carbon was removed by the hydrogen treatment. Flashing to 1373K regenerated the clean spectrum with Q = 0.80 as shown in Figure 10(d). These results suggest that there are two types of carbon associated with the catalyst. One type is rapidly removed by hydrogen treatment and the other type remains behind, being unreactive toward hydrogen in the time period of the exposure.

To demonstrate that this second type of carbon is indeed different from the first in reactivity and did not remain behind merely because the reaction was quenched when the hydrogen was pumped out after 300 seconds the following experiment was performed. The catalyst was exposed to the same carbon monoxide-hydrogen dose (138 μ of carbon monoxide and 8.63 torr of hydrogen). This was followed by a series of cleaning hydrogen doses without flashing the sample until the end of the study. The results are summarized in Table 6 (t = 0 corresponds to the first addition of hydrogen). Hydrogen was present at all times after the reactant gases were pumped out except while running spectra.

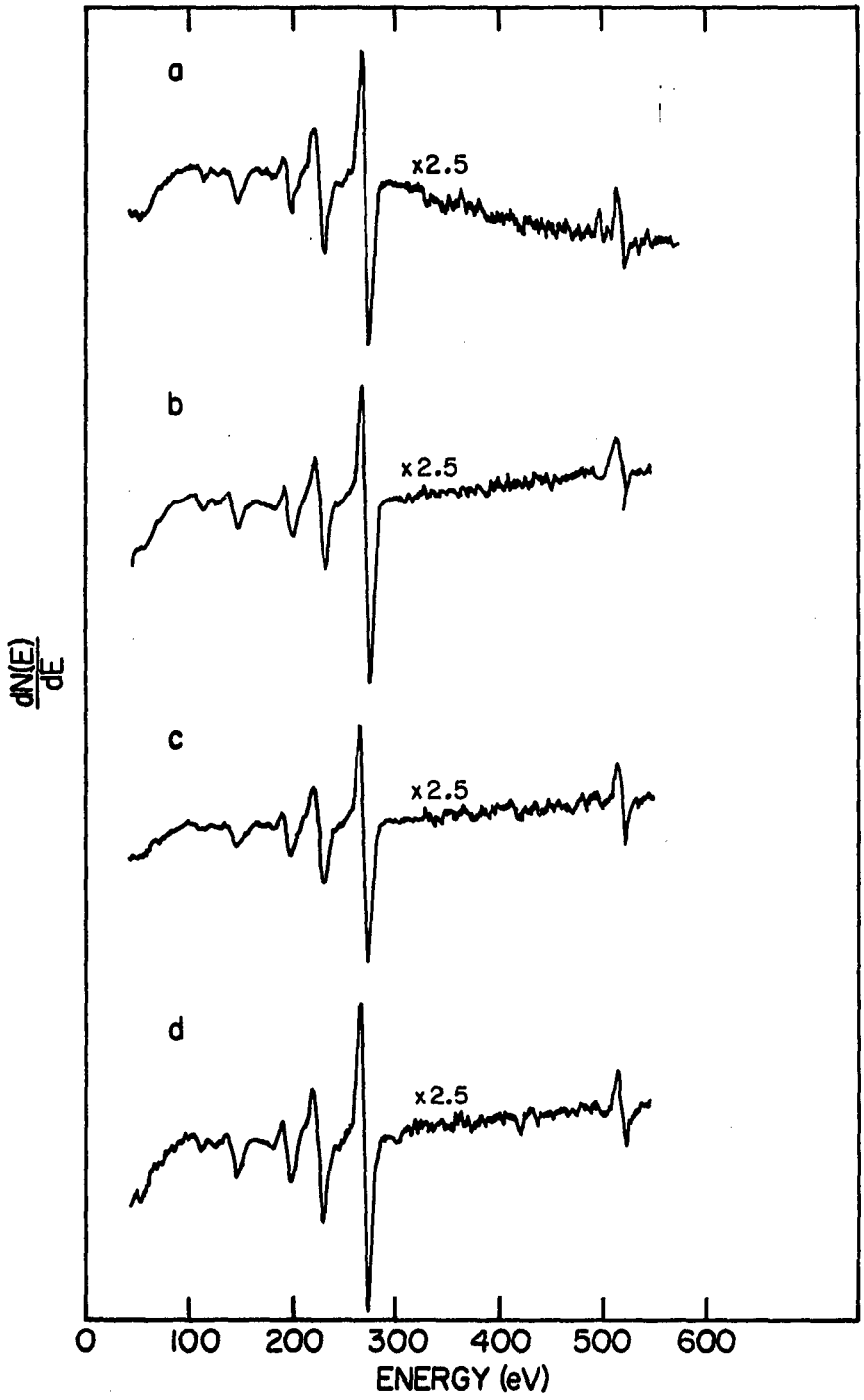

Figure 10. Auger characterization of the catalyst before and after methanation: (a) clean ruthenium sample, (b) after carbon monoxide-hydrogen dose, (c) after "standard hydrogen dose", (d) clean sample obtained by flashing to 1373K.

Table 6. Carbon coverage as a function of hydrogen exposure

Catalyst Condition	Q
clean ruthenium	0.79
after methanation ($138\ \mu$ CO-8.63 torr H_2)	0.61
standard hydrogen dose	
t = 0	0.61
t = 400 s	0.71
t = 1145 s	0.70
t = 2680 s	0.70
t = 13 hrs	0.75
flash	0.79

The noteworthy thing in this data set is the fact that the amount of carbon removed at 400 seconds is the same as the amount removed at 2680 seconds. This demonstrates that there is a less reactive carbon species associated with the catalyst in addition to the reactive carbonaceous methanation intermediate. After 13 hours in 3.5 torr of hydrogen at 573K, only half of the unreactive carbon had been removed. Flashing to 1373K immediately restored the clean ruthenium sample.

One additional point should be made concerning the data presented thus far. When the carbon monoxide-hydrogen dose was made and the Auger spectrum was run, no change in the oxygen peak was detected. This is a very interesting observation and will be discussed in more detail below.

An experiment was performed in which carbon monoxide and hydrogen were dosed onto the sample at 573K under reaction conditions with the $CO:H_2$ ratio being increased steadily to see if the quantity of carbonaceous material on the surface was affected by the pressure of carbon

monoxide in the dose. The results are summarized in Table 7 ($\Delta Q = Q_{clean} - Q_{carbon\ covered}$):

Table 7. Variation in carbon coverage as a function of the $CO:H_2$ ratio

CO (μ)	H_2 (torr)	ΔQ
154	8.82	0.15
154	8.82	0.17
516	8.92	0.18
1270	8.84	0.16
1790	8.81	0.15

As can be seen, the values of ΔQ do not vary in a systematic manner. The average of the ΔQ values is 0.16. All values are within ±10% of this value. This suggests that the $CO:H_2$ ratio can be varied by an order of magnitude without changing the amount of carbon present on the surface. This is a very interesting and somewhat surprising result. One would expect that an increase in the carbon monoxide gas phase concentration by an order of magnitude would favor adsorption of more carbon on the catalyst surface. These Auger results do not support this idea. Catalyst fouling has been observed to occur on industrial type catalysts at $CO:H_2$ ratios of 1:3 and at very high pressures relative to those in this study (100 atm.). Quite likely, the large excess of hydrogen always present in this study interferes with the formation of the carbonaceous material responsible for catalyst fouling. The concentration of adsorbed hydrogen must be high enough to prevent the interaction of neighboring adsorbed carbon species to form higher molecular weight materials. An interaction of this sort might produce either graphite

or some very high molecular weight wax-like material which does not desorb from the catalyst surface under reaction conditions and could explain the observed decline in rate with time.

As has been pointed out, one interesting feature of all the Auger spectra presented thus far is the stability of the oxygen peak. Table 8 reports the oxygen associated with the catalyst during the various steps of a methanation study:

Table 8. Oxygen peak intensity at various stages of a methanation study

Catalyst Condition	Oxygen Intensity
clean	31 (Fig. 10(a))
methanation dose	30 (Fig. 10(b))
standard hydrogen dose	29 (Fig. 10(c))
flashed (clean)	29 (Fig. 10(d))

The oxygen intensity remained unchanged throughout the methanation cycle. This suggests that even though carbon monoxide and hydrogen are dosed onto the catalyst, the surface concentrations of all species which contain oxygen must be negligible relative to the total concentrations of the species containing only carbon and hydrogen. These oxygen containing intermediates must be very reactive with the rate limiting step occurring after removal of the oxygen from the carbon and quite likely involving the hydrogenation of the carbon containing intermediate.

Two pathways are available for the conversion of adsorbed carbon monoxide into methane and water. One route involves the hydrogenation

of the carbon monoxide molecule to produce adsorbed alcohol type intermediates. The other process would involve the immediate dissociation of the carbon monoxide to yield adsorbed carbon and adsorbed oxygen, each of which is hydrogenated to the reaction products. An experiment was performed in an effort to develop an understanding of the ruthenium-oxygen interaction and to learn something about the reactivity of adsorbed oxygen. The results of this study are presented in Figure 11. Figure 11(a) is the Auger spectrum of the clean sample. Some residual oxygen which could not be removed by flashing to 1375K was present. A 138 μm oxygen dose was made with the catalyst at 573K. The dose lasted for 300 seconds. Figure 11(b) is the Auger spectrum which resulted after the oxygen dose. As can be seen, a huge oxygen peak is present. Note that in this case the oxygen and ruthenium peaks were measured on the same sensitivity scale. This was followed by an 8.9 torr hydrogen dose (reaction conditions). As can be seen from Figure 11(c), all of the adsorbed oxygen was removed by the 300 second hydrogen dose and the clean spectrum resulted.

This demonstrates clearly that two types of oxygen are associated with the ruthenium catalyst. The bulk oxygen is very unreactive and is not affected by any of the experiments performed except the initial cleaning step. The adsorbed oxygen atoms from the above study were shown to be extremely reactive when exposed to the same pressure of hydrogen used in some of the methanation studies.

It is difficult to quantify the amount of oxygen that adsorbed in terms of a fractional coverage of oxygen. A common practice is to

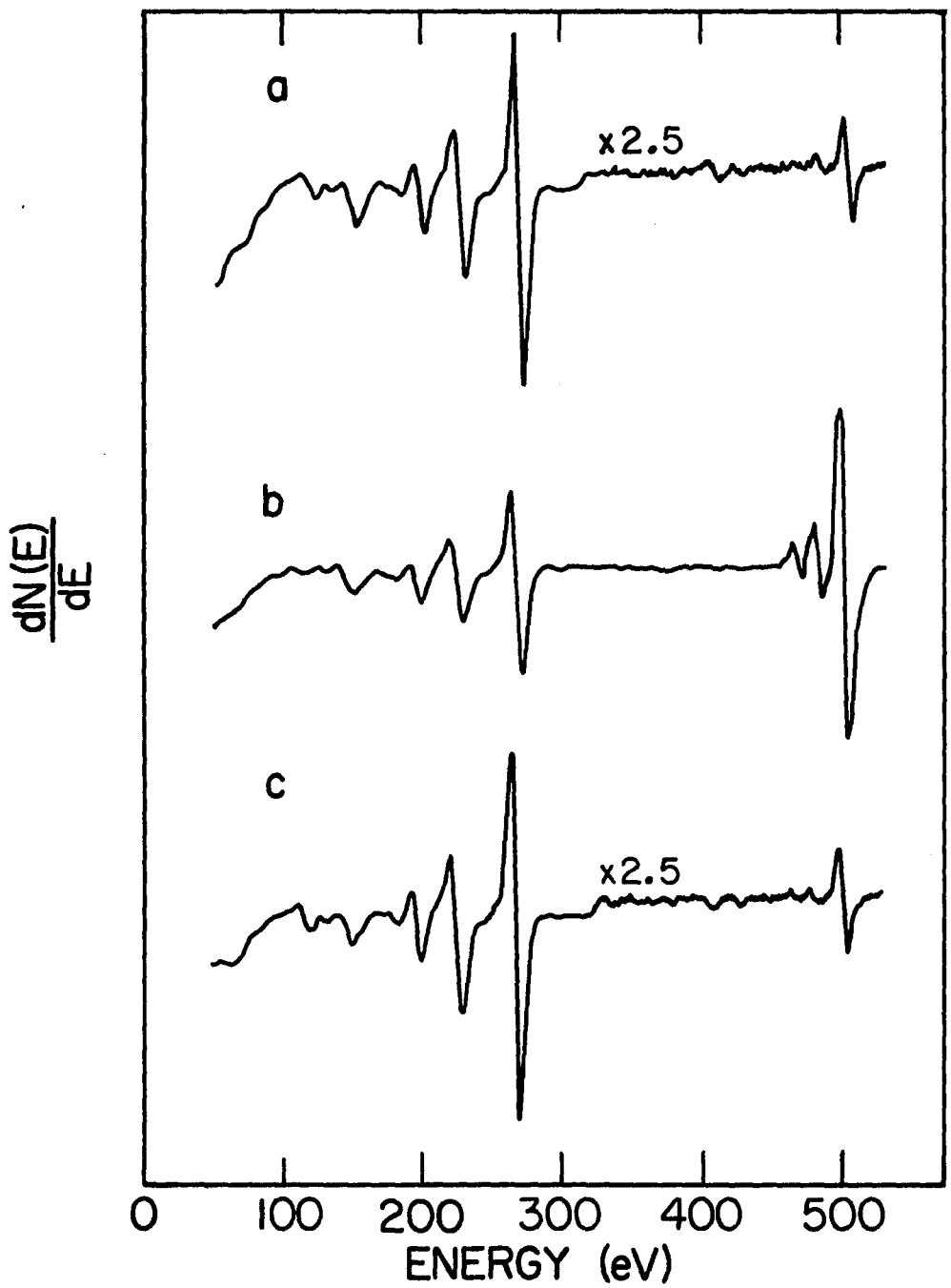

Figure 11. Oxygen adsorption study on ruthenium: (a) clean sample, (b) after 138 μm O_2 dose (300 s, 573K), (c) after 8.9 torr H_2 dose (300 s, 573K).

use a single crystal of ruthenium and quantify the amount of adsorbed oxygen by correlating LEED structures which are indicative of oxygen coverage with Auger intensities. By assuming that the relationship between Auger intensity and oxygen coverage is linear, coverage values can be assigned to any Auger intensity. Since the sample used in this study was not a single crystal, a direct LEED-Auger correlation could not be made. Previous studies using a ruthenium $(10\bar{1}0)$ single crystal demonstrated that a 2x1 structure resulted from a 10 Langmuir oxygen dose at 423K [91]. A series of oxygen doses were made on the polycrystalline sample. This is shown in Figure 12. If it is assumed that a 10 Langmuir dose yields a coverage of 0.5 then the correlation between Auger intensity and oxygen coverage is established (0.5 monolayer = 44 units of intensity). The results of this intensity-coverage study suggest that the previous oxygen dose of 4.1×10^7 Langmuirs produced an oxygen coverage of roughly 2 monolayers. This oxygen could easily be accommodated through multiple adatom adsorption. It is also possible that some could diffuse into the subsurface bulk. If this is the case then removal of this subsurface oxygen by hydrogen is a rapid process.

The noteworthy thing as far as this study is concerned is that adsorbed oxygen atoms are very reactive to hydrogen at 573K. If the mechanism of the methanation reaction involved dissociation of adsorbed carbon monoxide one would expect to see essentially no oxygen on the surface under reaction conditions.

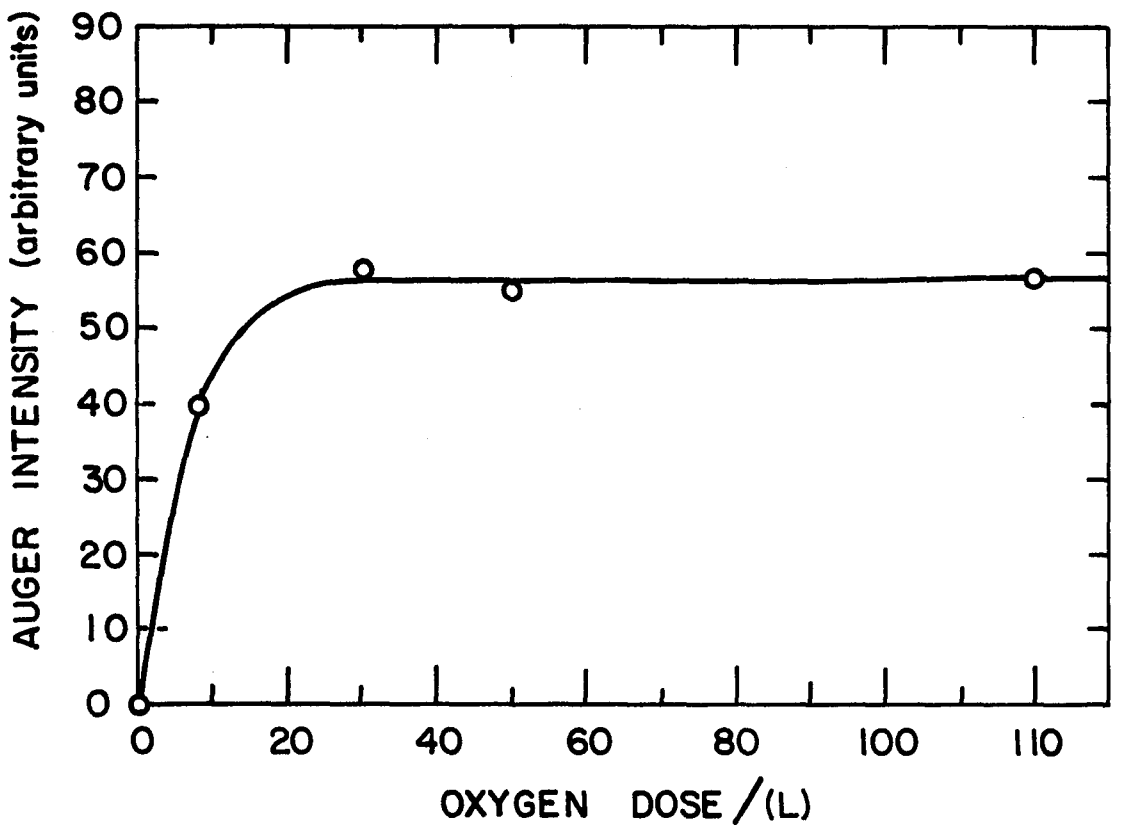

Figure 12. Auger intensity versus oxygen dose (coverage) correlation diagram for a polycrystalline ruthenium sample

The carbon monoxide disproportionation reaction was allowed to proceed on the clean ruthenium sample. Figure 13(a) shows the Auger spectrum of the clean catalyst and Figure 13(b) shows the spectrum that resulted after dosing the catalyst with 250 μm of carbon monoxide for 300 seconds at 573K. As expected the carbon intensity increased (ΔQ = 0.1) while the oxygen peak changed negligibly. An experiment was performed to enable a comparison of the Auger results of this high pressure carbon monoxide dose to those of a low pressure carbon monoxide dose. A 1×10^{-6} torr carbon monoxide dose was made at 573K for 300 seconds. No change in the carbon and oxygen peaks was detectable. Flash desorption results of Kraemer and Menzel [83] suggest that carbon monoxide is completely removed from a ruthenium field emitter tip upon heating to 500K. Other LEED/Auger studies suggest no interaction between carbon monoxide and ruthenium at low pressures (10^{-6} torr range) and elevated temperatures (473K or greater) [92]. The temperature of the crystal was lowered to 373K and the experiment was repeated. Figure 14(a) shows the clean ruthenium Auger spectrum and Figure 14(b) shows the spectrum that resulted from the light carbon monoxide dose at 373K. Small increases in both the carbon and oxygen peaks were detected. This suggests that some carbon monoxide has adsorbed but apparently the interaction is very weak since the coverage is so low. It is interesting to note that this carbon monoxide dose was followed by a 3.5 torr hydrogen dose and the clean surface was restored. No flash to 1373K was required to remove the adsorbed carbon.

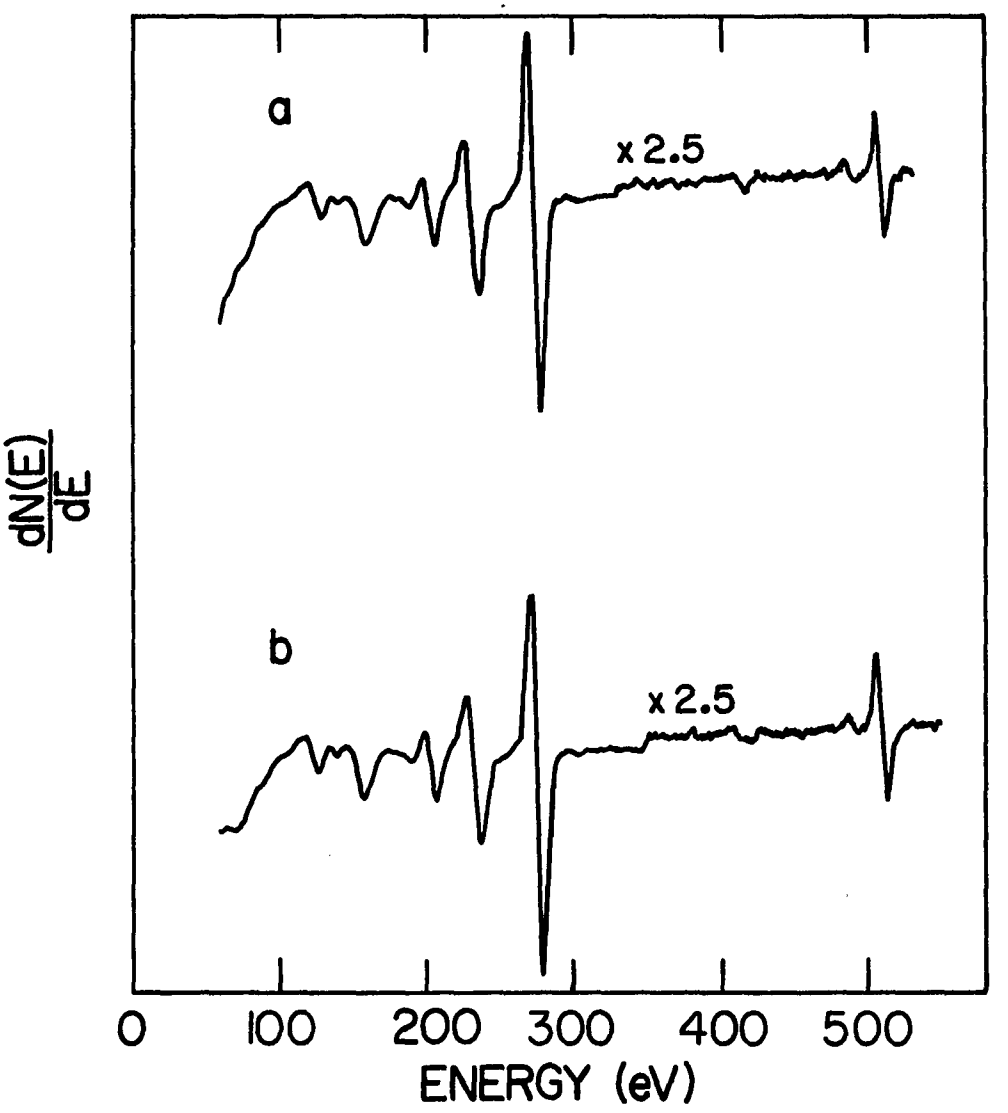

Figure 13. Interaction of a heavy carbon monoxide dose with the ruthenium sample: (a) clean ruthenium sample, (b) after carbon monoxide exposure (250 μm, 300 s, 573K).

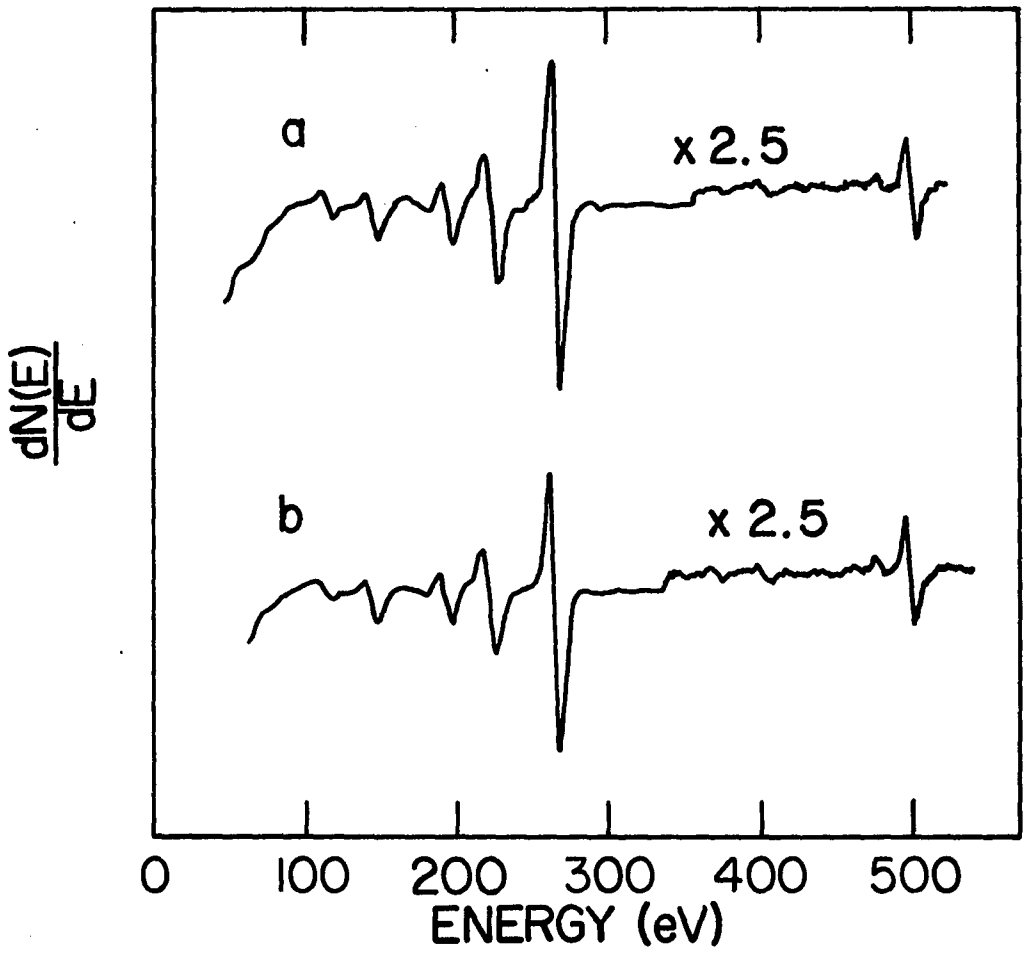

Figure 14. Interaction of a light carbon monoxide dose with the ruthenium sample: (a) clean ruthenium sample, (b) after carbon monoxide exposure (1×10^{-6} torr, 300 s, 573K).

A mixture of carbon monoxide and hydrogen at a 1:3 ratio was dosed to a pressure of $1x10^{-6}$ torr for 300 seconds at 573K. Figure 15(a) shows the clean spectrum and Figure 15(b) shows that carbon was adsorbed (ΔQ = 0.08) but no oxygen adsorption was detected. This suggests that carbon monoxide adsorption (based upon the amount of carbon on the surface) is greater when a carbon monoxide-hydrogen mixture at $1x10^{-6}$ torr is dosed than when carbon monoxide alone at $1x10^{-6}$ torr is dosed.

One final Auger study was made to monitor the amount of carbon and oxygen on the catalyst surface as a function of time at constant carbon monoxide and hydrogen pressures. A mixture of 138 μ of carbon monoxide and 9.1 torr hydrogen was dosed onto the sample for different exposure times (175 to 500 s). The amount of carbon present remained constant. The change in the oxygen peak was once again zero.

The ruthenium sample was removed from the Auger unit and transferred to an AEI XPS spectrometer. The purpose of the XPS work was to characterize the carbon which was associated with the sample after exposure to carbon monoxide and hydrogen under reaction conditions. The ruthenium $3d_{3/2}$ (284 eV) and $3d_{5/2}$ (280 eV [93]) electrons were analyzed. The carbon XPS peak occurs at 284.3 eV for atomic carbon. This overlaps the ruthenium $3d_{3/2}$ peak. Since ruthenium forms carbides only under rather rigorous conditions [94], no known ruthenium carbide spectrum has been run. However, several bulk carbides have been studied: HfC (281 eV), TiC (281.7 eV) and WC (282.9 eV). In all cases the carbon peak is shifted to lower binding energies in the metal carbide structure. A clean spectrum taken of the sample prior to catalytic treatment is shown

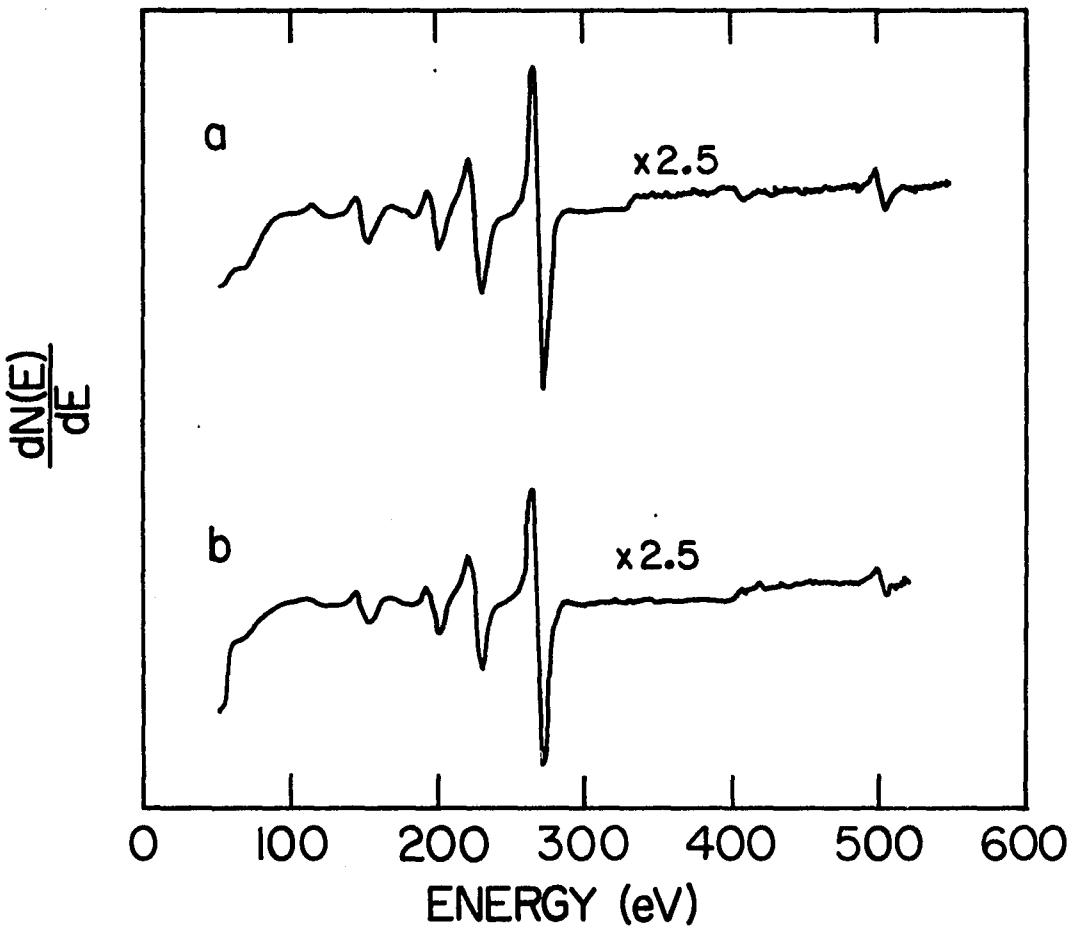

Figure 15. Interaction of carbon monoxide-hydrogen mixtures with ruthenium: (a) clean ruthenium sample, (b) after exposure a 1×10^{-6} torr $CO:H_2$ mixture for 300 s at 573K ($CO:H_2 = 1:3$).

in Figure 16(a). As can be seen the higher energy ruthenium-carbon peak is about two-thirds as intense as the lower energy peak. Shown in Figure 16(b) is the spectrum that resulted when the catalytically treated (138 μm of carbon monoxide, 8.63 torr of hydrogen, 573K, 300 s). sample was put into the XPS system. The higher energy peak is much too intense to be due to ruthenium alone. Some sort of surface carbon is also present. A light argon etch (4 minutes, 5 μ , 0.5 v) removed some of the carbon as shown in Figure 16(c). A repeat of this light etch removed more carbon and yielded the spectrum shown in Figure 10(d). These results indicate that neither the surface carbon (before etch) nor the subsurface bulk carbon (after 2 etches) was bonded in a manner analogous to the ruthenium carbide structure. All XPS energies reported are, unless otherwise noted, from a book by Carlson [95].

After all of the kinetic studies were completed an XPS analysis of the thin film was made. The film had been stored in hydrogen for about six weeks prior to its removal from the vacuum system. A glove bag was placed around the glass bulb prior to its removal. In an effort to prevent air contamination of the film it was constantly flushed with helium until it was loaded into the ESCA system. A small oxygen impurity was present which was almost completely removed by a very light argon ion etch. This oxygen quite likely diffused into the glove bag while the film was being transferred from the kinetic system to the ESCA unit. Essentially no carbon was detected. This is not too surprising since the film had been stored in hydrogen for such a long period of time. This suggests that even at room temperature the reduction of any surface

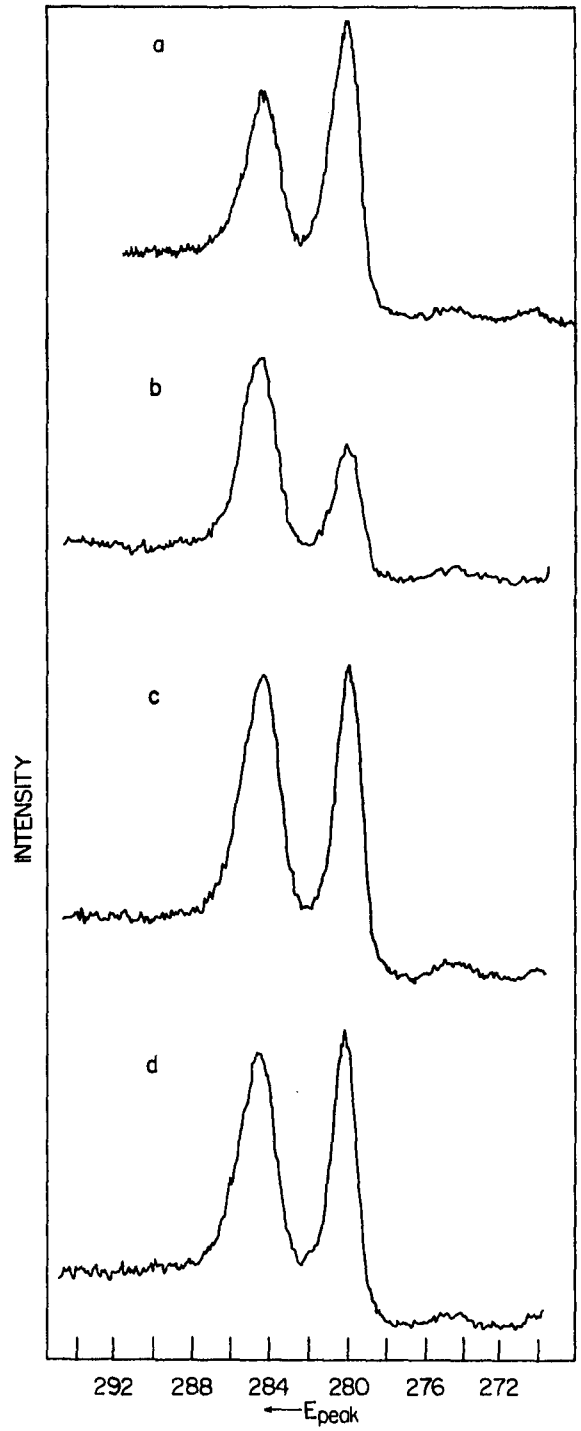

Figure 16. XPS analysis of ruthenium sample before and after methanation: (a) clean sample, (b) after methanation (138 μm CO, 8.63 torr H_2, 573K, 300 s), (c) after argon etch, (d) after another argon etch.

carbon remaining from the last kinetic run had occurred. These results support the Auger results which suggest that the unreactive form of carbon (type 2) is somewhat reactive toward hydrogen and will eventually be removed from a used catalyst.

Some XPS studies were performed on some of the early ruthenium films that were used only once. An XPS analysis was made at the end of the collection of the kinetic data. The results were essentially the same as those presented in Figure 16. This clearly demonstrates that carbon was present on the used catalyst in fairly high concentrations. This suggests a direct correlation between the properties of the surfaces of the thin films used for the kinetic work and that of the polycrystalline disc used in the Auger work.

An attempt was made to use LEED to characterize the structure of the carbon remaining on the catalyst surface after methanation. A ruthenium $(10\bar{1}2)$ surface was used in this study. The atomic arrangement of the ruthenium atoms is shown in Figure 17. The unit cell is a rectangle defined by two adjacent atoms in the highest row and their counterparts in the next row of elevated atoms. Figure 18(a) shows the LEED pattern of the clean surface. The sample was maintained at 573K and exposed to 138 μm of carbon monoxide and 8.63 torr of hydrogen. The methanation reaction proceeded for 300 seconds and then the system was evacuated. The LEED pattern shown in Figure 18(b) resulted. An Auger analysis indicated the presence of carbon on the ruthenium surface ($\Delta Q = 0.1$). This second LEED pattern suggests a 2x1 structure for the carbon overlayer relative to the ruthenium unit cell. Figure 19 gives

Figure 17. The atomic arrangement of atoms in a ruthenium $(10\bar{1}2)$ surface.

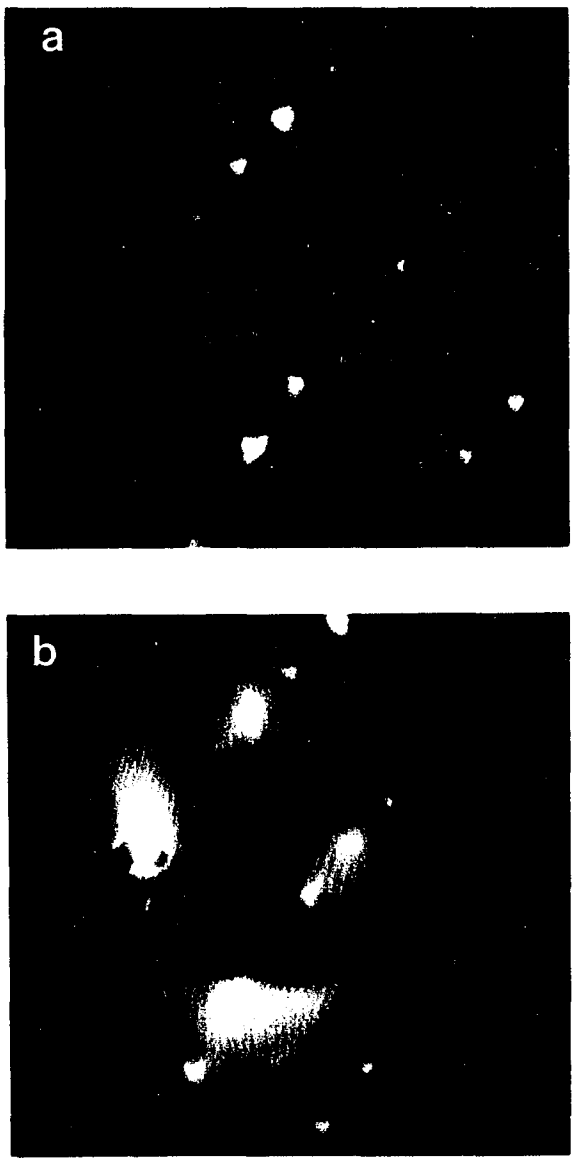

Figure 18. LEED study of the ruthenium $(10\bar{1}2)$ surface: (a) clean surface, (b) after methanation (138 μ CO, 8.63 torr H_2, 573K, 300 s).

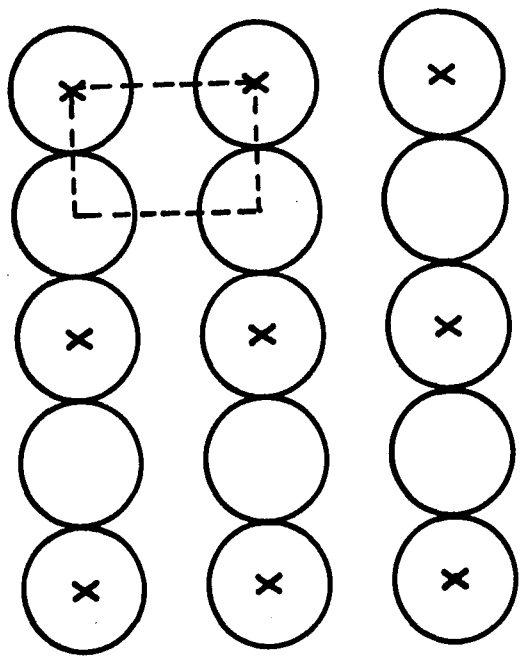

Figure 19. A representation of the ruthenium $(10\bar{1}2)$ surface using only the atoms in the elevated rows. Each X represents a possible site for adsorbed carbon based upon the LEED results. The rectangle defines the unit cell.

a representation of the ruthenium $(10\bar{1}2)$ surface using only the atoms in the elevated rows. Open circles represent ruthenium atoms and the dashed lines indicate the unit cell. Each adsorbed carbon structure is represented by an X. The positions of the carbon structures are only relative to the ruthenium atoms. The results presented here cannot distinguish between atoms adsorbed on top of the ruthenium rows or in bridge positions within the elevated rows. The carbon does not have to be associated with the elevated rows but could be associated with the atoms that make up the steps. The probable location of the carbon, as well as the mechanistic implications of these LEED results will be discussed later. The LEED pattern makes it evident, however, that the carbon is not graphitic. The only known report of graphite on ruthenium was made by Grant and Haas [87] on a ruthenium (0001) surface. The LEED pattern that resulted from their work demonstrated that rather than individual LEED spots they had a series of very closely spaced spots shaped like a hexagon. This was indicative of the symmetry of the graphite layer. It turns out that the (0001) plane of ruthenium is a very likely candidate for graphite overlayers since the position of the ruthenium atoms and the carbon atoms in the (0001) graphite basal plane coincide very well at every 9 ruthenium or 10 carbon meshes. Since the LEED pattern obtained from this work contained fairly sharp individual spots, a graphite overlayer is very unlikely.

Another LEED study was conducted in which the crystal was cleaned and then dosed with 138 μm of carbon monoxide and the disproportionation reaction occurred for 300 seconds. A LEED pattern was taken of this surface and a very diffuse 1x1 (unit cell) pattern resulted. This

suggests that the carbon overlayer was randomly dispersed on the catalyst surface. Auger analysis indicated a fairly heavy carbon deposit (ΔQ = 0.25).

ESCA Characterization of Ruthenium-Adsorbate Interaction

Several photoelectron spectroscopy studies have been performed which involve the interaction of carbon monoxide, oxygen, methanol and formaldehyde with ruthenium single crystals. Only one study is known in which XPS work was done on supported ruthenium [96]. These studies provide information which could be useful in predicting the bonding of various reaction intermediates in the methanation process. The following general conclusions have been drawn from the single crystal work. Oxygen dissociates and adsorbs atomically whereas carbon monoxide is believed to adsorb non-dissociatively via the carbon atom. At 80K methanol adsorbs non-dissociatively with the primary bonding involving the lone pair of electrons of the oxygen atom. Heating to T > 300K results in decomposition to primarily carbon monoxide and hydrogen [97]. At 80K formaldehyde is found to adsorb dissociatively [98]. The nature of the adsorbed species resulting from the dissociation of the formaldehyde at 80K remains unknown. It is known, however, that the complex is different than that obtained when hydrogen and carbon monoxide are coadsorbed on ruthenium. Flashing the formaldehyde surface complex yields carbon monoxide and hydrogen.

Some XPS experiments were performed in this study in which light doses of carbon monoxide, oxygen and methanol were made on the ruthenium

polycrystalline sample. Since this work had, in general, already been performed on single crystals the primary purpose of the study was to demonstrate that the polycrystalline Ru used in this study behaved similarly to the single crystals used in the other studies. This would provide a needed link between the polycrystalline work and the single crystal work and would help to demonstrate that the bonding to the surface in these two forms of catalyst is similar. All doses were in the 1 to 100 Langmuir range and were made with the sample at room temperature. Higher temperature doses (373K to 623K) were attempted but little or no adsorption was observed to occur. The results of this study are shown in Table 9:

Table 9. Binding energies (eV) of the O 1s level

Gas Dosed	Energy
O_2	529.8
CO	531.3
CH_3OH	531.3

These results are in excellent agreement with those of Kim and Winograd [93] and with those of Fuggle, et al. [81] who studied the ruthenium-oxygen-carbon monoxide system. In the latter study a difference of 1.8 eV was reported for the oxygen (1s) peak for adsorbed oxygen and adsorbed carbon monoxide. A difference of 1.5 eV was observed in this study. After dosing each gas and recording the XPS spectrum a light hydrogen dose was made and another XPS spectrum was recorded. No change in the spectrum occurred as a result of the hydrogen treatment. A good review

of the study of metal-adsorbate interactions using photoelectron spectroscopy has recently been published [99].

The Auger, ESCA and LEED results may be summarized as follows:

1) Neither diffusion of carbon into or out of the bulk occurs at a detectable rate at 573K.

2) A carbonaceous material is left on the surface after methanation. This material involves two types of carbon. Type 1 is reactive to the standard hydrogen dose after each run. Type 2 is relatively unreactive to hydrogen and can be removed only after 24-48 hours of hydrogen treatment (3.5 torr) at 573K. It diffuses into the bulk when the sample is flashed to 1373K.

3) No change in the oxygen surface concentration was observed during the course of a methanation study.

4) The quantity of carbonaceous material associated with the ruthenium did not vary as the carbon monoxide pressure was increased from 154 μm to 1790 μm with 8.8 torr of hydrogen.

5) Oxygen atoms adsorbed at 573K are very reactive toward hydrogen.

6) The carbon monoxide disproportionation reaction readily occurs with no surface oxygen being detected.

7) Light doses of carbon monoxide yield changes in both the carbon and oxygen Auger peaks.

8) No carbon buildup occurs if the methanation reaction is monitored as a function of time.

9) Flashing drives carbon into the bulk; argon ion bombardment exposes it.

10) XPS results confirm that no ruthenium carbides are formed.

11) Adsorbed oxygen is detected on the surface only in the absence of hydrogen.

12) LEED suggests that the carbon is not graphitic in nature.

13) XPS studies of the adsorption of carbon monoxide, oxygen and hydrogen on the polycrystalline ruthenium sample are in agreement with results obtained on single crystals.

Reaction Kinetics

The kinetics of the methanation reaction were studied over a wide pressure range. Most previous kinetic studies have been made over a fairly narrow range with a pressure variation of a factor of 2 or 3 with respect to both hydrogen and carbon monoxide. Although some general trends are evident, the results have in many cases been diverse and seemed contradictory. This study was performed over a 2 to 3 order of magnitude pressure range with respect to each reactant in an effort to demonstrate that the reaction follows Langmuir-Hinshelwood kinetics and to attempt to demonstrate that much of the existing data are not contradictory but were collected under such diverse conditions that different results were obtained.

Initial rates were measured throughout this work. The quantity of product never exceeded 25 μm in the time period in which the rate was measured. The data are presented in conventional ln R versus ln P plots. The slope of a data curve at any pressure represents the kinetic order of the reaction with respect to that reactant (or product) at the chosen pressure.

A typical carbon monoxide order plot is shown in Figure 20. This graph contains data taken on 4 different occasions over a period of several months. The data are unadjusted and reproduce well within a maximum scatter of about ±10%. It is evident that this curve has a shape that is indicative of a Langmuir-Hinshelwood interaction. The curve has, however, a very sharp maximum and can be easily approximated by two intersecting straight lines. The order of the reaction with

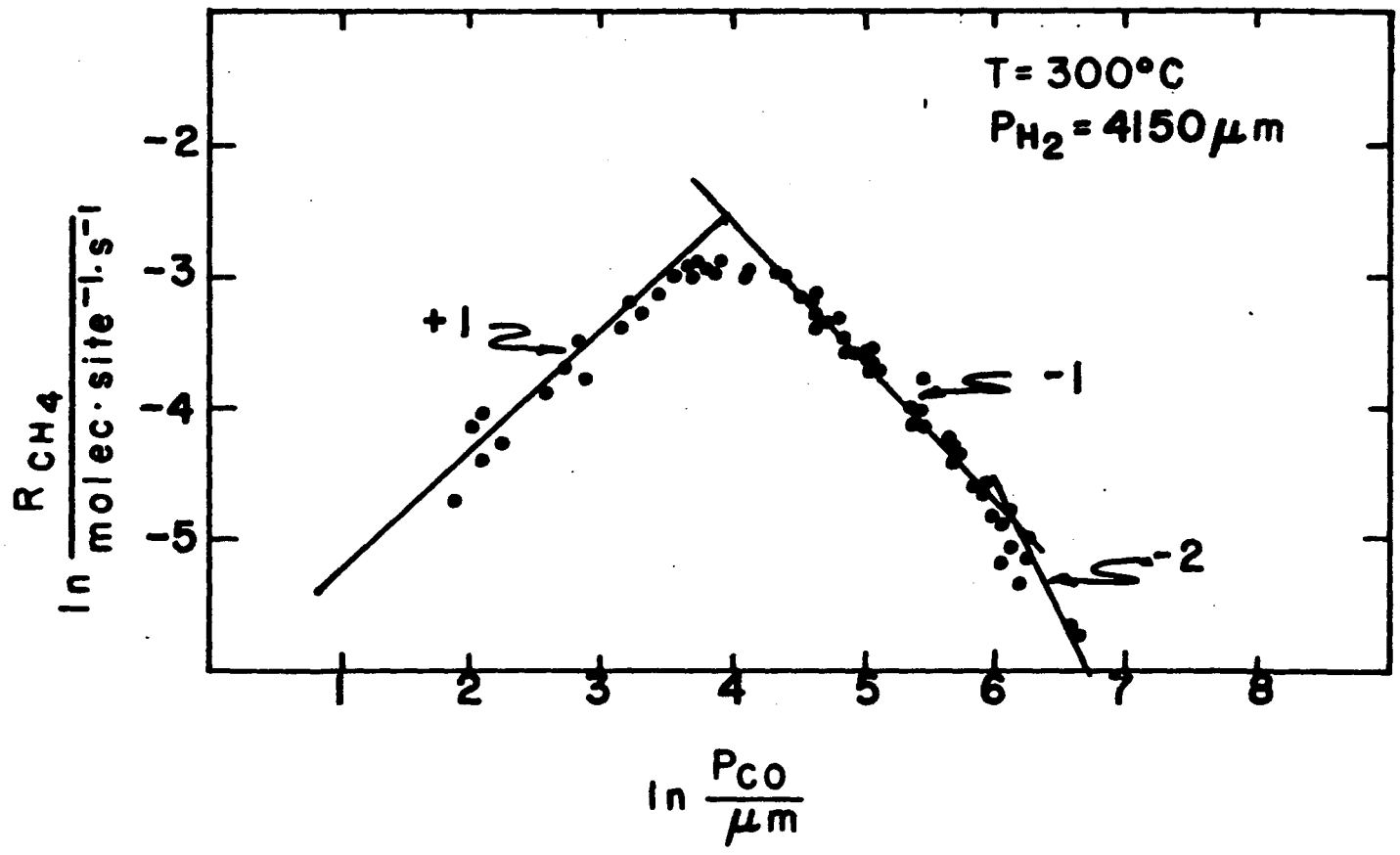

Figure 20. Order plot demonstrating that the carbon monoxide data can be roughly fit by straight lines. The order of the reaction with respect to carbon monoxide varies from +1 to -2.

respect to carbon monoxide is +1 at lower pressures and rather abruptly changes to -1 as the carbon monoxide pressure is increased. Data taken at the upper end of the carbon monoxide pressure range suggest that the kinetic order is more negative than -1 and may approach a value of -2. In general, kinetic orders for carbon monoxide from earlier studies are between -0.5 and -1.0.

A typical hydrogen order plot is shown in Figure 21. These data were collected on eleven different days over a period of 14 months. Like the carbon monoxide data, these results suggest that the hydrogen interacts in a fashion suggestive of Langmuir-Hinshelwood kinetics. This curve also has a very sharp maximum and can be represented by two intersecting straight lines. At lower hydrogen pressures the reaction order is +2. However, as the hydrogen pressure is increased, the reaction abruptly becomes -1 order in hydrogen. In general, earlier studies have yielded a hydrogen kinetic order in the range of +1 to +2. No report of a negative order in hydrogen has been found.

Figure 22 shows the results of two studies performed to get the reaction order with respect to methane. Both studies demonstrate clearly that the reaction is zero order in methane in the pressure range of 5 to 60 μm of methane. The study at the lower carbon monoxide pressure suggests that the reaction might become negative order in methane at pressures greater than 60 μm methane. The data in Figure 23 suggest that the reaction is zero order in water in the pressure range of 5 to 50 μm of water. At higher water pressures the reaction appears to become negative order in water. In the case of both methane and water, however, the negative order dependencies never exceed -0.06 in the pressure ranges

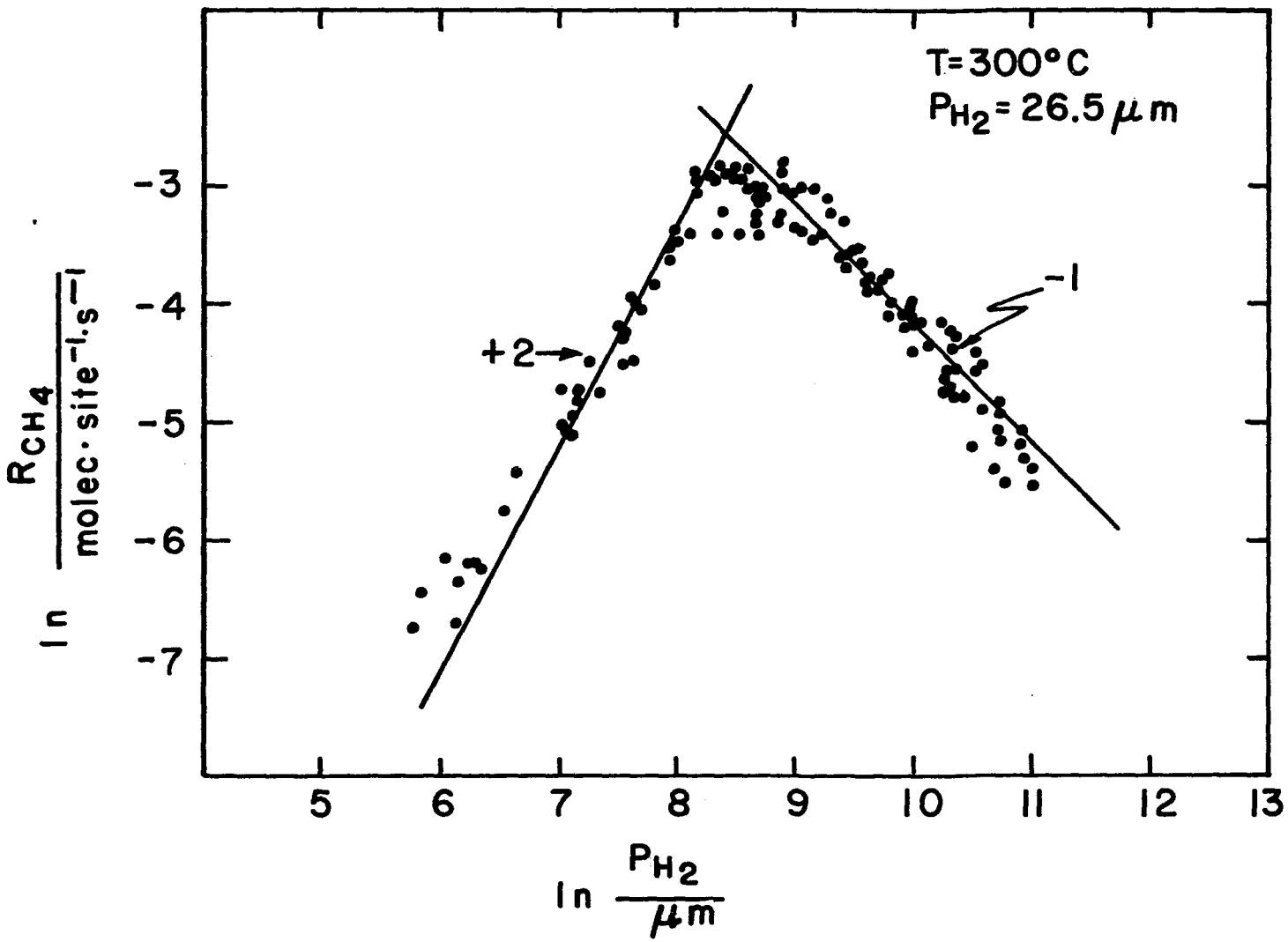

Figure 21. Order plot demonstrating that the hydrogen data can be roughly fit by straight lines. The order of the reaction with respect to hydrogen varies from +2 to -1.

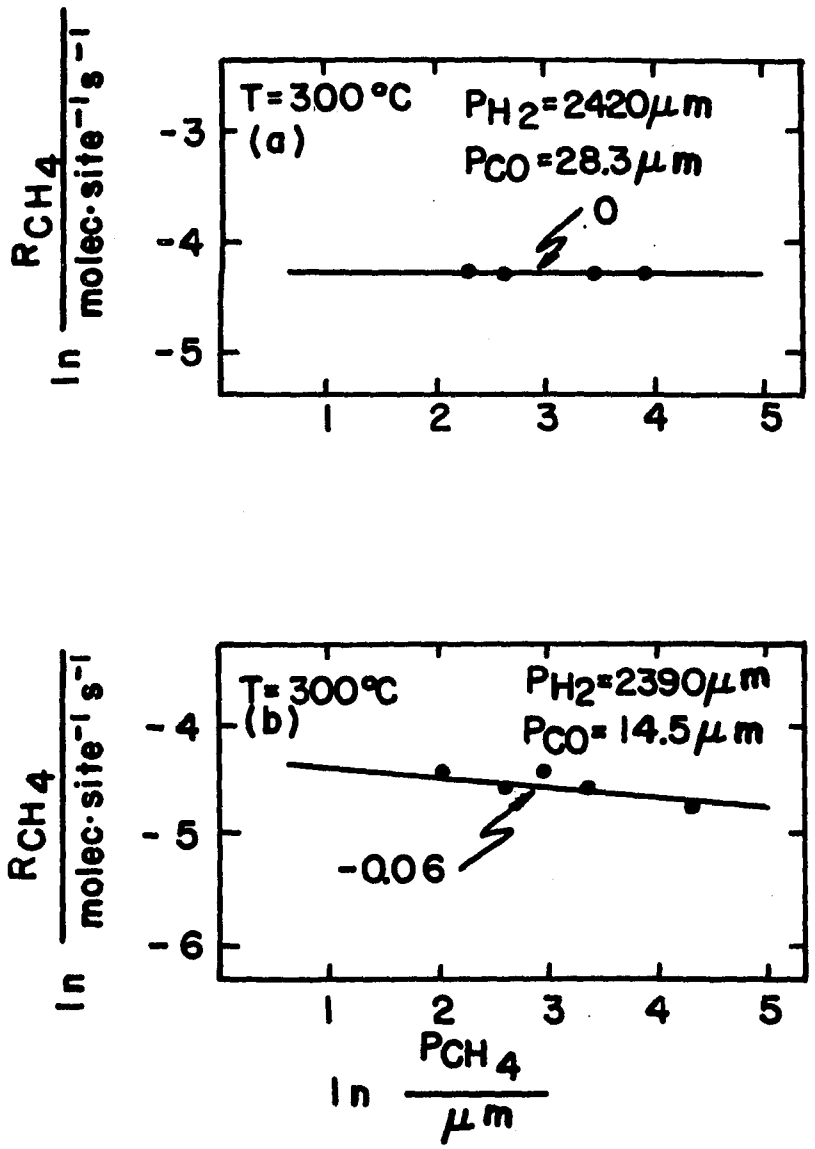

Figure 22. Order plot indicating that the reaction is zero order in methane.

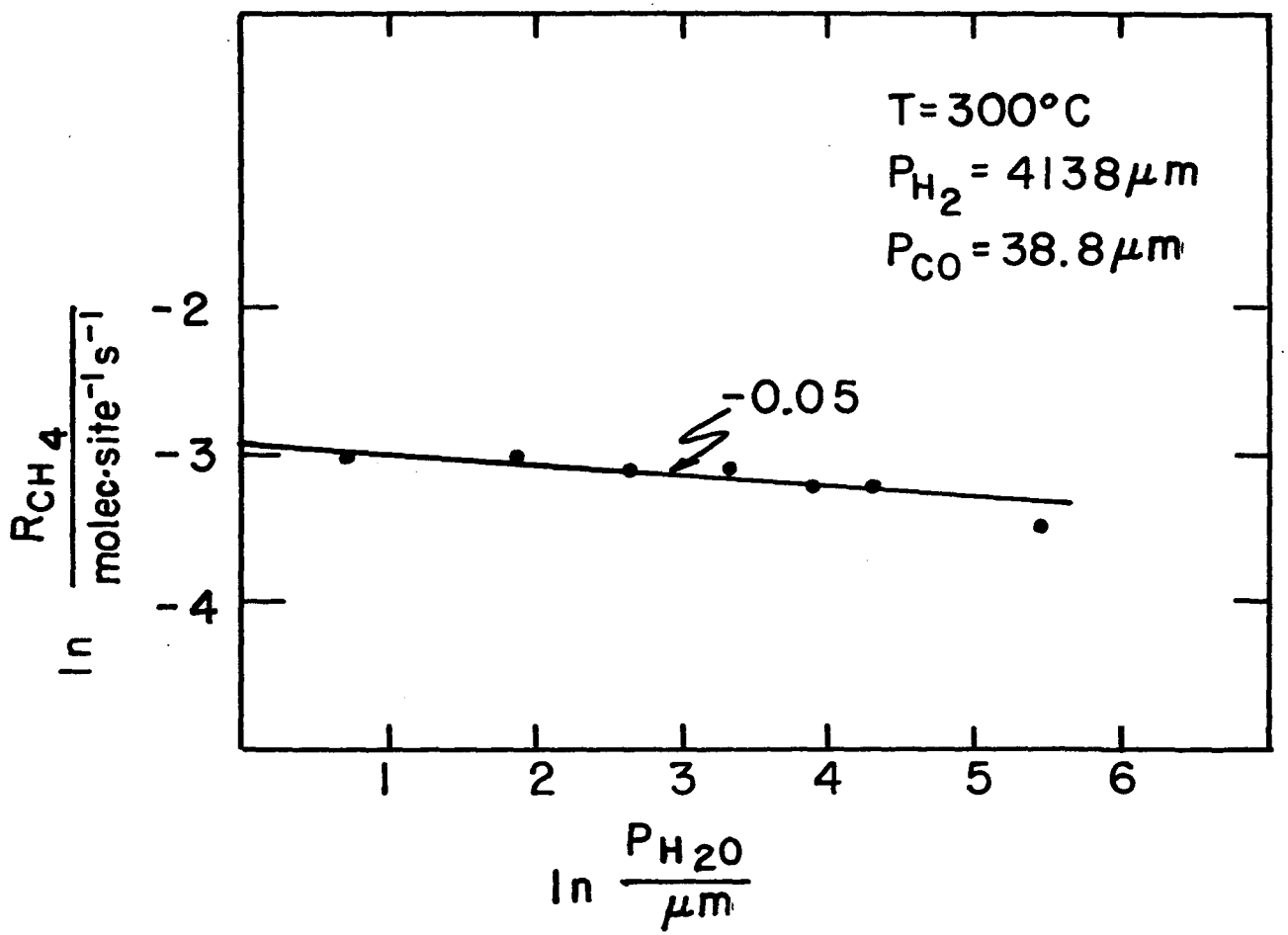

Figure 23. Order plot demonstrating that the reaction is zero order in water.

studied. Therefore, for all practical purposes the reaction is zero order in both methane and water over the entire pressure ranges studied. Few kinetic studies have been reported which measured the kinetic order dependence of the products. In fact, no report of the kinetic order dependence of the methanation reaction for water could be found for any metal. A few reports of methane kinetic orders are available. In all cases either a zero or negative order dependence was reported.

The apparent activation energy of the methanation reaction can be obtained from Figure 24. The slope of this curve at any point is $-E_{app}/R$. The activation energy obtained in this manner is not the actual activation energy of any step in the mechanism but represents the apparent activation energy resulting from a rate expression which involves products and quotients of actual rate constants. This accounts for the non-linearity of the curve. At 573K the apparent activation energy is 21.9 kcal/mole. Other reported activation energy values for the methanation reaction on ruthenium catalysts are listed in Table 10:

Table 10. Apparent activation energy values of the methanation reaction on various ruthenium catalysts.

Catalyst	P_{total} (atm)	E_{app} (kcal/mole)	Reference
5% Ru/Al_2O_3	1	24.2	33
Ru (powder)	0.01-0.16	9.0	49
0.5% Ru/Al_2O_3	1	37.2	51
1% Ru/SiO_2	1	26.5	36
5% Ru/SiO_2	1	27.0	36
1.5% Ru/Al_2O_3	1	24.0	100
5% Ru/SiO_2	1	24.0	47

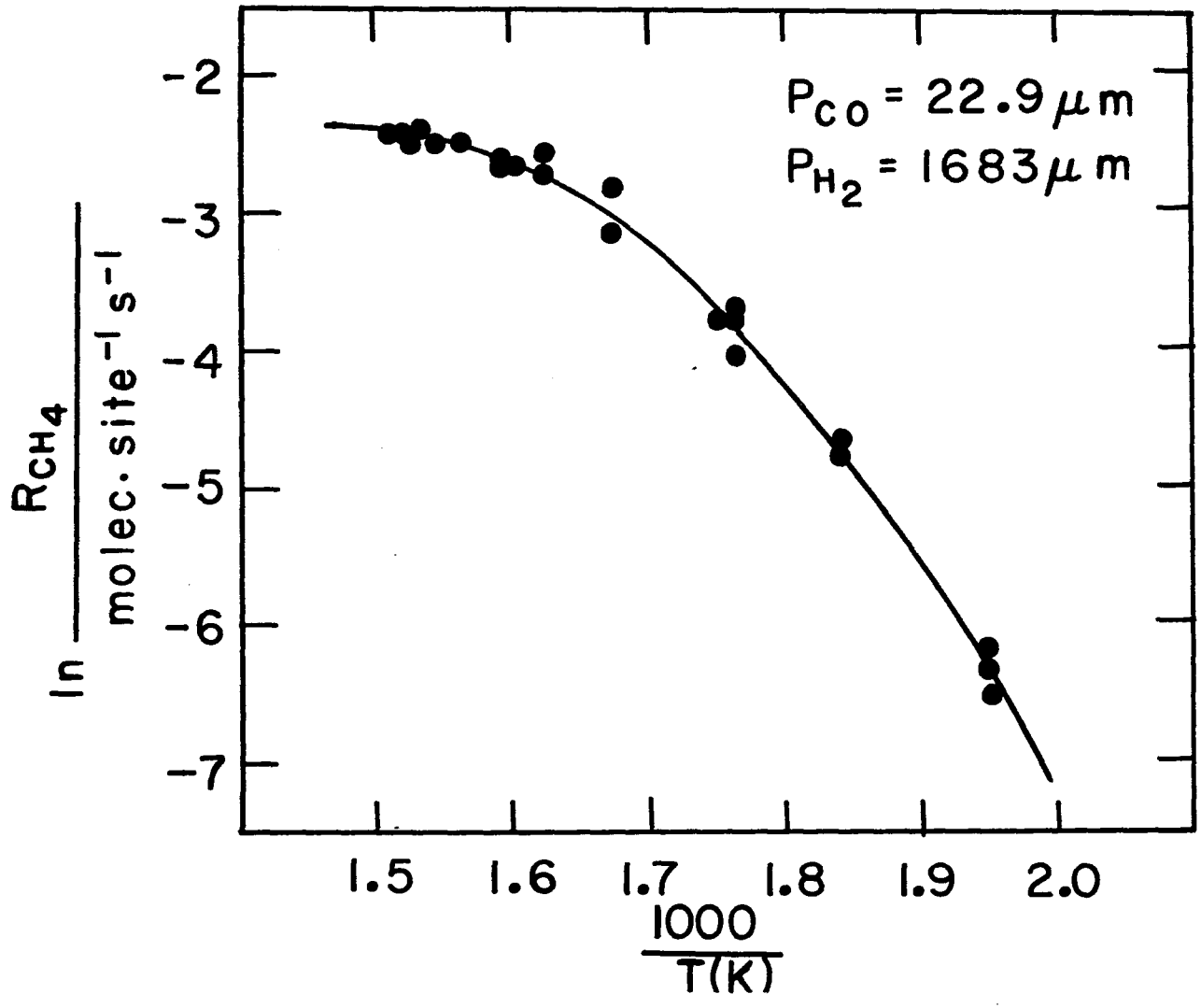

Figure 24. Temperature dependence of the methanation reaction on ruthenium thin films.

The value of 21.9 kcal/mole is in good agreement with the values that fall in the 24.0-27.0 kcal/mole range. Some deviation from this range might be expected since all of the values in this range were obtained using supported ruthenium catalysts. The values of McKee [49] and Randhava, et al. [51] are in serious disagreement with all others. McKee's work was done on a ruthenium powder whereas that of Randhava, et al. was done on a supported catalyst. Both catalysts were prepared by the experimenters by reduction of a ruthenium salt. The catalysts were not characterized before use and quite likely some sort of impurity caused the observed deviation from the expected activation energy value. It is also possible in the latter case that an impurity in the support would account for the unexpected result.

An experiment was performed to study the effect of carbon deposition upon the rate of the methanation reaction. The rate of the "clean" catalyst was obtained in the usual manner by dosing the catalyst with a mixture of carbon monoxide and hydrogen and monitoring the amount of methane produced. This was defined as the reaction rate at $\theta_C = 0$ (an initial carbon coverage of zero). Once this value was obtained the catalyst was exposed to the cleaning dose of hydrogen. Then carbon monoxide was dosed onto the catalyst and the disproportionation reaction was allowed to occur for various lengths of time to produce different fractional coverages of carbon atoms. After each disproportionation reaction the catalyst was dosed with the same carbon monoxide-hydrogen dose and the reaction rate was measured. A graph of the rate of methanation as a function of the initial carbon coverage is shown in Figure 25. This graph demonstrates that the rate of methanation first

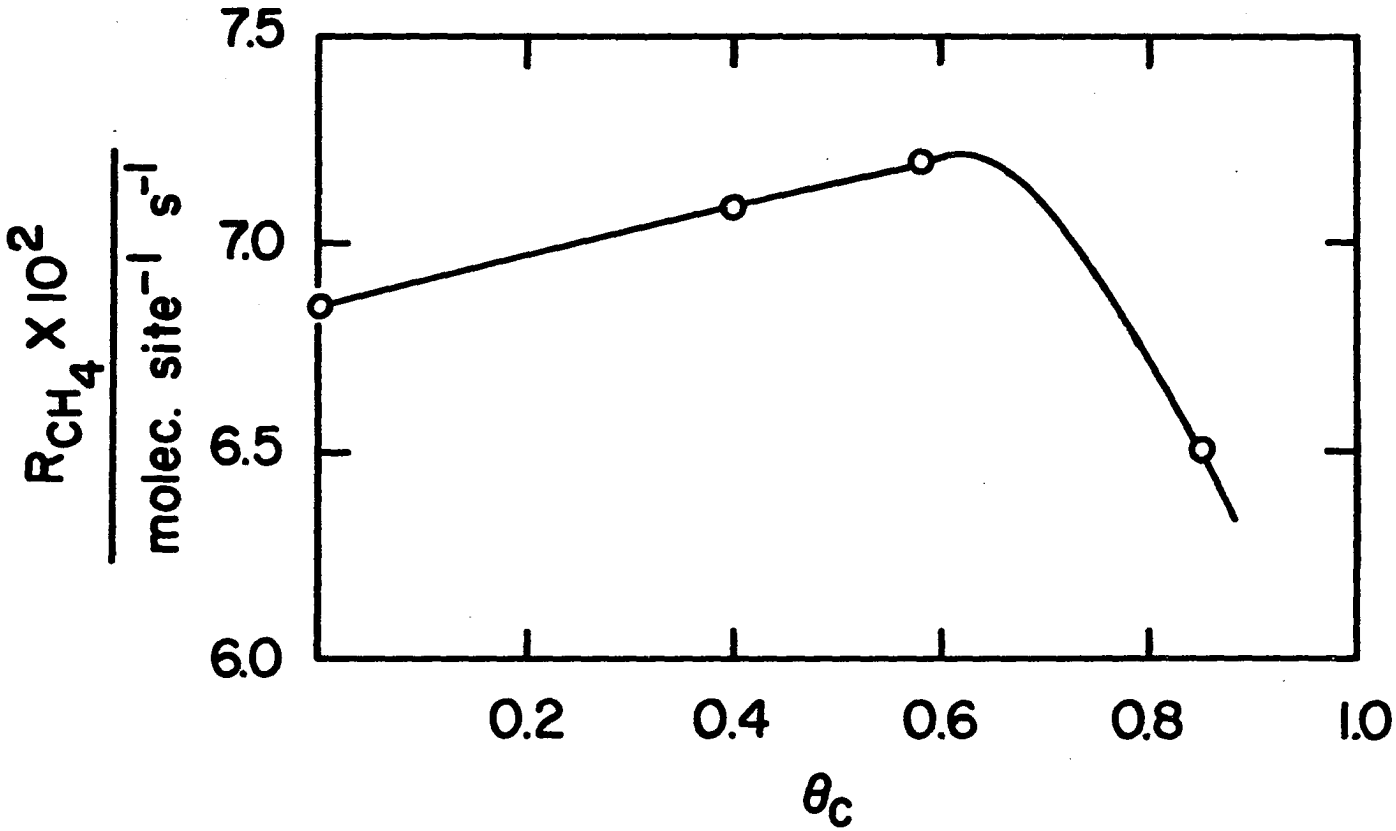

Figure 25. Variation in the rate of methanation as a function of the fractional coverage of reactive carbon.

increases in a linear fashion as the number of carbon atoms on the surface increases until a carbon coverage of about 0.65 is reached, and thereafter declines dramatically.

An additional experiment was performed at $\theta_c = 0.4$ in which the methanation rate was measured over the partially carbon covered surface. It was observed that the rate of methanation over the carbon covered surface using carbon monoxide and hydrogen in the gas phase was equal to the rate of methanation of the carbon monoxide and hydrogen over the clean catalyst plus the rate of methanation of the carbon layer using only hydrogen as a reactant gas. This is an interesting observation and suggests that the increased rate observed for $\theta_c \leq 0.80$ is due to the increased availability of surface carbon.

These observations suggest two fairly important facts. First, it demonstrates (as did Figure 7) that adsorbed carbon atoms are reactive toward hydrogen and could possibly be intermediates in the methanation reaction. It is not required that carbon atoms be intermediates in the methanation sequence since the reaction could occur in such a manner that carbon atoms are not produced. Once produced, however, they are reactive. Secondly, this experiment demonstrates that adsorbed hydrogen is necessary to produce methane. If the reaction merely occurred between the adsorbed carbon atoms and gas phase hydrogen, then the rate would be expected to increase as the carbon coverage increases for all values of θ_c. The decrease in rate as the coverage of adsorbed carbon gets above 0.65 indicates that a competition for sites is involved with hydrogen being unable to displace an adsorbed carbon atom.

A study was made in which ^{13}C atoms were deposited on the catalyst using the disproportionation of $^{13}C^{18}O$. This was followed by a dose of $^{12}C^{16}O$ and hydrogen. The production of both $^{12}CH_4$ and $^{13}CH_4$ was monitored. Initially, they were produced at about the same rate, however, the rate of $^{13}CH_4$ production dropped rather quickly due to the depletion of ^{13}C from the surface. This lends support to the previous conclusion that adsorbed carbon atoms are reactive toward hydrogen and lead to the production of methane.

As has already been discussed, a standard hydrogen dose was used between all kinetic runs to remove any reactive carbon remaining on the catalyst surface after pumping away the gases. In general a very negligible amount of methane was produced (often too little to detect). In cases in which the $CO:H_2$ ratio had been fairly large in the previous run some methane was detected. It was observed that for a given $CO:H_2$ ratio which produced methane during the standard hydrogen dose, the amount of product was a function of the length of time that the system was pumped between the end of the kinetic run and the dosing of the standard hydrogen dose. This is shown in Figure 26. This indicates that some (or all) of the intermediates present on the surface at the end of the kinetic run are unstable in vacuum at 573K. They undergo some sort of decomposition (or interaction) process which leads to the removal of carbon from the surface.

The standard hydrogen dose could be completely eliminated from the experimental procedure with very little effect upon the observed rates. Omission of the standard hydrogen dose between runs in which the $CO:H_2$

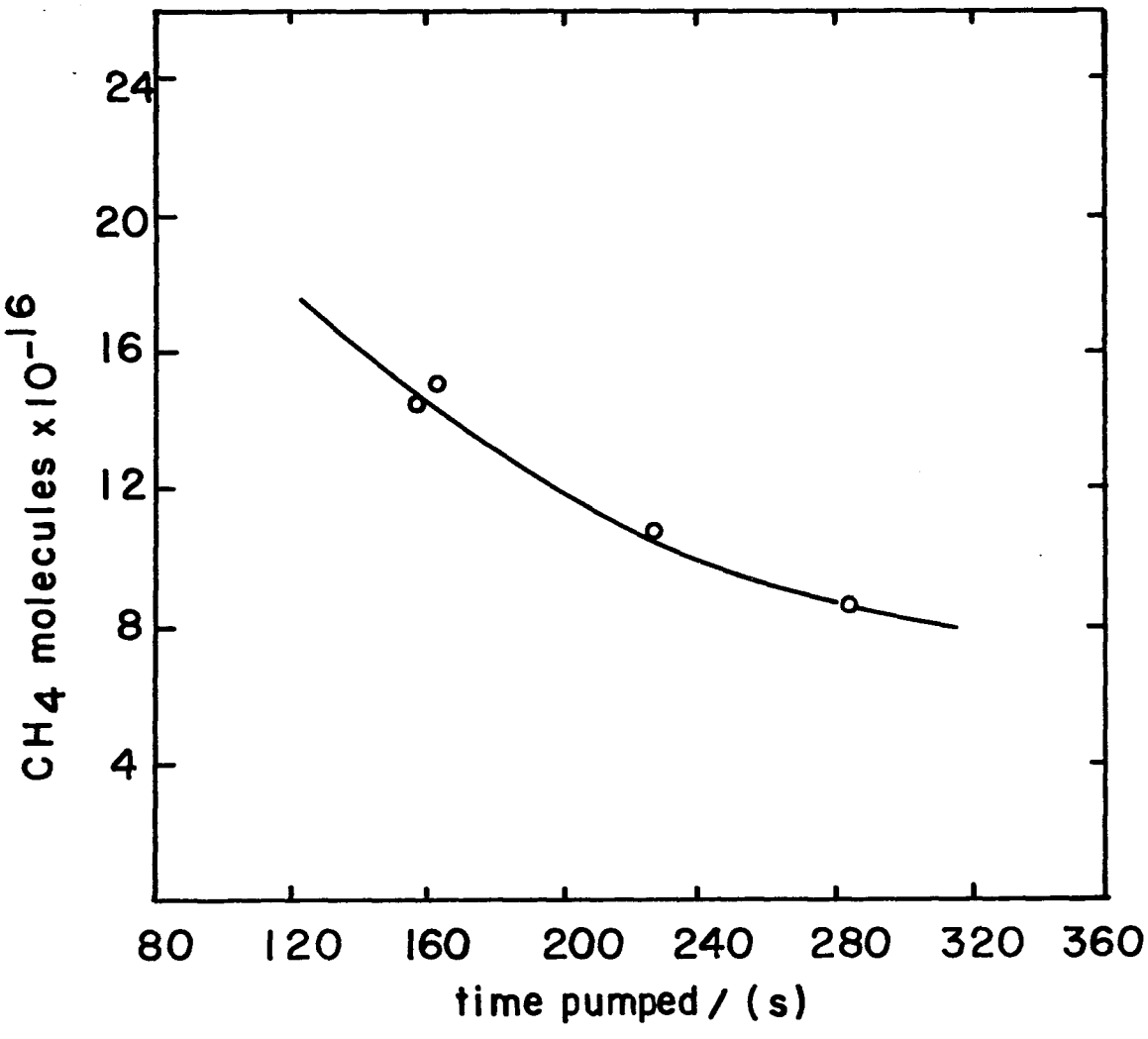

Figure 26. The quantity of methane produced during a standard hydrogen dose as a function of the length of time that the system was pumped prior to the dose.

ratio was moderate or low had no effect upon the rates of the subsequent runs. Omission of the standard hydrogen dose after a run involving a large $CO:H_2$ ratio led to a slight enhancement of the rate of the next kinetic run. This is actually predicted from Figure 25. Since the system was by necessity pumped between the two runs being discussed, and since some of the carbonaceous intermediates were removed by this pumping, θ_c was surely below 0.80 and an enhancement of the rate of the next run would be expected.

The ruthenium thin film was always stored under 3.5 torr of hydrogen at room temperature when it was not in use. It was always the case that after about 48 hours this hydrogen contained substantial amounts of methane. Since no reactive carbon was left on the surface prior to this hydrogen dose, there must be carbon associated with the catalyst which is removed only after long hydrogen exposures. This would be the "type 2" carbon suggested by the Auger results. The possible structure of this carbon will be discussed in a subsequent section.

One very reasonable reaction intermediate in the methanation reaction would be a partially hydrogenated adsorbed carbon monoxide molecule with the following structure:

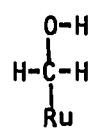

This looks very much like an adsorbed methanol molecule with the bonding occurring through the carbon atom. Since the Auger results indicated that no oxygen was on the surface of the catalyst after a methanation study, the rate limiting step must occur after the removal of the oxygen

from the reaction intermediates. Therefore, it would be expected that if the above structure is a reaction intermediate methanol would be converted to methane at a rate comparable to that for the conversion of carbon monoxide to methane. This assumes, of course, that adsorbed methanol has the above structure. A series of runs was made using methanol instead of carbon monoxide in the reactant feedstream. The production of methane was observed to occur at approximately the same rate as when carbon monoxide was used. This suggests that an adsorbed methanol type intermediate could be involved in the methanation reaction.

An attempt was made to perform the same study using formaldehyde. Since high purity formaldehyde cannot be purchased, an attempt was made to prepare some using the technique of Yates, et al. [101] involving the vacuum decomposition of paraformaldehyde (trioxymethylene). It was not possible using this technique to get the formaldehyde purity to an acceptable level. Therefore, this experiment could not be performed.

It was observed that with high $CO:H_2$ ratio feedstreams some carbon dioxide was produced. Ruthenium is known to be a good catalyst for the hydrogenation of carbon dioxide to methane. Therefore, there was a possibility that the primary oxygen containing product was carbon dioxide instead of water and that the carbon dioxide was either hydrogenated to methane and water or that it underwent the water-gas shift reaction (5) before leaving the cell. This was checked by mixing an equal molar mixture of carbon monoxide and carbon dioxide with hydrogen and dosing this feedstream onto the catalyst at 573K. The rate of methane production as well as the rate of disappearance of carbon monoxide and

carbon dioxide was monitored. Methane production was observed to occur immediately upon introduction of the reactant feedstream. However, no carbon dioxide was used up until all of the carbon monoxide had been converted to methane. The carbon dioxide was then hydrogenated. These results indicate that although both gases can be converted to methane over ruthenium catalysts, carbon dioxide in a mixture of the two will not be converted until the carbon monoxide is depleted. This difference in reactivity is believed to be due to the different manners in which the two gases interact with ruthenium. Carbon monoxide interacts strongly with ruthenium whereas the ruthenium-carbon dioxide interaction is relatively weak. Therefore the methanation reaction involving carbon monoxide will predominate as long as there is carbon monoxide available. Since the total depletion of carbon monoxide never occurred during the kinetic studies, neither the hydrogenation of carbon dioxide nor its removal by the water-gas shift reaction could have occurred. This proves that the primary oxygenated reaction product was at all times water.

It was also noted at relatively high $CO:H_2$ ratios that the rate of methanation tended to drop with time. This was not due to a reduction in the carbon monoxide concentration since under these conditions the rate was so slow that very little carbon monoxide was used. This drop in rate with time is very likely due to the production of some sort of surface poison which removes active sites. This has been observed before and is generally believed to be due to the formation of some sort of carbonaceous overlayer which is relatively unreactive under reaction conditions.

Exchange Studies

The exchange reactions of hydrogen and carbon monoxide were studied on the ruthenium thin film. Even though the experiments are fairly easy to perform with results that a very useful in predicting the structure of the adsorbed gas, no report of either reaction on ruthenium has been found. A dose was made in which 616.85 μm of hydrogen and 577.05 μm of deuterium was introduced into the reaction cell at 573K. The hydrogen-deuterium exchange occurred instantly with equilibrium being reached in a matter of seconds after the dose was made. This suggests very strongly that the hydrogen adsorbs dissociatively.

The $^{12}C^{16}O$-$^{13}C^{18}O$ exchange reaction was also found to proceed readily on the ruthenium thin film. The reaction was studied at approximately equal molar mixtures of the two isotopes over a fairly wide pressure range. The total carbon monoxide pressure was varied from $2x10^{-7}$ torr to 80 μm. The exchange reaction was quite rapid, however it could be measured on the basis of the rate of appearance of $^{12}C^{18}O$. The ready exchange would be most simply explained by a model involving dissociative adsorption of the carbon monoxide with both carbon and oxygen atoms available to exchange. The exact nature of the adsorption states of carbon monoxide on most metals is not well-understood. Some results suggest molecular adsorption and others suggest dissociative adsorption. In an effort to explain isotopic exchange of carbon monoxide on tungsten using a non-dissociative moded Madey, et al. [102] proposed a four-center bimolecular exchange intermediate in which both the carbon and oxygen atoms are bound to the surface as well as to each other.

Exchange could then occur *via* the interaction of these horizontally bound carbon monoxide molecules. Presumably, if such a structure is possible on tungsten then an analogous structure should be possible on ruthenium. This explanation does, however, seem rather far-fetched. An alternative model involves both dissociated and non-dissociated carbon monoxide in equilibrium on the surface. The carbon monoxide molecule adsorbs molecularly to a ruthenium site *via* the carbon atom. This molecular carbon monoxide can then dissociate to form adsorbed carbon and oxygen atoms. This model seems to be more reasonable than that proposed by Yates, *et al*. The exchange would of course occur among the adsorbed atoms.

An activation energy for the carbon monoxide exchange reaction was determined from the data shown in Figure 27. The value was found to be 6.1 kcal/mole which is considerably lower than the apparent activation energy of the methanation reaction.

A very interesting observation was made when the carbon monoxide exchange rate was measured with varying amounts of hydrogen present in the gas mixture. This was done in an effort to better characterize the adsorbed state of carbon monoxide under reaction conditions. A plot of this exchange rate versus the quantity of hydrogen in the mixture is shown in Figure 28. As can be seen the exchange rate drops with increasing hydrogen pressure. Methane production begins to occur around 2.5 to 3.0 torr of hydrogen although only very small amounts of methane are produced under these conditions. Since the Auger results suggest that the catalyst surface is free of oxygen after a methanation study, this hydrogen effect

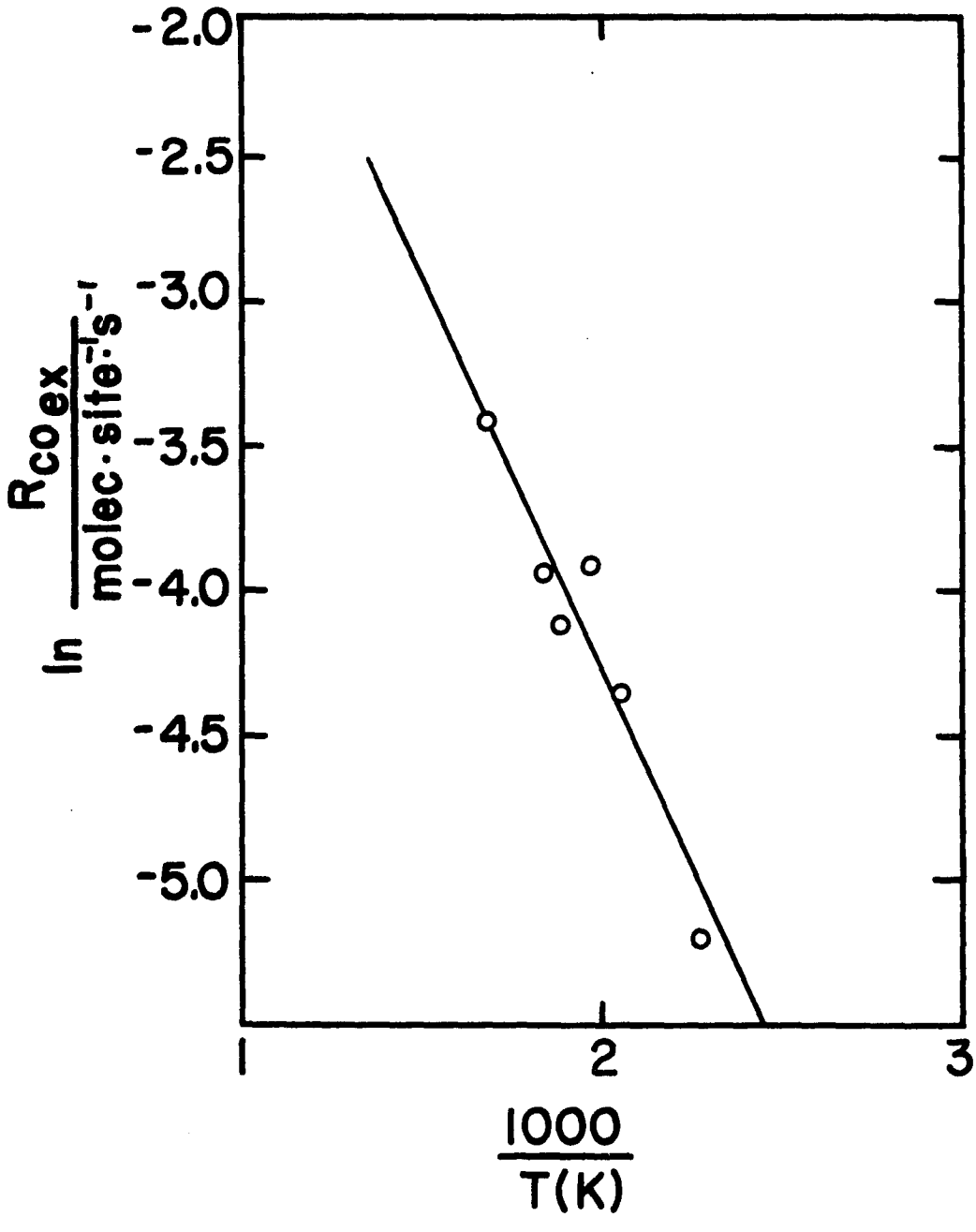

Figure 27. Temperature dependence of the $^{13}C^{18}O$-$^{12}C^{16}O$ exchange reaction on ruthenium thin films.

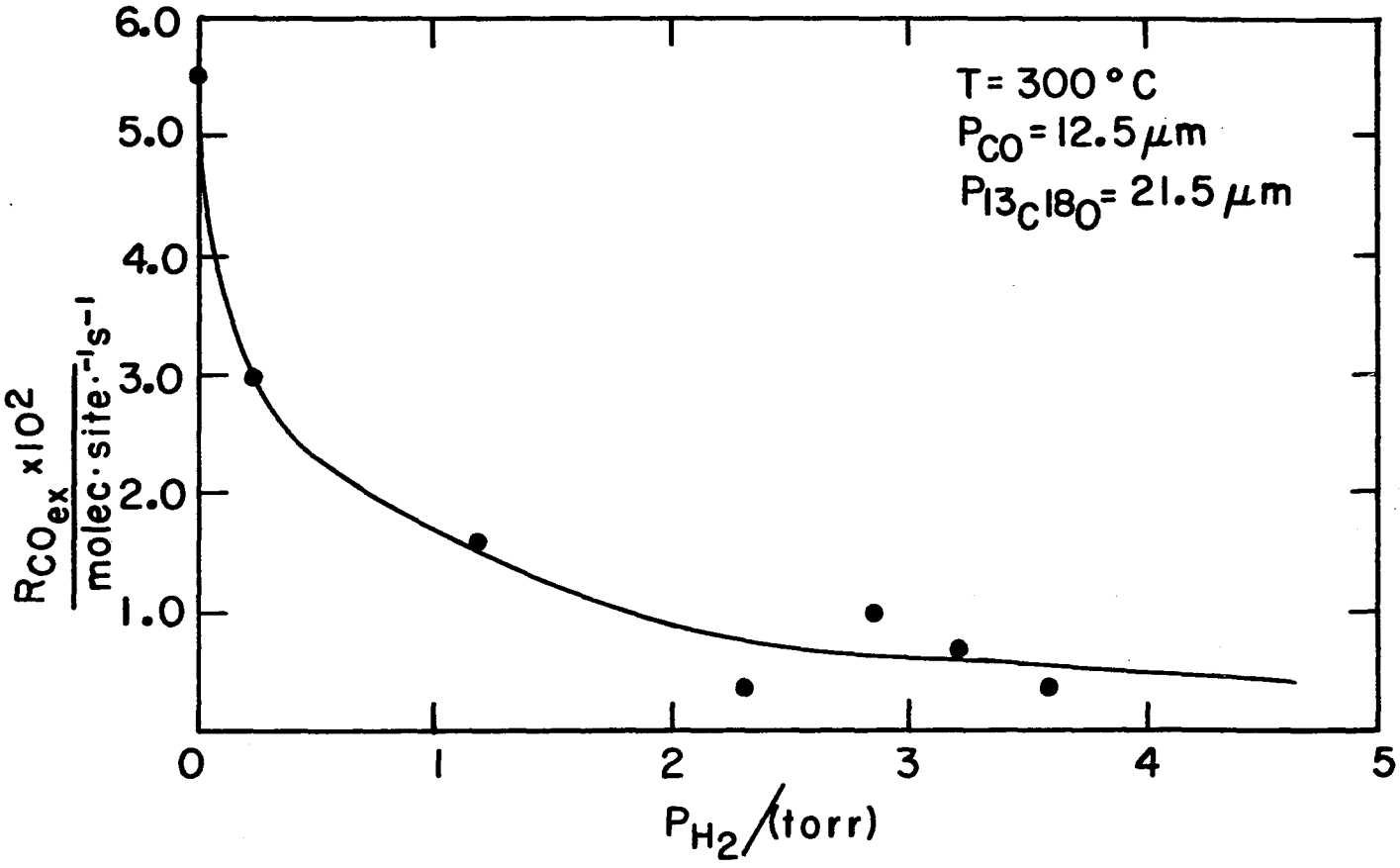

Figure 28. Variation in the rate of the $^{13}C^{18}O$-$^{12}C^{16}O$ exchange as a function of the quantity of hydrogen present in the background.

might be due to the rapid removal of the oxygen as water leaving no oxygen available for the exchange reaction. Whether the oxygen is removed by the hydrogen before or after carbon monoxide dissociation will be discussed thoroughly in the discussion of the proposed mechanism.

Flash Desorption Study

A series of flash desorption spectra for carbon monoxide from ruthenium was determined. The results are shown in Figure 29. The doses ranged from 0.6 to 12 Langmuirs. As can be seen, at low carbon monoxide doses there is one state on the polycrystalline sample. This carbon monoxide desorbs at about 488K. The second state begins to fill with doses of about 4 Langmuirs. The peak maximum for this low energy state occurs at 403K. These results are in fairly good agreement with those of Ku et al. [103] who report two states of carbon monoxide on ruthenium $(10\bar{1}0)$, with peak maxima at about 403 and 495K. Since one study involves a single crystal and the other involves polycrystalline ruthenium, perfect correlation is not really expected. Qualitatively, however, the results are identical. The flashes were continued to about 1000K and no further desorption was detected. This observation is in agreement with the work of Kraemer and Menzel [83] who observed that all carbon monoxide was removed from ruthenium field emitter tips by 500K. While this flash work is not extremely useful in terms of predicting a mechanism for the methanation reaction, it does lend support to the contention that work done on single crystal ruthenium is very useful in predicting observations made on polycrystalline ruthenium.

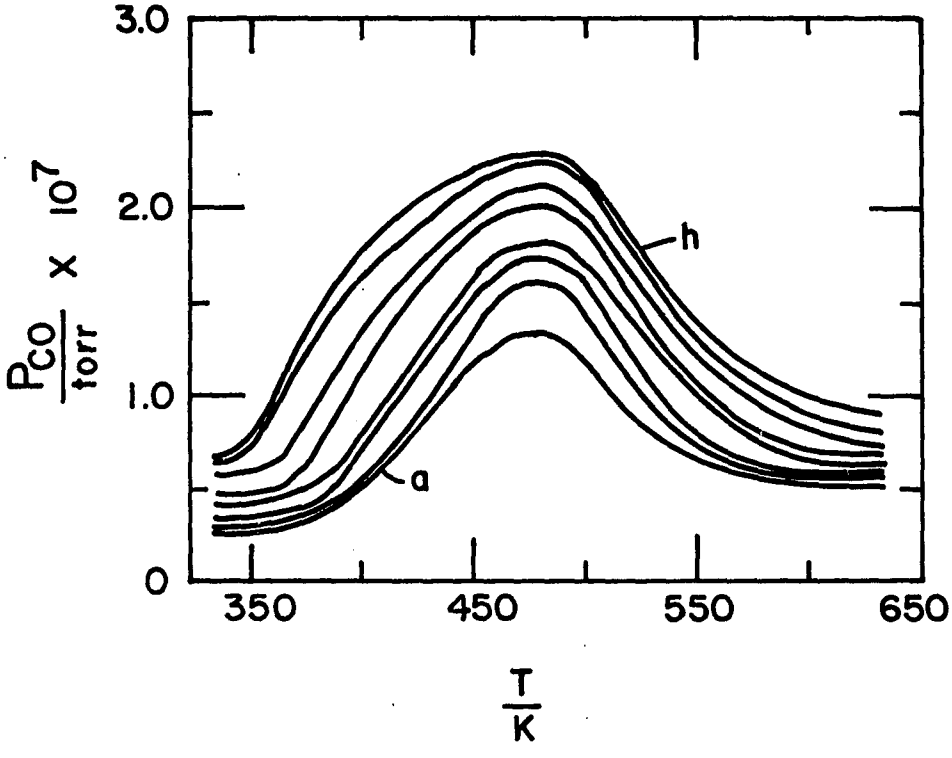

Figure 29. Flash desorption spectra for carbon monoxide on ruthenium: (a) 0.6 L CO dose, (b) 1.2 L CO dose, (c) 1.5 L CO dose, (d) 2.6 L CO dose, (e) 3.9 L CO dose, (f) 4.4 L CO dose, (g) 8.0 L CO dose, (h) 12.0 L CO dose.

Mechanistic Considerations

An attempt has been made to develop a mechanism which is quantitatively consistent with the kinetic studies as well as qualitatively consistent with the isotopic exchange studies, the flash desorption work and the surface characterization studies (Auger, LEED and ESCA). The major portion of the data suggest a carbon monoxide kinetic order varying between +1 and -1 and a hydrogen kinetic order varying between +2 and -1. The kinetic orders with respect to both methane and water are zero in the pressure range employed in this study. The shapes of the order plots suggest a Langmuir-Hinshelwood type mechanism which involves the interaction of adsorbed hydrogen and adsorbed carbon monoxide. Consider the following sequence of elementary steps:

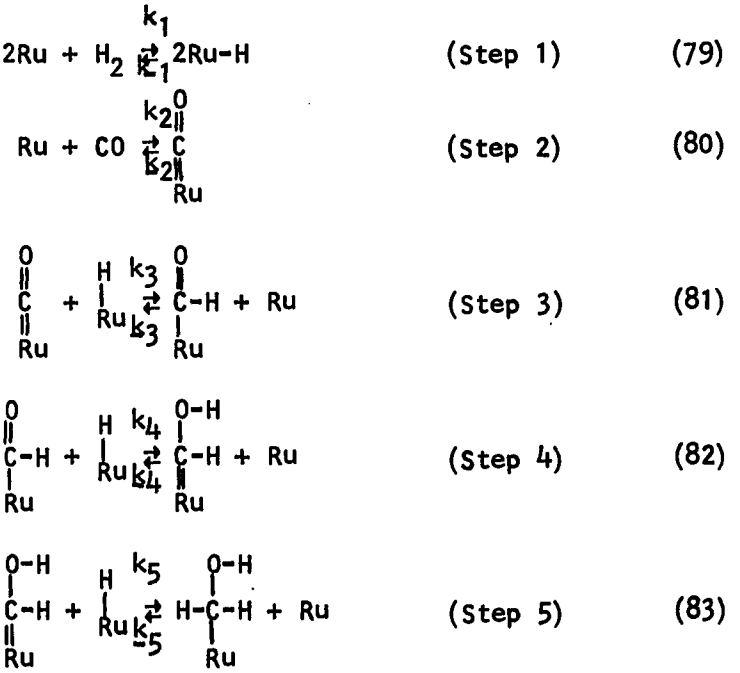

(Step 1) (79)

(Step 2) (80)

(Step 3) (81)

(Step 4) (82)

(Step 5) (83)

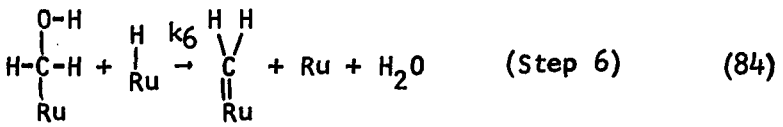

(Step 6) (84)

(Step 7) (85)

(Step 8) (86)

This mechanism proposes the existence of seven surface complexes. A steady state development would lead to a series of simultaneous equations which for all practical purposes are unsolvable. Although a mathematical solution can be obtained using this approach, the physical significance of the result is ambiguous. A more informative approach in this case would be that of Kemball [104] involving the establishment of some but not necessarily all of the possible equilibria between gas and surface and between different kinds of species on the surface. Each equilibrium established exerts a thermodynamic influence upon the amounts of the intermediates which take part in the reaction.

In the mechanism listed above, Ru designates a ruthenium surface atom, Ru-H represents a hydrogen atom adsorbed to a ruthenium surface atom and Ru=C=O represents an undissociated carbon monoxide molecule bonded <u>via</u> a double bond to one surface atom. An attempt has been made to maintain at all times four bonds to an adsorbed carbon, two bonds to oxygen and one bond to each hydrogen atom. The step designated by (86) is chosen as the rate determining step (Actually, steps (84) and (86) are in balance, and so in that sense both are rate limiting). Neither steps

(84) nor (86) are equlilibium steps since the reaction is zero order with respect to both products. The mathematical development proceeds as follows:

$$K_1 = \frac{[RuH]^2}{[H_2][Ru]^2} \rightarrow [RuH] = (K_1[H_2])^{1/2}[Ru] \quad (87)$$

$$K_2 = \frac{[RuCO]}{[CO][Ru]} \rightarrow [RuCO] = K_2[CO][Ru] \quad (88)$$

$$K_3 = \frac{[RuCHO][Ru]}{[RuCO][RuH]} \rightarrow [RuCHO] = K_2K_3(K_1[H_2])^{1/2}[Ru] \quad (89)$$

$$K_4 = \frac{[RuCHOH][Ru]}{[RuCHO][RuH]} \rightarrow [RuCHOH] = K_1K_2K_3K_4[H_2][CO][Ru] \quad (90)$$

$$K_5 = \frac{[RuCH_2OH][Ru]}{[RuCHOH][RuH]} \rightarrow [RuCH_2OH] = K_2K_3K_4K_5(K_1[H_2])^{3/2}[CO][Ru] \quad (91)$$

The overall reaction stoichiometry requires the production of water and methane at equal rates. This leads to the following equality:

$$k_6[RuCH_2OH][RuH] = k_8[RuCH_3][RuH] \quad (92)$$

From equations (91) and (92) it is evident that:

$$[RuCH_3] = \frac{k_6}{k_8}K_2K_3K_4K_5(K_1[H_2])^{3/2}[CO][Ru] \quad (93)$$

$$K_7 = \frac{[RuCH_3][Ru]}{[RuCH_2][RuH]} \rightarrow [RuCH_2] = \frac{k_6K_1K_2K_3K_4K_5}{k_8K_7}[H_2][CO][Ru] \quad (94)$$

Each of these expressions represents the surface coverage of the particular intermediate under reaction conditions. Fractional coverages will be used in this development. The sum of the fractional coverages of all intermediates and empty sites must be unity as indicated below:

$$1 = Ru + RuH + RuCO + RuCHO + RuCHOH + RuCH_2OH + RuCH_2 + RuCH_3 \quad (95)$$

Substitution of the above expressions for the fractional coverages of the surface intermediates into equation (95) yields the following expression

for the fractional coverage of bare ruthenium sites:

$$[Ru] = 1/\{1 + (K_1[H_2])^{1/2} + K_2[CO] + K_2K_3(K_1[H_2])^{1/2}[CO] + \tag{96}$$

$$(K_1K_2K_3K_4 + \frac{k_6K_1K_2K_3K_4K_5}{k_8K_7})[H_2][CO] + (K_2K_3K_4K_5 + \frac{k_6}{k_8}K_2K_3K_4K_5)(K_1[H_2])^{3/2}[CO]\}$$

Now that expressions have been derived for each of the surface intermediates as well as the ruthenium surface atoms, the rate can now be written:

$$\frac{d[CH_4]}{dt} = k_8[RuCH_3][RuH] = k_6K_1^2K_2K_3K_4K_5[H_2]^2[CO][Ru]^2 \tag{97}$$

Using the fractional coverage for bare ruthenium sites (96) leads to the following rate expression:

$$\frac{d[CH_4]}{dt} = (k_6K_1^2K_2K_3K_4K_5[H_2]^2[CO])/\{1 + (K_1[H_2])^{1/2} + K_2[CO] +$$

$$K_2K_3(K_1[H_2])^{1/2}[CO] + (K_1K_2K_3K_4 + \frac{k_6K_1K_2K_3K_4K_5}{k_8K_7})[H_2][CO] + (K_2K_3K_4K_5 +$$

$$\frac{k_6}{k_8}K_2K_3K_4K_5)(K_1[H_2])^{3/2}[CO]\}^2 \tag{98}$$

Recall that the surface characterization studies indicated that there was essentially no oxygen on the catalyst surface after methanation. There was, however, a significant carbon coverage. If it is assumed that the total coverage of all oxygen containing intermediates is at all times quite low then equation (98) reduces to the following:

$$\frac{d[CH_4]}{dt} = (k_6K_1K_2K_3K_4K_5[H_2]^2[CO])/\{1 + (K_1[H_2])^{1/2} + \frac{k_6K_1K_2K_3K_4K_5}{k_8K_7}[H_2][CO]$$

$$+ \frac{k_6}{k_8}K_2K_3K_4K_5(K_1[H_2])^{3/2}[CO]\}^2 \tag{99}$$

This expression can be rewritten as follows:

$$\frac{d[CH_4]}{dt} = A[H_2]^2[CO]/\{1 + B[H_2]^{1/2} + C[H_2][CO] + D[H_2]^{3/2}[CO]\}^2 \qquad (100)$$

The meaning of the constants A through D is obvious. This rate expression does predict the observed limiting kinetic orders for both hydrogen and carbon monoxide (ignoring the -2 order in carbon monoxide).

In order to fit this expression to the data the constants must be determined. It would be desirable to be able to linearize the expression or use some other mathematical approach to evaluate them absolutely. However, this expression is too complex so the trial and error method of iteration must be used. An attempt was made to fit the carbon monoxide order curve using equation (100) with the hydrogen pressure constant. The curve was found to be much too broad to fit the data. No choice of constants would increase the sharpness of the curve maximum. What this indicates is that the model presented thus far does not adequately describe the role of carbon monoxide in the reaction. Since the carbon monoxide order plot could not be fit with this theory, no effort was made to fit the hydrogen order plot.

As has already been mentioned some data collected at relatively high carbon monoxide pressure indicated a higher negative order dependence than -1. Actually, at high carbon monoxide pressures the kinetic order seems to be approaching -2. This suggests an interaction between two adsorbed carbon containing intermediates. It is difficult to understand how such an interaction could lead to methane production. The mass spectral output of some of the higher pressure carbon monoxide runs was examined and the production of a small amount of carbon dioxide was detected. A step was

added to the mechanism to account for the interaction leading to carbon dioxide production. Perhaps the simplest interaction that could lead to carbon dioxide production would be as follows:

$$2RuCO \xrightarrow{k_9} RuC + CO_2 + Ru \qquad \text{(Step 9)} \qquad (101)$$

If only this additional step were added then the catalyst would poison due to the formation of unreactive RuC. Since this is not observed to occur, the hydrogenation of the adsorbed carbon atom must be also included. This requires the addition of the following two steps:

$$RuC + RuH \underset{k_{-10}}{\overset{k_{10}}{\rightleftarrows}} RuCH + Ru \qquad \text{(Step 10)} \qquad (102)$$

$$RuCH + RuH \underset{k_{-11}}{\overset{k_{11}}{\rightleftarrows}} RuCH_2 + Ru \qquad \text{(Step 11)} \qquad (103)$$

The development of a rate expression for this new mechanism proceeds in the same fashion as the previous development. The expressions for [RuH], [RuCO], [RuCHO], [RuCHOH] and [$RuCH_2OH$] are unchanged from the results of equations (87) to (91). The principal change occurs as a result of the production of not only water but also carbon dioxide as an oxygen containing product. Actually, two different processes are occurring simultaneously:

$$CO + 3H_2 \rightleftarrows CH_4 + H_2O$$

$$2CO + 2H_2 \rightleftarrows CH_4 + CO_2$$

At low carbon monoxide to hydrogen ratios, only the first reaction occurs at a detectable rate. However, as the carbon monoxide pressure is increased relative to the hydrogen the second reaction begins to occur.

Products from both reactions are detected, therefore both must be considered in the development of the rate expression. It must be true that the rate of formation of methane equals the rate of formation of water plus the rate of formation of carbon dioxide. This leads to the following expression:

$$k_8[RuCH_3][RuH] = k_6[RuCH_2OH][RuH] + k_9[RuCO]^2 \tag{104}$$

Using the previously determined values for $[RuCH_2OH]$, $[RuCO]$ and $[RuH]$ we can now solve for $[RuCH_3]$:

$$[RuCH_3] = \{\frac{k_6}{k_8}K_2K_3K_4K_5(K_1[H_2])^{3/2}[CO] + \frac{k_9K_2^2[CO]^2}{k_8(K_1[H_2])^{1/2}}\}[Ru] \tag{105}$$

Using this expression and the surface equilibria relationships we can generate the following expressions for the other intermediates:

$$[RuCH_2] = \{\frac{k_6}{k_8K_7}K_1K_2K_3K_4K_5[H_2][CO] + \frac{k_9K_2^2[CO]^2}{k_8K_1K_7[H_2]}\}[Ru] \tag{106}$$

$$[RuCH] = \{\frac{k_6}{k_8K_7K_{11}}K_2K_3K_4K_5(K_1[H_2])^{1/2}[CO] + \frac{k_9K_2^2[CO]^2}{k_8K_7K_{11}(K_1[H_2])^{3/2}}\}[Ru] \tag{107}$$

$$[RuC] = \{\frac{k_6K_2K_3K_4K_5[CO]}{k_8K_7K_{10}K_{11}} + \frac{k_9K_2^2[CO]^2}{k_8K_7K_{10}K_{11}K_1^2[H_2]^2}\}[Ru] \tag{108}$$

The following expression for the fractional coverage of bare ruthenium sites results when the fractional coverages of all intermediates are summed and set equal to unity:

$$[Ru] = 1/\{1 + (K_1[H_2])^{1/2} + K_2[CO] + K_2K_3(K_1[H_2])^{1/2}[CO] +$$

$$K_1K_2K_3K_4[H_2][CO] + K_2K_3K_4K_5(K_1[H_2])^{3/2}[CO] + \frac{k_6}{k_8}K_2K_3K_4K_5(K_1[H_2])^{3/2}[CO] +$$

$$\frac{k_9K_2^2[CO]^2}{k_8(K_1[H_2])^{1/2}} + \frac{k_6}{k_8K_7}K_1K_2K_3K_4K_5[H_2][CO] + \frac{k_9K_2^2[CO]^2}{k_8K_7K_1[H_2]} +$$

$$\frac{k_6K_2K_3K_4K_5}{k_8K_7K_{11}}(K_1[H_2])^{1/2}[CO] + \frac{k_9K_2^2[CO]^2}{k_8K_7K_{11}(K_1[H_2])^{3/2}} + \frac{k_6K_2K_3K_4K_5[CO]}{k_8K_7K_{10}K_{11}} +$$

$$\frac{k_9K_2^2[CO]^2}{k_8K_7K_{10}K_{11}(K_1[H_2])^2}\} \qquad (109)$$

The rate limiting step is still chosen as the one involving methane production with the steps involving water and carbon dioxide production in balance with it. This leads to the following equation

$$\frac{d[CH_4]}{dt} = k_8[RuCH_3][RuH] \qquad (110)$$

Using the equations for the fractional coverages of these intermediates in conjunction with equation (109) yields the following rate expression:

$$\frac{d[CH_4]}{dt} = (k_6K_1^2K_2K_3K_4K_5[H_2]^2[CO] + k_9K_2^2[CO]^2)/\{1+ (K_1[H_2])^{1/2} +$$

$$(K_2 + \frac{k_6K_2K_3K_4K_5}{k_8K_7K_{10}K_{11}})[CO] + (K_2K_3 + \frac{k_6K_2K_3K_4K_5}{k_8K_7K_{11}})(K_1[H_2])^{1/2}[CO] +$$

$$(K_1K_2K_3K_4 + \frac{k_6K_1K_2K_3K_4K_5}{k_8K_7})[H_2][CO] +(K_2K_3K_4K_5 + \frac{k_6}{k_8}K_2K_3K_4K_5)(K_1[H_2])^{3/2}[CO]$$

$$+ \frac{k_9K_2^2[CO]^2}{k_8(K_1[H_2])^{1/2}} + \frac{k_9K_2^2[CO]^2}{k_8K_1K_7[H_2]} + \frac{k_9K_2^2[CO]^2}{k_8K_7K_{11}(K_1[H_2])^{3/2}} + \frac{k_9K_2^2[CO]^2}{k_8K_7K_{10}K_{11}K_1^2[H_2]^2}\}^2 \qquad (111)$$

If, once again, terms in the denominator associated with oxygen-containing intermediates are neglected based on the Auger results then equation (111) reduces to the following:

$$\frac{d[CH_4]}{dt} = (k_6K_1K_2K_3K_4K_5[H_2]^2[CO] + k_9K_2^2[CO]^2)/\{1+ (K_1[H_2])^{1/2} +$$

$$(\frac{k_6K_2K_3K_4K_5}{k_8K_7K_{10}K_{11}})[CO] + (\frac{k_6K_2K_3K_4K_5}{k_8K_7K_{11}})(K_1[H_2])^{1/2}[CO] + (\frac{k_6K_1K_2K_3K_4K_5}{k_8K_7})[H_2][CO] +$$

$$(\frac{k_6}{k_8}K_2K_3K_4K_5)(K_1[H_2])^{3/2}[CO] + \frac{k_9K_2^2[CO]^2}{k_8(K_1[H_2])^{1/2}} + \frac{k_9K_2^2[CO]^2}{k_8K_1K_7[H_2]} +$$

$$\frac{k_9K_2^2[CO]^2}{k_8K_7K_{11}(K_1[H_2])^{3/2}} + \frac{k_9K_2^2[CO]}{k_8K_7K_{10}K_{11}K_1^2[H_2]^2}\}^2 \qquad (112)$$

This equation can be rewritten in the following form:

$$\frac{d[CH_4]}{dt} = (A[H_2]^2[CO] + B[CO]^2)/\{1 + C[H_2]^{1/2} + D[H_2]^{3/2}[CO] + E[H_2][CO] +$$

$$F[H_2]^{1/2}[CO] + G[CO] + \frac{I[CO]^2}{[H_2]^{1/2}} + \frac{J[CO]^2}{[H_2]} + \frac{K[CO]^2}{[H_2]^{3/2}} + \frac{L[CO]^2}{[H_2]^2}\}^2 \qquad (113)$$

In this expression the correlation between the constants (A-L) and the rate constants and equilibrium constants is obvious. No direct correlation between the constants of this expression and those of equation (100) is intended. When the hydrogen pressure is held constant as in the case with a carbon monoxide order plot this expression assumes the much simpler form:

$$\frac{d[CH_4]}{dt} = \frac{(A'[CO] + B'[CO]^2)}{(1 + C' + D'[CO] + E'[CO]^2)^2} \qquad (114)$$

This expression could be fit rather nicely to the data with the maximun deviation between theory and experiment being 10%.

An attempt was made to fit the hydrogen order results using equation (113) and the constants of equation (114) obtained from the carbon monoxide order plot. The positive order region of the curve was fit very well but

serious deviation occurred in the negative order region of the curve. This suggests that the mechanism as listed does not adequately describe the hydrogen interaction at very high hydrogen pressures. A modification of the model increasing the negative hydrogen order dependency of the rate expression would involve multiple bonding of intermediates to ruthenium atoms. This would allow more than one hydrogen atom to bond to a ruthenium atom and it would also permit the bonding of hydrogen atoms and carbon containing intermediates to the same ruthenium atom. Since all kinetic data were taken with excess hydrogen and since at times the hydrogen pressure was as high as 2000 times the carbon monoxide pressure it is not unreasonable to suppose enhanced hydrogen adsorption. Upon looking through the eight or so intermediates predicted in the mechanistic discussion thus far it is apparent that a variety of structures could exist that would involve multiple bonding to the surface atoms. Quite a few of these would, however, not change the order dependence of the rate law in the desired manner. If we examine equation (112) it is apparent that in order to increase the negative order dependence in terms of hydrogen we must either change the rate limiting step such that the exponent of the hydrogen term in the numerator is less than +2 or we must add a term in the denominator which goes as the hydrogen pressure raised to a power greater than +3/2. The numerator has a very significant effect upon the fit of the theory to the data, especially in the positive order region of the hydrogen order plot. Since this region of the curve fits fairly well the approach will be to introduce new intermediates that would modify the denominator as described above.

When data are collected to yield a hydrogen order plot the carbon monoxide pressure is held constant. In this instance equation (112) reduces to the following:

$$\frac{d[CH_4]}{dt} = (A''[H_2]^2 + B'')/\{1 + C''[H_2]^{1/2} + D''[H_2]^{3/2} + E''[H_2] + G'' + \frac{I''}{[H_2]^{1/2}} + \frac{J''}{[H_2]} + \frac{K''}{[H_2]^{3/2}} + \frac{L''}{[H_2]^2}\}^2 \quad (115)$$

As will be evident later the denominator terms which are inverse order in hydrogen have negligible contribution (I'' - L'' are zero). In an attempt to improve the fit to the hydrogen order plot a term such as $M[H_2]^2$ was added to the denominator. It was observed that proper selection of the constants gave a fairly good fit to the data. It is evident that when hydrogen adsorbs as an adatom, a term $(C[H_2])^{1/2}$ in the denominator of equation (113) describes its pressure dependency. Also evident is the fact that the carbonaceous species RuCH has a term with the same hydrogen pressure dependency. In fitting the hydrogen order data no distinction between these terms can be made. However, their relative magnitude will affect the carbon monoxide order plot since one is independent of the carbon monoxide pressure and the other varies as the carbon monoxide pressure. An identical situation exists with the $M[H_2]^2$ term. If the adsorbed species with this hydrogen pressure dependency contains only hydrogen atoms then the C' term in equation (114) would include this term. If this species contains a carbon atom then the term is actually represented by $M[CO][H_2]^2$ with a first order carbon monoxide dependency. This term would appear in the D'[CO] term of equation (114). It is possible that both surface species contribute. The result of this analysis is that

either C' or D' or both must include a term with a +2 hydrogen pressure dependency.

It was observed that some variation in the values of both C' and D' was possible without sacrificing the carbon monoxide order plot fit. Maximum values of the two constants were found to be C' = 0.1 and D' = 0.01. These maximum values could not be used simultaneously to give the optimum fit. An attempt was made to fit the hydrogen order plot using constants from the carbon monoxide order plot with C' = 0.1. It was found that this led to an improved hydrogen order fit but the error at high hydrogen pressure was still too high. Similarly, D' was maximized and a hydrogen order curve fit was attempted. An acceptable fit resulted. What this suggests is that if only one new intermediate is introduced into the mechanism to accomplish a simultaneous fit of both order plots its surface concentration must vary as $[H_2]^2$ and [CO]. Alternatively, two new intermediates may be introduced. The first would have the pressure dependencies just mentioned and the second would have a surface concentration that varies as $[H_2]^2$. Introduction of the second intermediate alone will not yield an acceptable fit to the data. The approach at this point will be to attempt to introduce examples of both intermediates and use data other than kinetics to make a final judgement.

One interaction which might be expected to occur when hydrogen is present in large excess is the adsorption of more than one hydrogen atom per ruthenium atom. Consider the following:

$$Ru + H_2 \underset{k_{-12}}{\overset{k_{12}}{\rightleftharpoons}} \begin{matrix} H & H \\ \diagdown & \diagup \\ Ru & \end{matrix} \qquad \text{(Step 12)} \qquad (116)$$

$$K_{12} = \frac{[RuH_2]}{[H_2][Ru]} \rightarrow [RuH_2] = K_{12}[H_2][Ru] \qquad (117)$$

Of course, a species of this sort would be expected to be reactive. A simple mechanism could be written which would involve only this form of adsorbed hydrogen:

$$RuCO + RuH_2 \rightleftarrows RuCHOH + Ru$$

$$RuCHOH + RuH_2 \rightarrow H_2O + RuCH_2 + Ru$$

$$RuCH_2 + RuH_2 \xrightarrow{k_{13}} CH_4 + 2Ru \qquad \text{(Step 13)} \qquad (118)$$

The rate expression derived from this sequence of steps (including carbon monoxide and hydrogen adsorption steps) indicates that this sort of interaction does not yield a positive kinetic order in hydrogen. It is possible, however, that this mechanism could be occurring simultaneously with the one developed previously. This would lead to a rate expression identical to equation (113) except that some of the coefficients would have a slightly different form when expressed as rate constants and equilibrium constants. The important thing to be gained from this is that the introduction of the RuH_2 species has no effect upon the fit of the theory to the data. Since the only effect of the two unnumbered steps above is to modify the form of some of the coefficients in the rate expression they will not be considered subsequently.

It is also conceivable that the RuH_2 species could interact with some of the intermediates produced in the previous mechanism. Interactions could occur in which either one or both of the hydrogen atoms would be involved. All such interactions were considered and once again the rate expression was identical to equation (113) except for the correlations

between some of the coefficients and the rate constants and equilibrium constants.

It is quite conceivable that additional hydrogen could be adsorbed in the following manner:

$$RuH_2 + H_2 \underset{k_{-14}}{\overset{k_{14}}{\rightleftharpoons}} \begin{matrix} H & H \\ H\diagdown & \diagup H \\ Ru & \end{matrix} \qquad \text{(Step 14)} \qquad (119)$$

$$\therefore \quad K_{14} = \frac{[RuH_4]}{[RuH_2][H_2]} \rightarrow [RuH_4] = K_{14}[H_2]^2[Ru] \qquad (120)$$

This species has the desired hydrogen pressure dependency and would improve the fit to the data. Interactions between this intermediate and the oxygen containing intermediates could occur without modification of equation (113) except to change the rate constant-equilibrium constant dependence of a few of the coefficients. The same is true of interactions with RuC, RuCH and $RuCH_2$ to yield higher hydrogen containing intermediates. Therefore, such interactions will not be listed explicitly in the mechanism. An interaction between RuC and RuH_4 to yield methane could possibly occur but since such a step does not really resemble an elementary process, it will not be considered. The interactions between RuH_4 and each of the species RuCH, $RuCH_2$ and $RuCH_3$ to yield methane does not follow the observed kinetics and therefore must have negligible occurrence.

The major role of an RuH_4 species would be to serve as a reversible surface poison. At high hydrogen pressures the surface would become predominately covered with this species and therefore the number of sites available for adsorption of carbon monoxide would be quite low. A severe drop in rate would be expected. Upon pumping the system, the hydrogen

would be flashed off to yield the original surface. This sort of reversible poisoning would be expected to yield an order plot with a very sharp peak. As was observed in Figure 21, this is the case with the data of this study.

All intermediates postulated thus far have been of such a nature that no hydrogen atoms could be attached to a ruthenium atom which had a carbonaceous species also bound to it. To eliminate such structures is apparently incorrect as was noted in a previous discussion. Several species of this sort could be written involving the addition of extra hydrogen to the intermediates already postulated. Most such interactions lead to results that are kinetically indistinguishable from the theory already developed and would therefore not improve the fit of the theory to the data. Also, species that involve additional hydrogen adsorption onto oxygen containing intermediates are not likely because of the Auger results previously discussed.

Consider interactions involving the addition of one hydrogen atom. Only one such interaction will produce an intermediate whose surface concentration varies as $[H_2]^2[CO]$. Consider the following

$$\overset{CH_3}{\underset{Ru}{|}} + RuH \rightleftarrows \overset{H\ CH_3}{\underset{Ru}{\diagdown\!/}} + Ru$$

$$[RuHCH_3] = K[RuCH_3][RuH]$$

Before attempting to modify the theory to include this species, interactions involving the addition of two hydrogen atoms will be considered. Two such interactions would change the hydrogen order dependency of the previous theory. The first involves the interaction of two hydrogen atoms

with adsorbed methylene as follows:

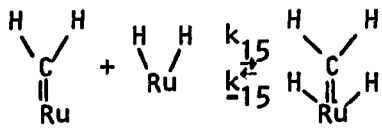

(Step 15) (121)

$$[RuH_2CH_2] = K_{12}K_{15}[RuCH_2][H_2] \qquad (122)$$

This intermediate clearly has the proper pressure dependency in both the hydrogen and carbon monoxide. One additional interaction would involve an adsorbed methyl group and a hydrogen molecule as follows:

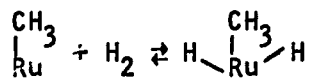

$$[RuH_2CH_3] = K[RuCH_3][H_2]$$

This species has a pressure dependency of $[H_2]^{5/2}[CO]$ and will be considered briefly.

Before proceeding with the mathematical development of the rate expression a few words must be said about the plausibility of these three hypothetical new surface structures. Comments will concern the mode of bonding and the stability of each intermediate. A more thorough discussion of this matter will follow the derivation of the rate expression.

The bonding of an adsorbed methyl group is most certainly <u>via</u> an sp^3 hybrid orbital. The hydrogen atom is bound to the surface <u>via</u> a σ bond. This, of course, assumes that bonding orbitals are available in the metal to accommodate the bonding of both structures. For the moment we will assume that this is the case and discuss it in more detail later. Since both the hydrogen atom and the methyl group are bound to the ruthenium <u>via</u> σ bonds, both adsorbates are free to "wiggle" and "flop around" on the ruthenium atom. It is quite likely that in doing this they will

collide with one another and form methane which desorbs rapidly as follows:

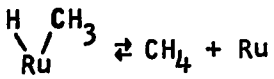

This structure is believed to be quite unstable and its surface concentration would be expected to be negligible. The same arguments can be made about the RuH_2CH_3 structure and likewise it must be eliminated as a species that could achieve relatively high coverages under reaction conditions.

It seems quite reasonable to expect that the RuH_2CH_2 surface intermediate could be present in significant concentrations. If it is assumed that the carbon atom has already undergone conversion to sp^3 hybrid orbitals then the bonding to the ruthenium would be as follows:

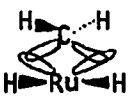

The methylene group is fairly rigidly bound to the surface such that the sort of movements that led to decomposition of the two previous structures is severely limited. The hydrogen atoms are bound to the ruthenium atom through directional bonds such that they are not positioned close enough to the carbon atom to allow rapid decomposition. This will be discussed in more detail later.

Once the RuH_2CH_2 species is present on the surface it can either remain on the surface as a reversible poison or it can slowly undergo decomposition to form methane. If the species remains on the surface during a run as a poison then it would have the effect of removing reactive ruthenium sites. This would lead to a very rapid decline in the rate and

would produce a sharp peak in the hydrogen order plot. A sharp change from a kinetic order of +2 to -1 was experimentally observed.

If the RuH_2CH_2 undergoes decomposition to methane, then it must do so in a manner which fits the observed kinetics. Consider the following dissociation step:

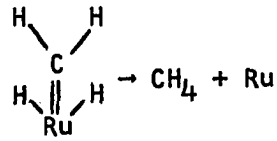

The rate of this simple decomposition would go as the number of ruthenium atoms. Examination of equation (110) indicates that in order for the theory to fit the data the rate must go as the number of ruthenium atoms squared. The following interaction would meet that requirement:

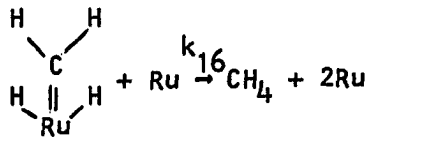

(Step 16) (123)

This suggests that because of the relative positions of the hydrogen atoms with respect to the carbon atom an interaction between the adsorbed methylene-hydrogen structure and a bare ruthenium atom is necessary to produce methane. This will be discussed in more detail later. It is believed, however, that this step is not a major pathway to the production of methane.

A rate expression will now be derived using steps 1-16 as a complete mechanism. Since the rate of formation of methane must equal the sum of those for water and carbon dioxide we get the following equation:

$$k_8[RuCH_3][RuH] + k_{13}[RuCH_2][RuH_2] + k_{16}[RuH_2CH_2][Ru] = k_6[RuCH_2OH][RuH] + k_9[RuCO]^2 \quad (124)$$

Substitution into this equation leads to the following expression for the fractional coverage of $RuCH_2$:

$$[RuCH_2] = \frac{1}{Z}\{k_6K_1K_2K_3K_4K_5[H_2][CO] + \frac{k_9K_2^2[CO]^2}{[H_2]}\}[Ru] \quad (125)$$

with $Z = (k_8K_1K_7 + k_{13}K_{12} + k_{16}K_{12}K_{15})$

Similarly, expressions for the other carbonaceous intermediates may be derived:

$$[RuCH_3] = \frac{1}{Z}\{k_6K_1^{3/2}K_2K_3K_4K_5K_7[H_2]^{3/2}[CO] + \frac{k_9K_2^2K_1^{1/2}K_7[CO]^2}{[H_2]^{1/2}}\}[Ru] \quad (126)$$

$$[RuCH] = \frac{1}{Z}\{\frac{k_6}{K_{11}}K_1^{1/2}K_2K_3K_4K_5[H_2]^{1/2}[CO] + \frac{k_9K_2^2[CO]^2}{K_{11}K_1^{1/2}[H_2]^{3/2}}\}[Ru] \quad (127)$$

$$[RuC] = \frac{1}{Z}\{\frac{k_6K_2K_3K_4K_5[CO]}{K_{10}K_{11}} + \frac{k_9K_2^2[CO]^2}{K_{10}K_{11}K_1[H_2]^2}\}[Ru] \quad (128)$$

$$[RuH_2CH_2] = \frac{1}{Z}\{k_6K_1K_2K_3K_4K_5K_{12}[H_2]^2[CO] + k_9K_2^2K_{12}[CO]^2\}[Ru] \quad (129)$$

The rate may be determined from equation (124) as follows:

$$\frac{d[CH_4]}{dt} = \{k_6K_1K_2K_3K_4K_5[H_2]^2[CO] + k_9K_2^2[CO]^2\}[Ru]^2 \quad (130)$$

The expression for the fractional coverages of the surface intermediates has the following form:

$$1 = [Ru] + [RuH] + [RuH_2] + [RuCO] + [RuCHO] + [RuCHOH] + [RuCH_2OH] +$$
$$[RuCH_3] + [RuCH_2] + [RuCH] + [RuC] + [RuH_2CH_2] + [RuH_4] \quad (131)$$

This expression may be used to solve for the fraction coverage of bare ruthenium sites. When the resulting expression is substituted into

equation (130) the following rate expression is obtained:

$$\frac{d[CH_4]}{dt} = (k_6K_1K_2K_3K_4K_5[H_2]^2[CO] + k_9K_2^2[CO]^2)/\{1 + (K_1[H_2])^{1/2} + K_{12}[H_2] + \frac{k_6K_1^{1/2}K_2K_3K_4K_5[H_2]^{1/2}[CO]}{ZK_{11}} + \frac{k_9K_2^2[CO]^2}{ZK_{11}K_1^{1/2}[H_2]^{3/2}} + \frac{k_6K_1K_2K_3K_4K_5[H_2][CO]}{Z} + \frac{k_9K_2^2[CO]^2}{Z[H_2]} + \frac{k_6K_1^{3/2}K_2K_3K_4K_5K_7[H_2]^{3/2}[CO]}{Z} + \frac{k_9K_2^2K_7K_1^{1/2}[CO]}{Z[H_2]^{1/2}} + \frac{k_6K_2K_3K_4K_5[CO]}{ZK_{10}K_{11}} + \frac{k_9K_2^2[CO]^2}{K_1K_{10}K_{11}[H_2]^2} + \frac{k_6K_1K_2K_3K_4K_5K_{12}[H_2]^2[CO]}{Z} + \frac{k_9K_2^2K_{12}[CO]}{Z} + K_{14}[H_2]^2\}^2 \quad (132)$$

This expression may be rewritten in a simpler form as follows:

$$\frac{d[CH_4]}{dt} = (A[H_2]^2[CO] + B[CO]^2)/\{1 + C[H_2]^{1/2} + D[H_2] + E[H_2]^{1/2}[CO] + \frac{F[CO]^2}{[H_2]^{3/2}} + G[H_2][CO] + \frac{I[CO]^2}{[H_2]} + J[H_2]^{3/2}[CO] + \frac{K[CO]^2}{[H_2]^{1/2}} + L[CO] + \frac{M[CO]^2}{[H_2]^2} + N[H_2]^2[CO] + O[CO]^2 + P[H_2]^2\}^2 \quad (133)$$

where the definition of the constants in terms of rate constants and equilibrium constants is obvious. This theory was fit to the data with the constants shown in Table 11. They are functionally dependent only upon the temperature.

It was observed in fitting the carbon monoxide order plot that the denominator term which is independent of the carbon monoxide pressure (C' of equation (114)) could be varied by two orders of magnitude

Table 11. Values of the constants in the rate expression

Constant	Value	Units
A	1.26×10^{-10}	molec·site^{-1}·s^{-1}·μm^{-3}
B	1.64×10^{-6}	molec·site^{-1}·s^{-1}·μm^{-2}
C	1.0×10^{-3}	μm$^{-1/2}$
D	3.0×10^{-6}	μm^{-1}
E	0	
F	0	
G	9.58×10^{-8}	μm^{-2}
I	0	
J	2.64×10^{-8}	μm$^{-3/2}$
K	0	
L	0	
M	0	
N	3.27×10^{-10}	μm^{-3}
O	3.98×10^{-5}	μm^{-2}
P	5.33×10^{-9}	μm^{-2}

without severely affecting the fit to the data. The major effect of this term is at low carbon monoxide pressures where the other terms are fairly small. The fit of the data to the hydrogen order plot yielded a more accurate value of C'. In the final equation $C' = C[H_2]^{1/2} + D[H_2] + P[H_2]^2$. This term was dominated by the $[H_2]^2$ contribution. The data of both curves were fit by initially optimizing P and then C and D. Since the $[H_2]^2$ term was dominant the values of C and D could vary by a factor of 2 or 3 without severely affecting the fit. All constants that are assigned values of zero in Table 11 were found to contribute negligibly to the value of the rate as defined by equation (133) and the non-zero constants.

The fit to a typical carbon monoxide order plot is shown in Figure 30. The overall fit is quite good with the only deviation occurring near the peak maximum. This deviation amounts to about 10% at worst. Figure 31

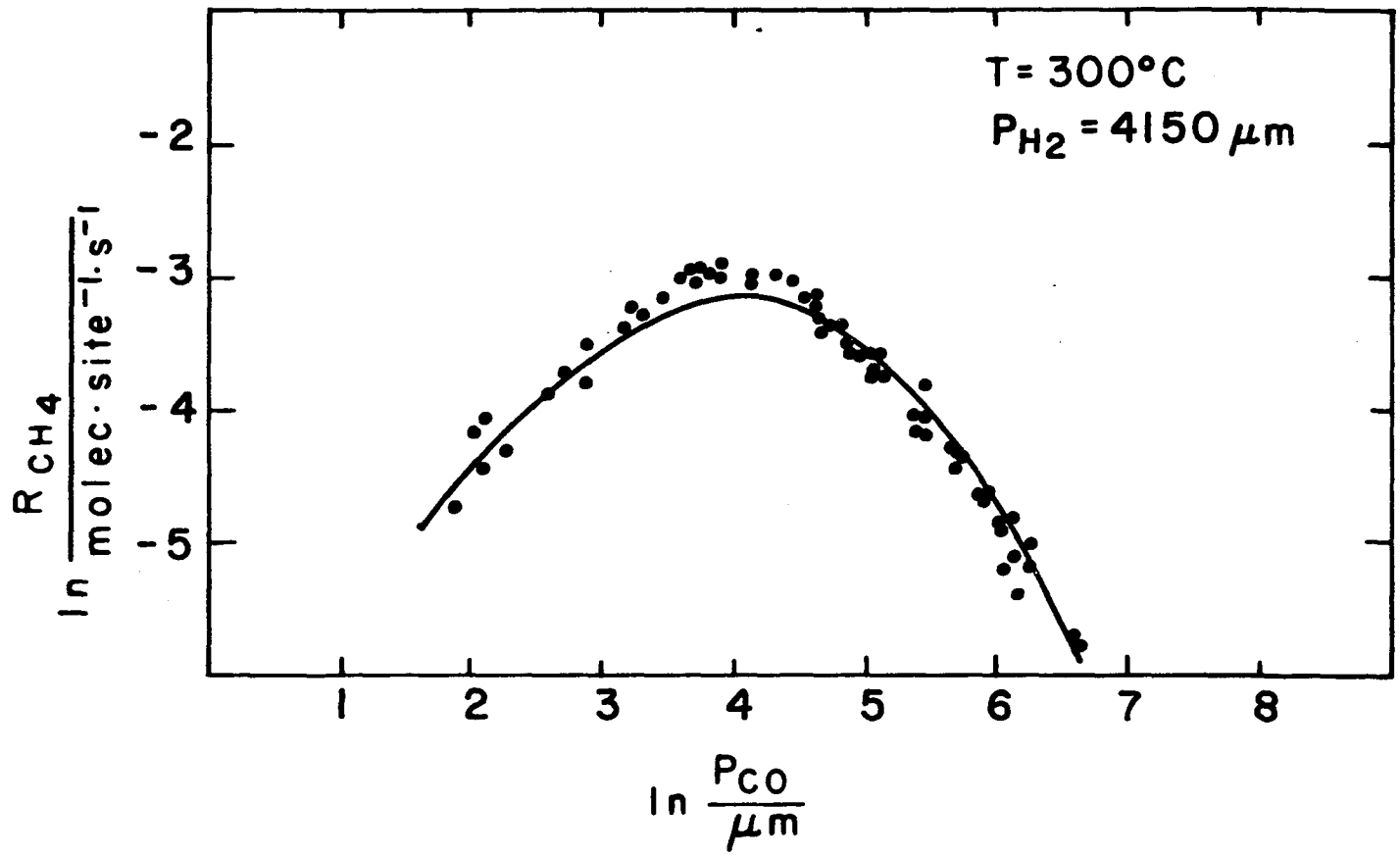

Figure 30. The fit of the theory to a carbon monoxide order plot with $[H_2]$ = 4150 μm.

shows the fit of the theory to a typical hydrogen order plot. The maximum deviation in this case occurs at hydrogen pressures just below the peak maximum. The deviation in this case is about 15%. At extremely low hydrogen pressures it is noted that the theory predicts a leveling off of the order plot. The $[CO]^2$ term in the numerator dominates yielding a constant rate. In the case of the data shown in Figure 31 this leveling off begins to occur at a hydrogen pressure of about 400 μm. The scatter in the data in this region is higher than usual because the rates are so slow. As a result it is not certain that the rate actually levels off as predicted by the theory. The minimum rate detectable in this study was about 4×10^{-4} molec·site^{-1}s^{-1}. The fit of the theory to the water and methane order plots is shown in Figures 32 and 33 respectively. Two methane order plots are shown. They were taken at different carbon monoxide pressures. Both were fit quite well by the theory.

The constants that were presented in Table 11 were obtained by fitting the theory to the data shown in Figures 30 and 31. These data were chosen because they were collected over a fifteen month period with excellent reproducibility. Also, because there are so many data points in these two order plots it is obvious where the curve should lie. To demonstrate that the theory will correctly predict the results of studies conducted at the same temperature but at different pressures, fits were made to the data in Figures 34 and 35 using the constants from Table 11. As can be seen the fit is quite good for each curve. It might be possible to improve the fit in Figures 34 and 35 by modifying some of the constants while attempting to maintain the fit in Figures 30 through 33. This,

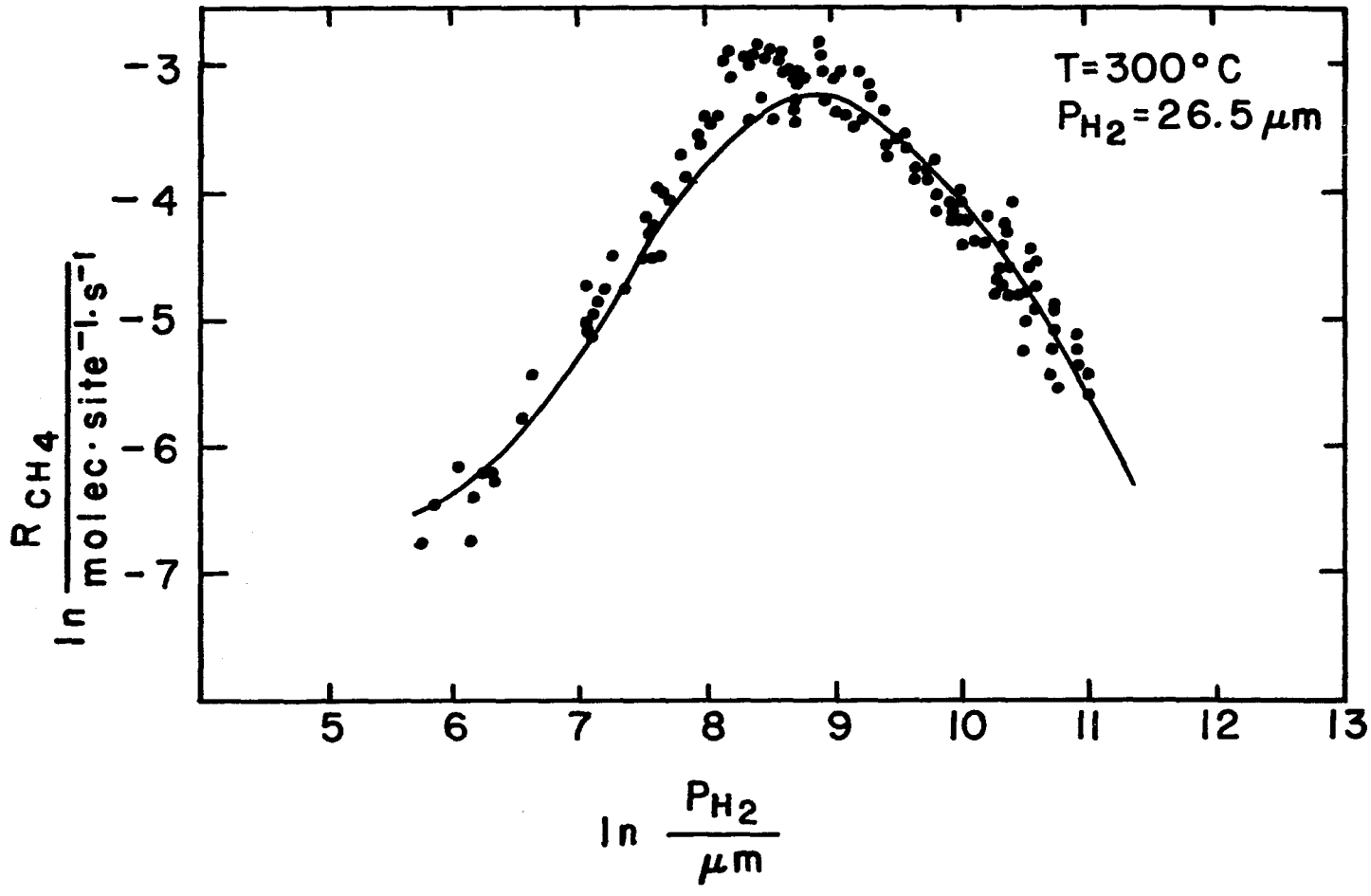

Figure 31. The fit of the theory to a hydrogen order plot with [CO] = 26.5 μm.

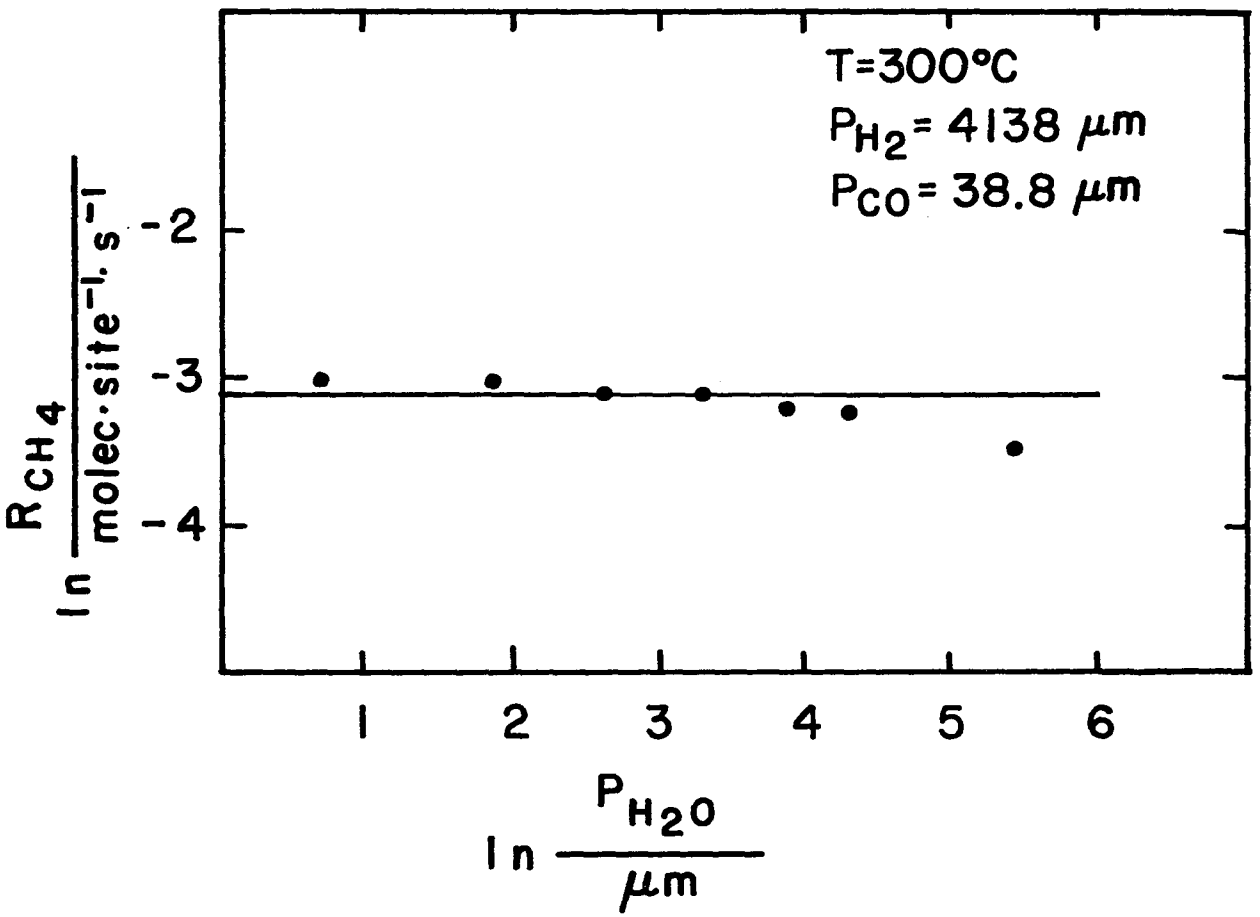

Figure 32. The fit of the theory to a water order plot with $[H_2]$ = 4138 μm and [CO] = 38.8 μm.

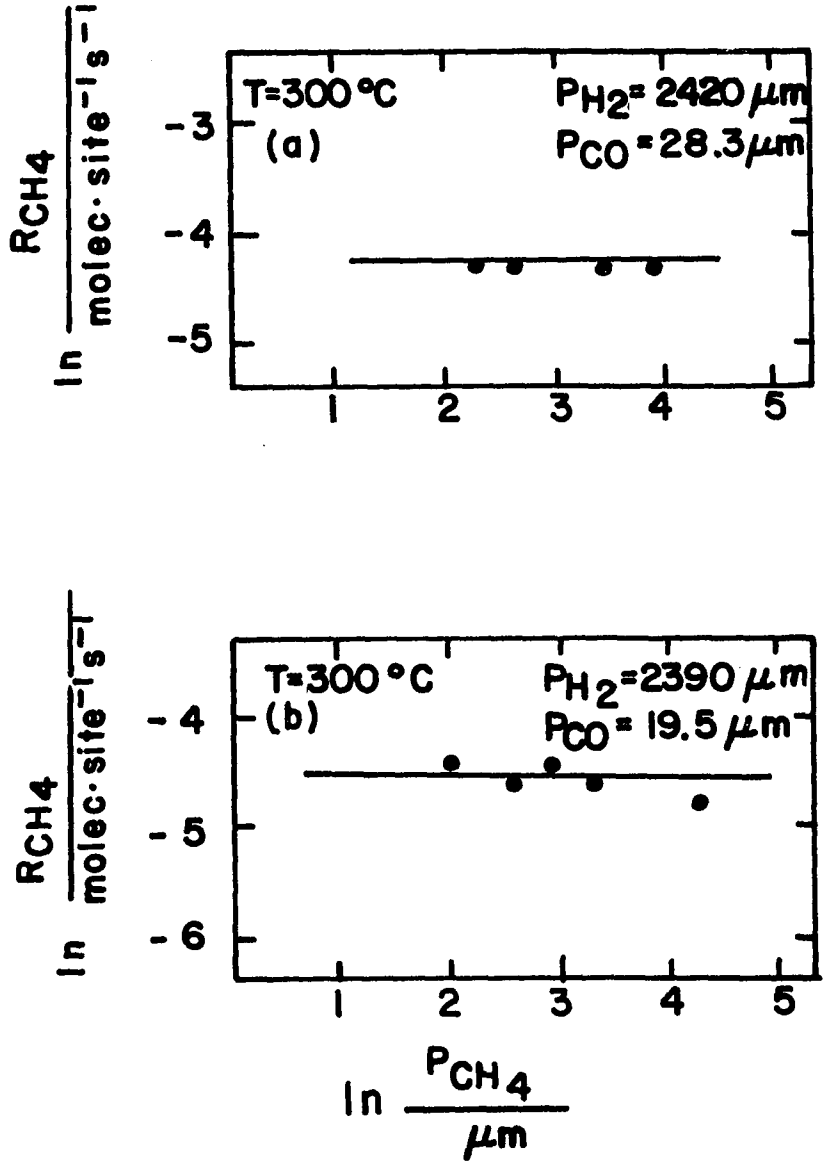

Figure 33. The fit of the theory to two methane order plots: (a) $[H_2]$ = 2420 μm and $[CO]$ = 28.3 μm, (b) $[H_2]$ = 2390 μm and $[CO]$ = 19.5 μm.

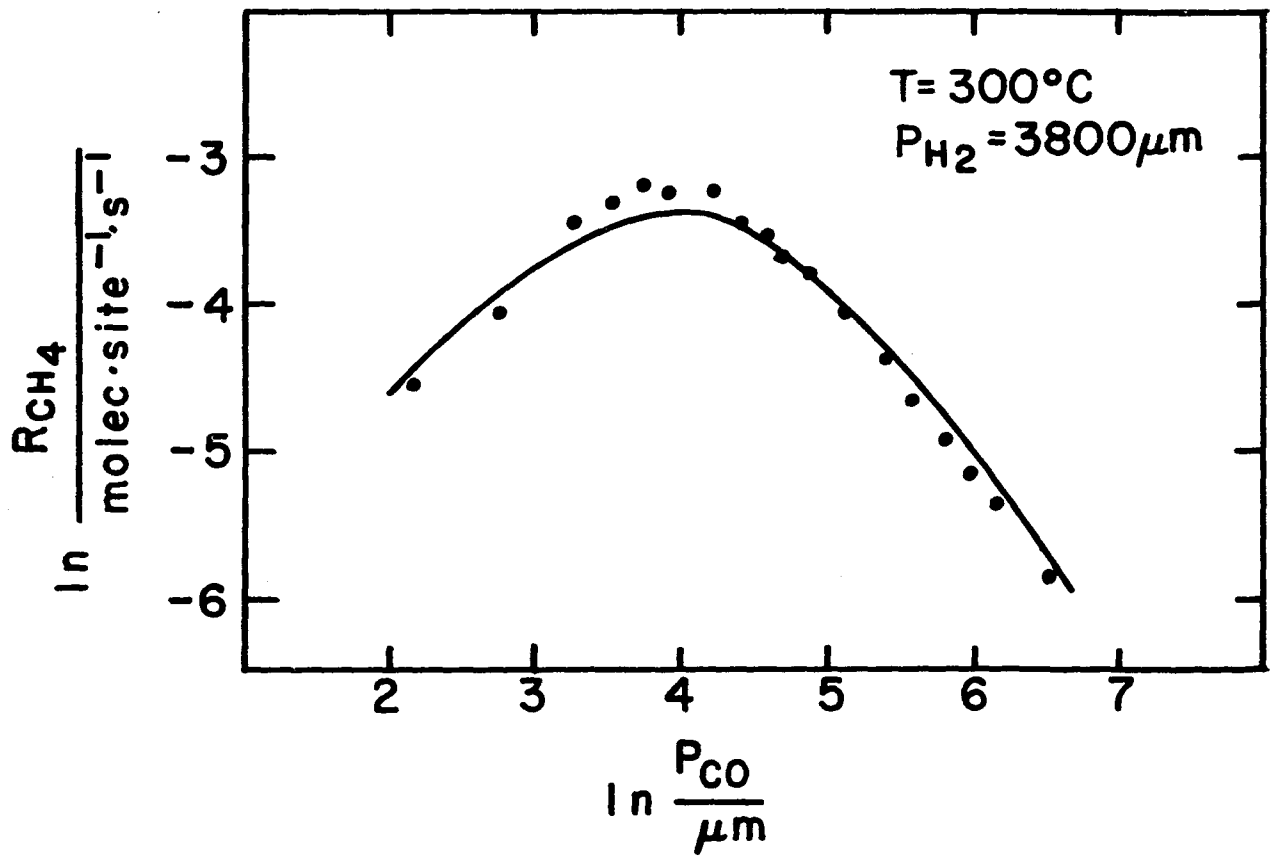

Figure 34. The fit of the theory to a carbon monoxide order plot with $[H_2]$ = 3800 μm.

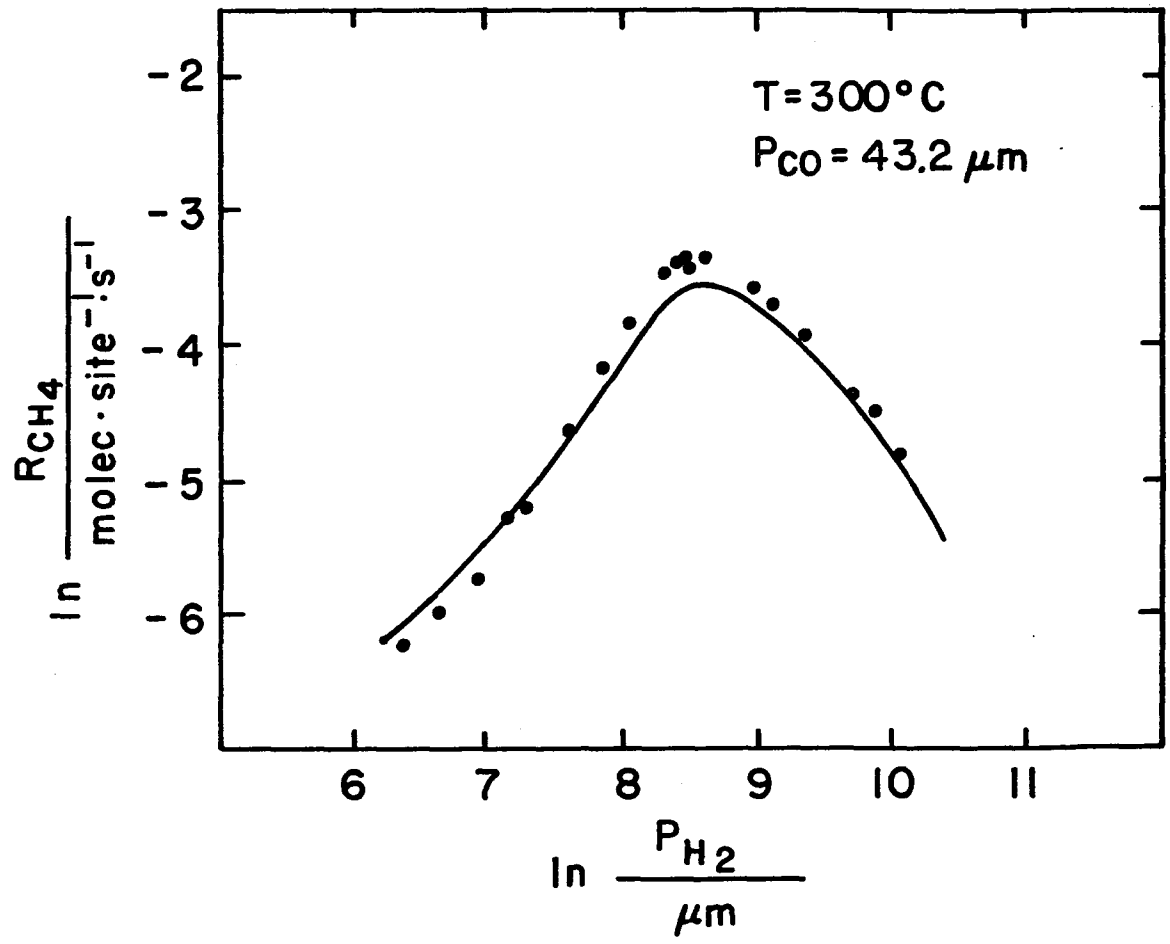

Figure 35. The fit of the theory to a hydrogen order plot with [CO] = 43.2 μ m.

however, was not done. No attempt was made to fit all of the data collected quantitatively. However, all data were in qualitative agreement with the theory.

Some comparisons among these figures can be made which demonstrate that the theory correctly predicts several trends relative to the reaction rates and the pressures of carbon monoxide and hydrogen. Figures 30 and 34 are carbon monoxide order plots taken at different hydrogen pressures. The rate at a hydrogen pressure of 3800 μm peaks at a rate of 0.035 molec$\cdot$site^{-1}s^{-1}. When the hydrogen pressure was increased to 4150 μm the maximum in the rate occurred at 0.043 molec$\cdot$site^{-1}s^{-1}. It can be observed in Figure 31 that both of these hydrogen pressures lie in the positive order region with respect to hydrogen, so an increase in hydrogen pressure would be expected to increase the rate for any given carbon monoxide pressure. The comparison of the peak maxima can be made since they occur at the same carbon monoxide pressure.

The hydrogen order plots can be compared in a similar manner (Figures 31 and 35). At a carbon monoxide pressure of 26.5 μm the maximum rate occurs at 0.041 molec$\cdot$site^{-1}s^{-1} whereas at 43.2 μm of carbon monoxide the peak is at 0.029 molec$\cdot$site^{-1}s^{-1}. Both of these carbon monoxide pressures lie in the positive order region in Figure 30. Therefore, the variation of rate with carbon monoxide pressure in a hydrogen order plot is as expected.

A careful examination of the relationships between the coefficients in the rate expression and the rate constants and equilibrium constants allows an approximation of the values of two equilibrium constants and one rate constant. From the value of C it is evident that $K_1 = 1 \times 10^{-6}$ μm^{-1}.

From D a value of $K_{12} = 3x10^{-6}\ \mu m^{-1}$ is obtained. These are considered good approximations but not absolute numbers because of the problem in determining C and D discussed previously. The final mechanism includes three steps that lead to the production of methane. It is believed, however, that the major pathway to methane production is step 8 of the mechanism. If this is assumed to be the case then $k_8K_1K_7 \gg k_{13}K_{12} + k_{16}K_{12}K_{15}$ and the value of k_8 can be calculated from the coefficients A and J. It is evident that $A/J = K_1^{1/2}k_8$. This yields a value of $k_8 = 4.77$ molec·site^{-1}s^{-1}.

It is difficult to comment upon these values since equilibrium constants and rate constants for surface reactions are not generally available. A value for the equilibrium constant K_1 has been reported on iridium thin films [105]. At 373K the value was reported to be 2.5 μm^{-1} while at 473K the value was approximately $2x10^{-2}\ \mu m^{-1}$. These values are obviously higher than that of this study. It must be kept in mind, however, that this work involves ruthenium rather than iridium and that the temperature was 573K. A value of $1x10^{-6}\ \mu m^{-1}$ is certainly not unreasonable when compared to the iridium results. It has been reported [106] that hydrogen flashes off ruthenium by 373K. Since this study was conducted at a temperature well above the desorption temperature the coverage of adsorbed hydrogen atoms would be expected to be quite low. The value of $K_2 = 3x10^{-6}\ \mu m^{-1}$ seems also to be in the correct range. A first glance might suggest that it should be approximately equal to K_1 since both involve the adsorption of two hydrogen atoms on ruthenium. No reported value of this equilibrium constant is available for comparison.

Before discussing the value of k_8 it might be useful to convert to the more conventional units of molec·cm^{-2}s^{-1}. This requires an estimate of the number of sites per cm^2 of catalyst surface area. The total number of sites was 2.54×10^{17}. If the surface area of the film is estimated at 250 cm^2 then a site density of 1×10^{15} sites/cm^2 is obtained. The 250 cm^2 represents the calculated internal surface area of the glass bulb. Actually, since the film is known to have many grain boundaries the density of sites might be expected to be higher. Competing with this effect is the apparent removal of sites by the type 2 carbon discussed earlier. Effectively these two phenomena cancel one another such that the actual density of sites is within an order of magnitude that of a relatively smooth surface. This density of sites leads to a value of $k_8 = 4.77 \times 10^{15}$ molec·cm^{-2}s^{-1}. In general, it has been observed that rate constants for bimolecular surface reactions (like step 8) tend to fall in the 10^{12} to 10^{16} molec·cm^{-2}s^{-1} range. The value reported here is certainly well within that range.

From the value of $k_8 = 4.77$ molec·site^{-1}s^{-1} and the value of 21.9 kcal/mole for the activation energy of the reaction at 573K the preexponential factor a may be calculated ($k = ae^{-E_a/RT}$). A value of $a = 9.5 \times 10^8$ is obtained. This is in excellent agreement with the value of 5.9×10^8 reported by Vannice for the methanation reaction on supported ruthenium [38]. This value of a falls within the rather broad range of values expected for a process that is surface reaction controlled [107]. The agreement between the rate constant of this study and that reported by Vannice suggests at least some agreement between this theory and the

data already available in the open literature. It also suggests that the assumption that step 8 of the mechanism is the major pathway to methane production is reasonable.

The equations developed previously can be used to predict the relative coverages of the various intermediates during the reaction process. This was done at different pressures of carbon monoxide and hydrogen. It is interesting to note that the coverages of those species which are reactive intermediates (RuH, RuH_2, $RuCH_2$ and $RuCH_3$) pass through maxima as the pressure of one gas is held constant and the other is varied. A graph of coverage versus pressure of reactant would look very much like the order plots of carbon monoxide and hydrogen. On the other hand, the coverages of the reversible poisons RuH_4 and RuH_2CH_2 increase with the pressure of each reactant gas.

The coverage of $RuCH_3$ is generally considerably higher than that of any other reactive intermediate. This is reasonable since the rate limiting step involves its removal. This observation lends additional support to the postulation that of the three possible pathways to methane production, step 8 of the mechanism accounts for most of the methane produced. One might argue that step 13, which involves the interaction of $RuCH_2$ and RuH_2 to yield methane, is sufficiently fast that most of the $RuCH_2$ is removed *via* this route. This is unlikely since $RuCH_2$ is a precursor to $RuCH_3$. If the $RuCH_2$ were being removed *via* an alternate route then the coverage of $RuCH_3$ would not be expected to build up. Also, since $RuCH_2$ and $RuCH_3$ are in dynamic equilibrium, any process which had the effect of removing the $RuCH_2$ at a rapid rate compared to the production of $RuCH_3$

would lead to the depletion of the $RuCH_3$ species. It might be possible to expect that step 16 could lead to significant amounts of methane. This would be expected to occur only under conditions where the fractional coverage of vacant sites was relatively high. The rate of methane production has been observed to peak at a hydrogen pressure of about 5 torr when the carbon monoxide pressure was 26.5 μm (Figure 31). Surface coverage calculations indicate that under these conditions ample vacant sites are available up to a hydrogen pressure of about 15 torr. The peak maximum in the hydrogen order plot seems to occur at too low a hydrogen pressure to expect step 16 to occur at an appreciable rate.

Perhaps the most surprising piece of information to result from these calculations is the very low coverage of the reactive forms of hydrogen. At 573K the sticking coefficient of hydrogen on ruthenium is extremely low. However, sufficient hydrogen must be available to rapidly remove the oxygen as water, leaving behind $RuCH_2$ as predicted by the surface characterization work. Also, sufficient hydrogen must be available to convert the $RuCH_2$ to $RuCH_3$. The pathways that lead to product formation are severely limited by the observed kinetics. In order to satisfy the Langmuir-Hinshelwood kinetics as well as to meet the stoichiometric requirements of the reaction the water and methane must be produced <u>via</u> the interactions specified in steps 6 and 8 of the mechanism (ignoring steps 13 and 16). All other steps have been written involving RuH attack of the various intermediates. Since all steps except those leading to products are treated as equilibria, the hydrogen could also be supplied by either of the reversible poisons or by gas phase hydrogen. Such steps are kinetically indistinguishable from

those listed in the mechanism. A few examples are as follows:

$$RuCO + H_2 \rightleftarrows RuCHOH$$

$$RuCH_2 + RuH_2CH_2 \rightleftarrows RuCH_3 + RuHCH_2$$

$$RuC + RuH_4 \rightleftarrows RuCH_2 + RuH_2$$

Quite a few other steps could also be written since any of the intermediates could be interconverted using any of the above hydrogen donors. Keep in mind that this applies only to those equilibrium steps that convert one intermediate into another and not to those irreversible steps that lead to products. With these possibilities the supply of reactive hydrogen is actually quite a bit higher than predicted by the surface coverage calculations for RuH and RuH_2.

Since the coverages of RuH and RuH_2 are relatively low at all times, it might be useful to consider why the coverages of RuH_2CH_2 and RuH_4 seem so high under certain conditions. In fitting the data to the theory it was observed that the total $[H_2]^2$ dependence of the denominator was very critical in getting a good fit to the hydrogen order plot. This says that N[CO] + P (from equation (133)) could be accurately determined. The relative magnitude of each term, however, was less critical for getting a reasonable fit to both the hydrogen and carbon monoxide order plots. Since it was known from Auger studies as well as kinetic results that the amount of carbon remaining on the surface after a kinetic run generally decreased with increasing hydrogen pressure it was felt that the contribution of the RuH_4 term should be maximized relative to the RuH_2CH_2 concentration. As a result the relative coverages of these two poisons are approximately equal under most conditions. The fit to the kinetic

order plots remains essentially unchanged, however, if the coverage of RuH_4 is decreased (P becomes smaller) and the coverage of RuH_2CH_2 is increased (N becomes larger). In fact, the values $N = 4.91 \times 10^{-10}$ and $P = 0$ could be used to predict order plots that fit the data just as well as when the values were as listed in Table 10. This suggests that the RuH_4 could be quite a bit lower than the RuH_2CH_2 and might even be comparable to the coverages of the RuH and RuH_2 intermediates. The structures of these adsorbates will be discussed shortly.

One final comment concerning enhanced adsorption should be made. It was observed that when one reactant was held constant and the pressure of the other was increased the coverage of both hydrogen and carbon containing intermediates was increased. This suggests a fairly strong interaction between the adsorbed gases and has been seen previously [49].

A model has been developed which quantitatively fits the kinetic data and qualitatively predicts all other observations made during this study. Step 1 involves the dissociative adsorption of hydrogen on ruthenium. Hydrogen which had been adsorbed on ruthenium (0001) at 100K was found to desorb with second order desorption kinetics in the 350 to 450K range [82]. Second order desorption kinetics suggest dissociative adsorption. Also, this mode of bonding is consistent with the observed hydrogen-deuterium exchange that occurred on the catalyst at 573K. This structure for adsorbed hydrogen with a H_{ads}:Ru ratio of about 1 has been suggested by Dalla Betta [69] and Taylor [70].

That other types of hydrogen bonding on ruthenium can occur simultaneously with that discussed above was suggested by Gostunskaya, et al. [108]. Indeed the work of Ghoneim, et al. [71] and Kubicka [72] suggests

that two hydrogen atoms can be simultaneously bound to a single ruthenium site as suggested in step 12.

Bulk ruthenium atoms, being in a hexagonal close packed structure, have a coordination number of 12 (number of nearest neighbors). Those atoms at the surface of a smooth plane have 9 nearest neighbors. The electron micrograph of this catalyst suggests a very high density of grain boundaries in this thin film. This suggests a high density of edge sites where a ruthenium atom may be bound to as few as 4 or 5 nearest neighbors. Such an atom is very highly uncoordinated and has many bonding sites (orbitals) available. It is not at all unreasonable then to expect multiple bonding to these ruthenium atoms. Such a structure involving hydrogen atoms is suggested in step 14 in which 4 hydrogen atoms are bound to one ruthenium atom. Hydrogen normally flashes off of ruthenium by 373K. Therefore any adsorbed hydrogen under reaction conditions must result from the shift of the adsorption equilibria (steps 1, 12 and 14) to the right at the elevated hydrogen pressures used in this study. When the system is pumped this hydrogen most certainly flashes off.

The carbon monoxide-ruthenium interaction has been the subject of several recent investigations and there is some disagreement as to whether the adsorption process results in adsorbed molecular carbon monoxide or dissociated carbon monoxide. Two field emission studies of the adsorption of carbon monoxide on ruthenium have been reported [83, 109]. Both involve the adsorption of carbon monoxide at about 100K. The tips were heated and were found to be clean at about 500K. Both authors reported that there was no indication that decomposition of carbon monoxide was

involved. The Kraemer and Menzel work also suggested that the carbon monoxide adsorption was not face specific. From the results of a flash desorption study of carbon monoxide on ruthenium (0001) Madey and Menzel [85] concluded that adsorbed carbon monoxide is non-dissociated. They were able to model their data quite well using first order desorption kinetics. An interesting observation was made during the LEED studies reported in this paper. An electron beam induced effect was observed in which molecularly adsorbed carbon monoxide was dissociated by the LEED beam. A more thorough study of this effect was made by Fuggle, et al. [110] and it was concluded that molecularly adsorbed carbon monoxide cannot be thermally dissociated at carbon monoxide pressures below $1x10^{-5}$ torr. Such a state could, however, be produced by electron impact onto a virgin carbon monoxide layer adsorbed on ruthenium. An XPS/UPS study by the same group led to the conclusion that carbon monoxide adsorbs on ruthenium non-dissociatively [81]. The same conclusion was reached by Bonzel and Fischer [111] as a result of a UPS study of carbon monoxide adsorption of ruthenium $(10\bar{1}0)$. Ku, et al. [103] have studied the same surface using LEED, AES and flash desorption and also concluded that carbon monoxide bonds molecularly to ruthenium. A very interesting study was reported by Reed, et al. [88] in which $^{18}O_2$ and carbon monoxide were coadsorbed on a ruthenium $(10\bar{1}1)$ single crystal at 300K. The sample was heated and the carbon monoxide that desorbed contained no labelled oxygen. The results of a flash desorption study involving carbon monoxide on ruthenium (1100) were recently reported by Goodman, et al. [86]. Their data could be fit quite nicely using first order desorption kinetics

which are indicative of non-dissociated carbon monoxide. These results are in agreement with those of Madey and Menzel on ruthenium (0001).

Several infrared studies involving carbon monoxide on supported ruthenium catalysts have been reported recently [112-116]. Each reports that the carbon monoxide molecule is non-dissociated on ruthenium. The paper by Brown and Gonzalez [113] alludes to the possibility that some of the molecules could be bound *via* the oxygen atom. This method of bonding was also favored in a recent series of papers by Sapienza, *et al.* [117, 118] in which they reported a generalized methanation reaction for most active metals. Although there are certainly electrons associated with the oxygen atom such that this mode of bonding could occur it is not believed to be a reasonable intermediate for the methanation reaction for two reasons. First, if the bonding of molecular carbon monoxide occurred through the oxygen atom, a very electron deficient carbon atom would result. This species would quite likely be very unstable. Secondly, the mechanism suggested by Sapienza, et al. involves the removal of the carbon atom *via* attack by adsorbed hydrogen atoms to leave an oxidized ruthenium surface. There is no evidence to support this. To the contrary, the vast majority of the data suggest carbon covered ruthenium catalysts after the methanation reaction has occurred on them.

Two recent studies have concluded that indeed carbon monoxide does not bond to ruthenium molecularly but the molecule dissociates upon adsorption. Singh and Grenga [119] observed that if single crystal ruthenium spheres were exposed to carbon monoxide, 1 atm. at 823K, for 6-96 hours a graphite layer was deposited. They concluded that the carbon monoxide

was adsorbed dissociatively and observed that the more active sites for the dissociation were the atoms located at surface steps. Rabo, et al. [120] performed a series of experiments involving the exposure of a 1.2% Ru/SiO_2 at 673K to several torr of carbon monoxide. They observed that this treatment produced a catalyst with a surface carbon coverage of about 0.8 with the remainder of the surface being covered with undissociated carbon monoxide. Subsequent dosing to this surface with hydrogen indicated that some of the surface carbon was converted to methane. This led to the conclusion that carbon monoxide is adsorbed dissociatively on ruthenium.

At first glance, these results which led to the conclusion that carbon monoxide adsorbs dissociatively on ruthenium might seem to contradict the work which suggested that carbon monoxide bonds non-dissociatively to ruthenium. However, this is not really the case. All of the work which reported non-dissociated carbon monoxide, except the infrared studies, was conducted at very low carbon monoxide pressures ($\leq 1 \times 10^{-5}$ torr) with the catalyst generally at room temperature or below when the gas was dosed. The infrared work was generally conducted at room temperature with an ambient carbon monoxide pressure of about 5 torr. The work that led to the conclusion that carbon monoxide adsorbs dissociatively was conducted at 673-873K with substantially higher carbon monoxide pressure (10-760 torr). Since the experiments were conducted under such different conditions it is quite likely that different surface processes are occurring which led to the different conclusions concerning the mode of bonding of the carbon monoxide to the ruthenium. That such a situation exists for carbon monoxide adsorption on tungsten has been discussed by Anders and Hansen [121].

Several studies were performed in this work to characterize the bonding of carbon monoxide to the ruthenium catalysts. The XPS studies in which carbon monoxide and oxygen were individually dosed onto the catalyst yielded a binding energy difference of 1.5 eV for the oxygen 1s electrons. This suggests that different modes of bonding are involved in the adsorption of these gases to ruthenium, lending support to the molecularly adsorbed carbon monoxide structure. Isotopic exchange studies were conducted in which the exchange occurred over a wide pressure range suggesting that the carbon molecule might be adsorbed dissociatively. The exchange rate was found to drop with increased hydrogen pressure in the feedstream suggesting that either the percent of the adsorbed carbon monoxide that was dissociated was decreasing with increased hydrogen pressure or that the oxygen was removed as water before the exchange could occur. The latter could occur via the interaction of adsorbed oxygen atoms with hydrogen (a process which is known to occur from the work of Ku, et al. [103] and from the Auger portion of this work) or via the interaction of molecularly adsorbed carbon monoxide with hydrogen to produce water and a carbonaceous residue. It is qualitatively correct that in a flash desorption study where only the dose is varied, the peak maximum temperature is independent of dose for first order desorption kinetics whereas for a second order desorption process it systematically decreases with increasing dose [57]. If this argument is applied to the carbon monoxide flash studies then a first order desorption process is found to be involved suggesting molecularly adsorbed carbon monoxide.

Consider the following reaction sequence:

$$Ru + CO \rightleftarrows RuCO$$

$$RuCO + Ru \rightleftarrows RuC + RuO$$

Since dissociation is a thermal process, the second step would be expected to occur only when the carbon monoxide coverage was high enough to cause substantial coverage at elevated temperatures. If it is assumed that the second step is necessary for methanation to occur then a mechanism may be written involving the adsorption and dissociation of hydrogen as well as the adsoprtion and dissociation of carbon monoxide with the subsequent hydrogenation of the carbon and oxygen adatoms to produce methane and water. Attempts were made to fit various forms of this mechanism to the observed kinetics. It was found that whenever the carbon monoxide dissociation step was involved, a rate expression was obtained, using the mathematical approach discussed earlier, in which the maximum carbon monoxide order was +0.5. A maximum carbon monoxide order of +1 was experimentally observed. This is a general consequence of the Langmuir model and is discussed briefly in Appendix II. Steady state kinetics were also investigated in conjunction with the mechanism involving dissociated carbon monoxide and once again no suitable fit to the kinetic data was obtained. It should be mentioned, however, that the steady state approach generated a large number of fairly complex expressions and in some cases the simultaneous solution of these expressions to yield a rate expression was not possible. Since it was apparent that the inclusion of the step involving the dissociation of adsorbed carbon monoxide yielded results which could not be fit to the kinetics, the mechanism involving undissociated carbon monoxide was developed.

The carbon monoxide adsorption step is represented as step 2 in the mechanism. The molecule is bonded in a linear fashion to a single ruthenium atom. Upon adsorption, the oxygen is rapidly removed by the successive attack of adsorbed hydrogen to ultimately yield $RuCH_2$ and H_2O (steps 3-6). The production of carbon dioxide is taken into account in step 9 in which two adsorbed carbon monoxide molecules interact. If the lateral interaction model proposed by Madey, et al. [102] to describe the exchange of undissociated carbon monoxide on tungsten is invoked then the exchange results are explained. If the dissociative model is used to describe the exchange results then it must be assumed that only a small fraction of the adsorbed carbon monoxide is dissociated. The major portion of the adsorbed carbon monoxide must be bound in the non-dissociated form. This is required in order to get a fit to the kinetics. The existence of oxygen containing intermediates is supported by the observation that methanol can be converted to methane at about the same rate as carbon monoxide.

It is quite likely that rather than having a simple dissociation step in which molecularly adsorbed carbon monoxide is converted to carbon atoms and oxygen atoms, a chemical reaction is occurring which results in the removal of the oxygen to produce a carbon overlayer. Kinetically this process would be favored at elevated temperatures and increased reactant pressure, exactly the conditions under which results have been obtained that led to the conclusion of dissociative adsorption.

It would be expected that the carbon monoxide disproportionation reaction would be most likely to occur on metals which form stable bulk

oxides and carbides. The formation of ruthenium oxides has been found to occur readily at 573K. This was discussed in the Auger results section. However, the formation of ruthenium carbide is very difficult to achieve. Liquid ruthenium dissolves carbon, which upon cooling is precipitated in the form of graphite [122, 123]. The solubility of carbon in molten ruthenium increases with temperature and at the boiling point of the metal it is 4.8%. It has been shown from an x-ray study of the products of the reaction of ruthenium with carbon that on heating a mixture of ruthenium and carbon black in the proportions of 1:10 in a helium atmosphere at 2873K for four hours, a product was formed whose x-ray diffraction pattern indicated a new phase identified as RuC [94, 124]. Nickel is another metal which is an active catalyst for the methanation reaction. It has been postulated that on nickel the reaction occurs via the dissociative adsorption of carbon monoxide. This is a reasonable prediction since, in contrast to ruthenium, the formation of bulk nickel carbides is easily accomplished [125].

Step 6 of the mechanism leads to the production of water and is represented as an irreversible step. This is suggested by the kinetic order of zero for water. A recent study of the interaction of water with ruthenium (0001) found that water which had been adsorbed at 100K was completely flashed off the sample by 250K [126]. This same study also indicated that the water was bound non-dissociatively via the oxygen atom. Since the experiments in this study were generally conducted at 573K it is not surprising that there is no detectable interaction between the catalyst and the water.

Since it is generally believed that carbon monoxide does not spontaneously dissociate on ruthenium, most of the structures that have been proposed for the intermediates of the methanation reaction contain oxygen, carbon and hydrogen atoms and are very similar to those proposed in steps 3-6 of this mechanism. Various flash desorption and kinetic studies have led to the conclusion that such structures are involved in the methanation reaction [33, 49, 86]. Each of these authors favors a methanation process involving the release of water from the intermediate resulting in an adsorbed carbonaceous material which is subsequently hydrogenated to methane as in steps 7, 8, 10, 11 and 13 of the mechanism proposed in this study.

The production of methane is treated as an irreversible step because, like water, methane has a zero kinetic order dependence. Several studies have been performed in an effort to understand the interaction of methane with various metal surfaces. The results suggest that on all metals studied the interaction is very weak. A recent study using ruthenium black has reported the isotopic exchange between CH_4 and D_2 [127]. This suggests that perhaps the step yielding methane should be written as slightly reversible to allow for this exchange process.

The relatively unique intermediate proposed in this mechanism is the RuH_2CH_2 produced in step 15. In order to fit the kinetics a species was required whose surface concentration varied as $[H_2]^2[CO]$. Such a species must by necessity contain four hydrogen atoms. The most reasonable structure of this surface species is as indicated in step 15 of the mechanism (equation (121)). Obviously, any ruthenium atom involved in

this sort of bonding would have to be relatively uncoordinated. There must be sufficient orbitals available to form four bonds. Let us assume the crystallite surfaces to be low index planes where there are generally nine nearest neighbors to a surface ruthenium atom. Since these atoms have three vacant coordination sites, RuH_2CH_2 would not be expected to exist on the crystallite planes. The grain boundaries, however, contain atoms which are more uncoordinated than those in the planes. There should be ample bonding orbitals available for the formation of the intermediate. The result is that this intermediate would be expected to preferentially adsorb on the relatively uncoordinated surface atoms associated with the grain boundaries. Since the electron micrograph indicated that the single crystal grains are quite small, it is reasonable to expect that a very large portion of the catalyst surface area involves grain boundaries. This could result in a fairly large coverage of RuH_2CH_2 under the proper conditions.

There is some precedence for assuming an intermediate of this sort. Kraemer and Menzel [128] have proposed a structure in which one carbon monoxide molecule and two hydrogen atoms are bound to a single ruthenium atom. Since this result arose from a field emission study and not a kinetic investigation, the kinetic implications of such a surface species were not discussed. As a result it is not certain whether this species would function as a surface poison or if perhaps under the conditions of the study it was an active reaction intermediate. In a different study involving the ruthenium catalyzed transformation of carbon monoxide into polymethylene (at a H_2:CO ratio of 2 and a total pressure of 1100 atm.

and 393K), Pichler detected the presence of $H_4Ru_4(CO)_{12}$ which was associated with a loss in catalytic activity [129]. It is not surprising that under the conditions of Pichler's work the surface poison was rich in carbon monoxide whereas under the conditions of this work the surface poison is rich in hydrogen. Although there is considerable difference between the structure of Pichler's poison and the one proposed in this mechanism, it does exemplify a case in which a ruthenium carbonyl hydride was formed under Fischer-Tropsch conditions and had the effect of blocking surface sites. In general the method of preparation for many metal carbonyl hydride compounds is to convert the metal to a metal carbonyl and then to react it with molecular hydrogen to yield the carbonyl hydride [130]. This is similar to the method in which RuH_2CH_2 was prepared beginning with ruthenium metal, forming a ruthenium methylene structure via interaction with hydrogen and carbon monoxide and then reacting with hydrogen to produce the ruthenium methylene hydride.

A plausible bonding model for the RuH_2CH_2 species proposed in this work can be developed. As has already been mentioned, the ruthenium atom involved is relatively uncoordinated. The bonding involved in bulk ruthenium has been discussed by Trost [131]. The electronic configuration of ruthenium is $[Kr]5s^14d^7$. Each bulk ruthenium atom has 12 nearest neighbors: 3 above, 3 below and 6 in the same plane. The bonding of the central atom to the 3 above and the 3 below is believed to involve d^5p hybridization. The bonding directions are toward the corners of a trigonal prism as shown in Figure 36(a). The solid lines represent the bonding lobes from the central atom to the nearest neighbors above and below. The

dashed lines represent d^5p hybrid orbitals between atoms other than the central atom. The bonding of the central atom to the 6 nearest neighbors in the same plane occurs via sp^2 hybridization as shown in Figure 36(b).

Of course, surface atoms are less coordinated than the central atom considered in this discussion. If the top 3 atoms in Figure 36(a) are removed then a smooth surface results with the central atom of the previous discussion at the surface. Since it has been previously concluded that the RuH_2CH_2 structure is most likely associated with the atoms of the grain boundaries a different "surface" must be considered. Once again, Figure 36(a) will be considered. The 8 atoms marked with an X will be removed and the bonding to the original central atom will be modeled. The method developed by Bond [132] and used extensively by Weinberg and Merrill [133] to model the emergence of orbitals from surface atoms will be used to describe the bonding of the RuH_2CH_2 structure. Figure 36(c) shows the 5 remaining atoms with the d^5p hybrid orbitals explicitly drawn in. The solid lines represent the hybrid orbitals from the central carbon atom to the remaining nearest neighbor above and below. The 4 lobes represent d^5p hybrid orbitals coming out of the surface. Clearly, these orbitals were involved in bonding to the two nearest neighbors above and below which have been removed. The angles between the orbitals are indicated. Each orbital makes an angle of 38° to the surface.

If it is assumed that the carbon atom of a methylene group is sp^3 hybridized then its structure is as shown in Figure 36(c). Note that the sp^3 lobes are positioned at 109° angles whereas the d^5p lobes are 104° apart. This allows for a great deal of overlap and should result

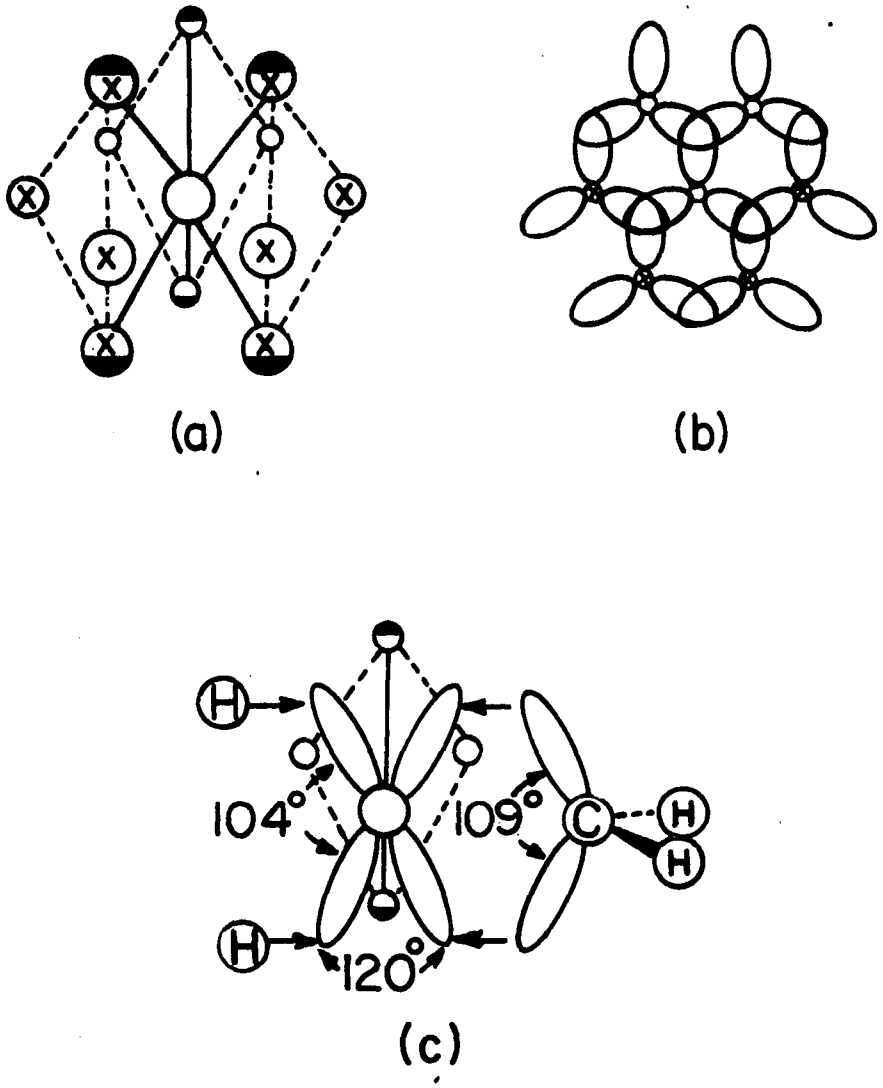

Figure 36. The bonding involved in the RuH_2CH_2 structure:
(a) d^5p orbitals involved in bonding a central atom to the nearest neighbors above and below,
(b) sp^2 hybrid orbitals involved in bonding a central atom to the nearest neighbors in the same plane,
(c) surface orbitals involved in the RuH_2CH_2 structure

in a fairly stable bond. The additional two hydrogen atoms are bound to the remaining lobes of the d^5p hybrid. By using the known structure of bulk ruthenium the distance between the carbon of the methylene and one of these hydrogen atoms was found to be 3.45 $\mathring{A}$. This is a fairly long distance over which to expect an interaction to occur and could account for the predicted stability of this species under reaction conditions. The d^5p and sp^2 hybrid orbitals need 9 electrons to have 1 electron per orbital. Since ruthenium has only 8 valence electrons, the structure is somewhat electron deficient. If it is assumed that there are 6 electrons in the d^5p orbitals and 2 electrons in the sp^2 orbitals then it can be quite easily shown that the sp^2 orbitals at the surface of structure (c) in Figure 36 contain no electrons. As a result they were not considered in the overall bonding model.

Previous results (Figure 26) have demonstrated that when the system was pumped some of the carbonaceous material on the surface was removed. The amount of material removed seems to increase with time up to about 300 seconds. Very likely, when the surface is exposed to vacuum the hydrogen which was attached to ruthenium atoms is desorbed. During the process of pumping the gas phase carbon monoxide is removed. This might shift some surface equilibria such that some carbon containing intermediates are removed. It is believed that pumping destabilizes the high pressure poison RuH_2CH_2. This would account for the removal of substantial amounts of carbon during the pumping period.

As a result of the Auger and kinetic studies it was determined that two types of carbon with quite different reactivities were associated

with the catalyst. Type 1 was the reactive form which was removed by a combination of pumping followed by a "standard hydrogen dose". This carbon is believed to be that associated with all of the intermediates proposed in the mechanism (including RuH_2CH_2). Type 2 was relatively unreactive and could be removed only after exposure to hydrogen for long periods of time (48 hours). There are two likely modes for binding this carbon to the ruthenium. Some carbon could be dissolved in the first few layers of the bulk. Migration out of the bulk would very likely be a relatively slow process and would account for the observed low reactivity. Some carbon could also be bound to the surface so tightly as to make its removal very difficult. This would likely occur in cases in which the carbon could simultaneously bond to several carbon atoms. Such sites are very likely available, especially near the bottom of a crevice or a grain boundary.

Overall, the surface is modeled as a combination of very rough grain boundaries with relatively smooth crystallites. The rough areas are generally good sites for the formation of the reversible poison RuH_2CH_2 and the strongly bound type 2 carbon. The smooth crystalline areas are believed to be sites that convert carbon monoxide and hydrogen to methane. Also, those grain boundary sites which are not blocked are believed to be active for methanation.

Quite a bit has already been said about those studies that tend to support the conclusions drawn in this work. However, very little has been said about those who disagree with a mechanism involving non-dissociated carbon monoxide. Perhaps the most convincing study which concluded

that methane is produced from carbon monoxide and hydrogen *via* a dissociated carbon monoxide molecule was that of Araki and Ponec on nickel [46]. Two subsequent papers by van Dijk, *et al.* [134] and Ponec [135] discussed the same system. These authors performed a fairly wide variety of experiments and came to the conclusion that the hydrogenation of adsorbed carbon atoms resulting from dissociated carbon monoxide was the major pathway to methane production. They performed no kinetic studies but commented that their mechanism was consistent with known kinetic results. They chose to describe the known kinetics by the same expression used to describe some of the kinetic studies discussed earlier (equation (9)). Ponec chose to consider the case with $m > 0$ and $n < 0$. It is quite likely that his mechanism could be fit to this expression. First of all the orders of the reaction are constant indicating that the data were taken over a fairly narrow pressure range and secondly, the region of the carbon monoxide order plot that cannot be fit by a dissociative adsorption process is the positive order region which was eliminated from consideration by choosing $n < 0$. Data exist for nickel which indicate a +1 order dependence at low carbon monoxide pressures [42]. At least one subsequent study has also concluded that dissociative adsorption of carbon monoxide leads to methane production on nickel catalysts [136].

It is very tempting to conclude that since the recent studies involving methanation on nickel suggest dissociative carbon monoxide adsorption the same sort of process is involved in the methanation reaction over other metals. Ekerdt and Bell [47] have recently proposed a dissociative carbon monoxide adsorption methanation process on ruthenium. Their work

involved infrared studies combined with very limited kinetic work. The infrared work suggested the presence of chemisorbed carbon monoxide structures with frequencies very close to those reported in the infrared work already discussed. Some additional bands near 3000 cm^{-1} were attributed to C-H stretching vibrations. The kinetic orders were +1.5 in hydrogen and -0.6 in carbon monoxide. Bell concluded that the adsorbed carbon monoxide was not an intermediate in the methanation reaction, although he could quite easily remove it by hydrogenation. He postulated that the structures causing the bands at 3000 cm^{-1} were adsorbed methyl and methylene groups and were active intermediates in the methanation reaction. This is quite likely correct, but the justification for concluding that these structures must result from dissociatively adsorbed carbon monoxide is not at all clear. Bell proposed a mechanism in which carbon monoxide adsorbed dissociatively with subsequent hydrogenation of the adsorbed carbon and oxygen by both adsorbed and gaseous hydrogen. A rate expression was derived using the equilibrium Langmuir kinetic approach used in the present study. The model could be fit to the observed kinetics only if it was assumed that the surface was covered with adsorbed carbon monoxide. Clearly, there are some inconsistencies in Bell's study which need clarification.

It is interesting to note that a recent study by Sachtler, et al. [137], has suggested that the methanation mechanisms are quite different on nickel and ruthenium. Ponec, who was responsible for the dissociative mechanism on nickel, was involved in this study. These authors have suggested that although the ruthenium surface appears to be covered

with a carbonaceous deposit under reaction conditions and even though a layer of carbon atoms can be readily hydrogenated to methane there is suffecient evidence to suggest that adsorbed oxygen containing intermediates are very likely involved in the reaction on ruthenium.

In conclusion, the methanation reaction on ruthenium thin films has been found to follow Langmuir-Hinshelwood type kinetics. The rate-limiting step involves the interaction of an adsorbed methyl group with adsorbed hydrogen. The surface concentration of all oxygen containing intermediates was found to be negligible. The reaction involves a reversible poison with the structure RuH_2CH_2. The surface is predominantly covered with $RuCH_2$, $RuCH_3$ and RuH_2CH_2. If all other species are neglected, a reasonable fit to the data can be obtained. Inclusion of the other intermediates in the rate expression improves the fit to the data. The terms in the denominator of the rate expression which involve hydrogen to the inverse power are assigned coefficients of zero because they affect the theory only in the region where the hydrogen pressure was very low, less than any pressure used in this study. The surface of the catalyst is at all times covered with a carbonaceous overlayer. This carbon can be classified according to its reactivity. Type 1 carbon is reactive under the conditions in which methane is produced. Type 2 carbon is much less reactive. The most active sites are believed to be relatively uncoordinated edge sites. These sites, however, are believed to become covered with the reversible poison leaving the less coordinated sites for methanation.

SUGGESTIONS FOR FUTURE RESEARCH

The mechanism proposed in this work has suggested that the surface is covered by series of carbonaceous intermediates under reaction conditions. The two most concentrated intermediates which contain carbon are $RuCH_3$ and RuH_2CH_2. Two experiments could be performed to attempt to observe these intermediates under reaction conditions. Nuclear magnetic resonance and electron loss spectroscopy could be used to distinguish between these intermediates and to look for others which might be present in relatively high concentrations.

It would also be informative to extend this study to high pressure using a Berty reactor and a supported ruthenium catalyst. Several such studies have been made but none has covered a wide enough pressure range to demonstrate Langmuir-Hinshelwood kinetics. Also, it would be useful to vary the $CO:H_2$ ratio such that higher hydrocarbons are produced. The effect of this process upon the mechanism of the methanation reaction could be established, as well as the mechanism for the higher hydrocarbon production.

APPENDIX I

Year	Event	Researcher
1902	First report of the catalytic conversion of carbon monoxide and hydrogen; normal pressure process at 523K using nickel to produce methane.	Sabatier and Senderens [8,9]
1913	Patent granted for high pressure synthesis (100 atm) of hydrocarbons and oxygenated chemicals using a variety of catalysts.	Badische Anilin-und-Soda-Fabrik A. G. [10]
1922	Production of a mixture of oxygenated compounds at 100 atm. and 673K using alkalized iron-filings (Synthol process).	Fischer and Tropsch [138]
1923	Patents granted for controlled production of methanol exclusively on ZnO-Cr_2O_3 at 200-300 atm. and 573-673K.	Badische Anilin-und-Soda-Fabrik A. G., Hanisch [11, 12, 139]
1925	Normal pressure synthesis of gasoline at 473-573K over Fe-ZnO and Co-Cr_2O_3 catalysts.	Fischer and Tropsch [13]
1931	Ni-ThO_2-kieselguhr catalysts were developed that allowed the normal pressure synthesis at 448K instead of 523K.	Fischer and Meyer [140]
1932	Co-ThO_2-kieselguhr catalysts were developed that yielded much lower methane formation.	Fischer and Koch [141]
1935	Fischer-Tropsch yield increased by 10-20% by doing the synthesis in steps with intermediate removal of products. The overall yield of methane was less with this process.	Fischer and Pichler [17]
1936	Startup of first normal pressure full scale synthesis plant using Co catalyst (Oberhausen-Holten, Ger.)	

Year	Event	Researcher
1936	Development of Co catalysts for a medium pressure (5-20 atm) moderate temperature (453-473K) process with more saturated products. The catalyst did not require regeneration.	Fischer and Pichler [142]
1937	Medium pressure synthesis with Fe catalysts, 5-30 atm and 473-593K.	Fischer and Pichler [143, 144]
1938	Use of ruthenium catalysts at high pressure (50-1000 atm) and 373-473K to produce compounds with very high molecular weight.	Pichler [18]
1938	Oxo synthesis involving the conversion of olefins in the presence of CO and H_2 to aldehydes.	Roelen [145]
1938	Start-up of first commercial Co medium pressure plant at Oberhausen-Holten, Germany.	Ruhrchemie
1941	High pressure (150-600 atm) synthesis of branched hydrocarbons (isosynthesis) using ThO_2 and other oxide catalysts at 673-773K.	Pichler and Ziesecke [146]
1943	Schwarzheide pilot plant studies of precipitated and fused Fe catalysts on the medium pressure synthesis.	KWI, Ruhrchemie, Rheinpreussen, Lurgi, Brabag, I. G.
1949	Carbon monoxide and water used as synthesis gas	Kolbel and Engelhardt [147, 148]
1950	Commercial scale medium pressure synthesis plant erected for conversion of CO and H_2 from natural gas with Fe at Brownsville, Texas.	Hydrocarbon Research, Inc. and American Oil Companies.
1955	Start-up of Sasol-large scale synthesis plant in Sosolburg, South Africa for medium pressure synthesis using Fe.	South Africa Coal, Oil and Gas Corp., L. T. D.
1962	Synthesis of polymethylene from CO and H_2 with activated ruthenium catalysts at high pressure below 423K.	Pichler and Firnhaber [149]

Year	Event	Researcher
1973	Copper catalysts developed that are more active than ZnO/Cr_2O_3 for methane production.	[150, 151]
1974	Use of a homogeneous rhodium catalyst at 523K and extremely high pressures (1400-3500 atm) to selectively produce ethylene glycol.	Pruett and Walker [20]

APPENDIX II

Consider the following very simple surface reaction in which two diatomic molecules adsorb and then interact to form products. One molecule, A_2, adsorbs molecularly while the other, B_2, adsorbs dissociatively. The sequence is as follows:

$$A_2 + Ru \rightleftarrows RuA_2$$

$$B_2 + 2Ru \rightleftarrows 2RuB$$

$$RuA_2 + RuB \rightarrow \text{Products}$$

Using the Langmuir surface equilibrium approach gives the following expressions for the fractional coverages of the intermediates

$$[RuA_2] = K_A[A_2][Ru]$$

$$[RuB] = (K_B[B_2])^{1/2}[Ru]$$

$$[Ru] = 1/\{1 + K_A[A_2] + (K_B[B_2])^{1/2}\}$$

The last step is the rate limiting step so that the rate may be expressed as follows:

$$\text{Rate} = k[RuA_2][RuB]$$

Using the above expressions for the intermediates leads to the following rate expression:

$$\text{Rate} = \frac{kK_A(K_B[B_2])^{1/2}[A_2]}{\{1 + K_A[A_2] + (K_B[B_2])\}^2}$$

Note that the maximum order of the diatomic that dissociated is +0.5. This is a general result and will be the same as long as the product contains only one atom of B. This is the case in the formation of CH_4 from CO.

Several times throughout this thesis reference was made to the fact that this reaction follows Langmuir-Hinshelwood kinetics. This means that the rate limiting step of the mechanism involves the interaction of two adsorbed intermediates. Both reactants are competing for the same surface sites. Rideal-Eley kinetics result from a sequence in which the rate limiting step involves the interaction of an adsorbed intermediate with a gas phase molecule.

LITERATURE CITED

1. Storch, H. H. Adv. Catal. 1948, 1, 115.
2. Pichler, H. Adv. Catal. 1952, 4, 271.
3. Pichler, H.; Hector, A. in "Kirk-Othmer Encyclopedia of Chemical Technology", John Wiley & Sons: New York, 1964; Vol. 4, p. 446.
4. Mills, G. A.; Steffgen, F. W. Catal. Rev. 1973, 8, 159.
5. Vannice, M. A. Catal. Rev. 1976, 14, 153.
6. Vlasenko, V. M.; Yuzefovich, G. E. Russ. Chem. Rev. 1969, 38, 728.
7. Vannice, M. A. Adv. Chem. Ser. 1977, 163, 15.
8. Sabatier, P.; Senderens, J. B. Compt. Rend. 1902, 134, 514.
9. Sabatier, P.; Senderens, J. B. Compt. Rend. 1902, 134, 689.
10. Badische Anilin-und-Soda-Fabrik A. G. Ger. Patent 293,787, 1913.
11. Badische Anilin-und-Soda-Fabrik A. G. French Patent 571,356, 1923.
12. Badische Anilin-und-Soda-Fabrik A. G. French Patent 580,905, 1923.
13. Fischer, F.; Tropsch, H. Chem. Ber. 1926, 59, 830.
14. Fischer, F.; Tropsch, H. Chem. Ber. 1926, 59, 832.
15. Fischer, F.; Tropsch, H. Chem. Ber. 1926, 59, 923.
16. Fischer, F. Brennst.-Chem. 1935, 16, 6.
17. Fischer, F.; Pichler, H. Brennst.-Chem. 1936, 17, 24.
18. Pichler, H. Brennst.-Chem. 1938, 19, 226.
19. Pichler, H. U. S. Bur. Mines Spec. Rep. 1947.
20. Pruett, R. E.; Walker, W. E. U. S. Patent 3,833,634, 1974.
21. Fischer, F.; Tropsch, H. Brennst.-Chem. 1926, 7, 97.
22. Craxford, S. R.; Rideal, E. K. J. Chem. Soc. 1939, 1604.

23. Craxford, S. R.; Rideal, E. K. Trans. Faraday Soc. 1946, 42, 576.

24. Kini, K. A.; Lahiri, A. J. Sci. Ind. Res. 1975, 34, 97.

25. Elvins, O. C.; Nash, A. W. Nature 1926, 118, 154.

26. Storch, H. H.; Golumbic, N.; Anderson, R. B. "The Fischer-Tropsch and Related Syntheses", John Wiley & Sons: New York, 1951; Chapter 6.

27. Pichler, H.; Schulz, H. Chem. Ing. Tech. 1970, 42, 1162.

28. Emmett, P. H. "Catalysis Then and Now", Franklin: Engelwood Cliffs, New Jersey, 1965; Chapter 10.

29. Sanstri, M. V. C.; Balaji Gupta, R.; Viswanathan, B. J. Indian Chem. Soc. 1974, 51, 140.

30. Kölbel, H.; Hanus, D. Chem. Ing. Tech. 1974, 46, 1042.

31. Blyholder, G.; Goodsel, A. J. J. Catal. 1971, 23, 374.

32. Rossini, F. D.; Pitzer, K. S.; Arnett, R. L.; Braun, R. M.; Pimentel, G. C. "Selected Values of Physical and Thermodynamic Properties of Hydrocarbons and Related Compounds", Carnegie Press: Pittsburgh, 1953.

33. Vannice, M. A. J. Catal. 1975, 37, 449.

34. Vannice, M. A. J. Catal. 1975, 40, 129.

35. Vannice, M. A. J. Catal. 1976, 44, 152.

36. Vannice, M. A. J. Catal. 1977, 50, 228.

37. Sinfelt, J. H. Catal. Rev. 1974, 9, 147.

38. Vannice, M. A. J. Catal. 1975, 37, 462.

39. Kozub, G. M.; Rusov, M. T.; Vlasenko, V. M. Kinet. Katal. 1965, 6, 244.

40. Schoubye, P. J. Catal. 1969, 14, 238.

41. Bousquet, J. L.; Gravelle, P.; Teichner, S. J. Bull. Soc. Chim. Fr. 1969, 2673.

42. Van Herwijnen, T.; Van Doesburg, H.; De Jong, W. A. J. Catal. 1973, 28, 391.

43. Fontaine, R. Ph. D. Dissertation, Cornell University, Ithaca, New York, 1973.

44. McGill, R. N.; Richardson, J. T. "Proceedings of the 41st Annual Chemical Engineering Symposium, I.&E.C. Division, American Chemical Society", Pittsburgh, 1975.

45. Bond, G. C.; Turnham, B. K. J. Catal. 1976, 45, 128.

46. Araki, M.; Ponec, V. J. Catal. 1976, 44, 439.

47. Ekerdt, J. G.; Bell, A. T. J. Catal., in press.

48. Karn, F. S.; Schultz, J. F.; Anderson, R. B. Ind. Eng. Chem. Prod. Res. Dev. 1965, 4, 265.

49. McKee, D. W. J. Catal. 1967, 8, 240.

50. Dalla Betta, R. A.; Piken, A. G.; Shelef, M. J. Catal. 1974, 35, 54.

51. Randhava, S. S.; Rehmat, A.; Camara, E. H. Ind. Eng. Chem. Prod. Res. Dev. 1969, 8, 482.

52. Everson, R. C.; Woodburn, E. T.; Kirk, A. R. M. J. Catal. 1978, 53, 186.

53. King, D. L. J. Catal. 1978, 51, 386.

54. Lunde, P. J. Ind. Eng. Chem. Proc. Des. Develop. 1974, 13, 226.

55. Lunde, P. J.; Kester, F. L. Ind. Eng. Chem. Proc. Des. Dev. 1974, 13, 27.

56. Rehmat, A.; Randhava, S. S. Ind. Eng. Chem. Proc. Des. Dev. 1970, 9, 512.

57. Hansen, R. S.; Mimeault, V. J. in "Experimental Methods in Catalytic Research", Anderson, R. B., Ed.; Academic Press, Inc.: New York, 1968; Chapter 5.

58. Dushman, S. "Scientific Foundations in Vacuum Technique", 2nd ed.; Lafferty, J. M., Ed.; John Wiley & Sons: New York, 1962.

59. Anderson, J. R. "Chemisorption and Reactions on Metallic Films", Academic Press: New York, 1971; Vol. I and II.

60. Holland, L. "Vacuum Deposition of Thin Films", Chapman and Hall, Ltd.: London, 1966.

61. Masterson, P. B. Ph.D. Dissertation, Iowa State University, Ames, Iowa, 1971.

62. May, J. W. Adv. Catal. 1972, 21, 151.

63. Bhasin, M. M. in "Catalysis in Organic Syntheses 1976", Rylander, P.; Greenfield, H., Eds.; Academic Press, Inc.: New York, 1976; Chapter 2.

64. Eastman, D. E.; Nathan, M. I. Phys. Today 1975, 28, 44.

65. Bradshaw, A. M.; Cederbaum, L. S.; Domcke, W. Struct. Bonding 1975, 24, 133.

66. Phillips, L. V.; Salvati, L.; Carter, W. J.; Hercules, D. M. in "Quantitative Surface Analysis of Materials", American Society For Testing and Materials: New York, 1978; Chapter 2.

67. Riggs, W. M.; Beimer, R. G. Chem. Technol. 1975, 5, 652.

68. Ogilvie, J. L.; Wolberg, A.; Roth J. F. Chem. Technol. 1973, 3, 567.

69. Dalla Betta, R. A. J. Catal. 1974, 34, 57.

70. Taylor, K. J. Catal. 1975, 38, 299.

71. Ghoneim, F. B.; Balandin, A. A.; Slovakhotova, T. A. Z. Phys. Chem. Leipzig 1972, 250, 243.

72. Kubicka, H. J. Catal. 1968, 12, 223.

73. Sinfelt, J. H.; Yates, D. J. C. J. Catal. 1967, 8, 82.

74. Guerra, C. R.; Schulman, J. H. Surf. Sci. 1967, 7, 229.

75. Kobayashi, M.; Shirasaki, T. J. Catal. 1973, 28, 289.

76. Buyanova, N. E.; Karnaukhov, A. P.; Doroleva, N. G.; Ratner, I. D.; Chernyavskaya, O. N. Kinet. Katal. 1973, 14, 1364.

77. Somorjai, G. A.; Blakely, D. W. Nature 1975, 258, 580.

78. Dwyer, D. J.; Somorjai, G. A. J. Catal. 1978, 52, 291.

79. Weast, R. C., Ed. "Handbook of Chemistry and Physics", 50th ed.; The Chemical Rubber Co.: Cleveland, Ohio, 1969.

80. Davis, L. E.; McDonald, N. C.; Palmberg, P. W.; Keach, G. E.; Weber, R. E. "Handbook of Auger Electron Spectroscopy", 2nd ed.; Physical Electronics Industries: Eden Prairie, Minnesota, 1976.

81. Fuggle, J. C.; Madey, T. E.; Steinkelberg, M.; Menzel, D. Surf. Sci. 1975, 52, 521.

82. Danielson, L. R.; Dresser, M. J.; Donaldson, E. E.; Dickinson, J. T. Surf. Sci. 1978, 71, 599.

83. Kraemer, K.; Menzel, D. Ber. Bunsenges. Phys. Chem. 1974, 78, 591.

84. Thomas, G. E.; Weinberg, W. H. J. Chem. Phys. 1979, 70, 954.

85. Madey, T. E.; Menzel, D. Japan J. Appl. Phys. Suppl. 2, Pt. 2 1974, 229.

86. Goodman, D. W.; Madey, T. E.; Ono, M.; Yates, J. T. J. Catal. 1977, 50, 279.

87. Grant, J. T.; Haas, T. W. Surf. Sci. 1970, 21, 76.

88. Reed, P. D.; Comrie, C. M.; Lanbert, R. M. Surf. Sci. 1977, 64, 603.

89. Madey, T. E.; Engelhardt, H. A.; Menzel, D. Surf. Sci. 1975, 48, 304.

90. Orent, T. W. Honeywell, Inc., Minneapolis, Minnesota, private communication.

91. Orent, T. W.; Hansen, R. S. Surf. Sci. 1977, 67, 325.

92. Tomcsik, T. L. Ph.D. Dissertation, Iowa State University, Ames, Iowa, 1978.

93. Kim, K. S.; Winograd, N. J. Catal. 1974, 35, 66.

94. Kempter, C. P.; Nadler, M. R. J. Chem. Phys. 1960, 33, 1580.

95. Carlson, T. A. "Photoelectron and Auger Spectroscopy", Plenum: New York, 1975.

96. Clausen, C. A.; Good, M. L. Charact. Met. Polymer Surf. (Symp) 1977, 1, 65.

97. Fisher, G. B.; Madey, T. E.; Waclawski, B. J.; Yates, T. E. "Proceedings of the 7th International Vacuum Congress and the 3rd International Conference on Solid Surfaces", Vienna, Austria, 1977.

98. Fisher, G. B.; Madey, T. E.; Yates, J. T. J. Vac. Sci. Technol. 1978, 15, 543.

99. Menzel, D. J. Vac. Sci. Technol. 1975, 12, 313.

100. Dalla Betta, R. A.; Piken, A. G.; Shelef, M. J. Catal. 1975, 40, 173.

101. Yates, J. T.; Madey, T. E.; Dresser, M. J. J. Catal. 1973, 30, 260.

102. Madey, T. E.; Yates, J. T.; Stern, R. C. J. Chem. Phys. 1965, 42, 1372.

103. Ku, R.; Gjostein, N. A.; Bonzel, H. P. Surf. Sci. 1977, 64, 465.

104. Kemball, C. Faraday Discuss. Chem. Soc. 1966, 41, 190.

105. Mahaffy, P.; Hansen, R. S. J. Chem. Phys. in press.

106. Kraemer, K.; Menzel, D. Ber. Bunsenges. Phys. Chem. 1974, 78, 728.

107. Baetzold, R. C.; Somorjai, G. A. J. Catal. 1976, 45, 94.

108. Gostunskays, I. V.; Trinko, A. I.; Dobroserdova, N. B. Dann SSR 1970, 193, 573.

109. Klein, R. Surf. Sci. 1970, 20, 1.

110. Fuggle, J. C.; Umbach, E.; Feulner, P.; Menzel, D. Surf. Sci. 1977, 64, 69.

111. Bonzel, H. P.; Fischer, T. E. Surf. Sci. 1975, 51, 213.

112. Dalla Betta, R. A. J. Phys. Chem. 1975, 79, 2519.

113. Brown, M. F.; Gonzalez, R. D. J. Phys. Chem. 1976, 80, 1731.

114. Brown, M. F.; Gonzalez, R. D. J. Catal. 1976, 44, 477.

115. Dalla Betta, R. A.; Shelef, M. J. Catal. 1977, 48, 111.

116. Davydov, A. A.; Bell, A. T. J. Catal. 1977, 49, 332.

117. Sapienza, R. S.; Spaulding, L. D.; Lynch, J. R.; Sansone, M. J. "Preprints of papers presented at the Symposium on New Tools in Catalysis" American Chemical Society: Washington, D.C. Meeting in Miami Beach, September, 1978, p. 1255.

118. Sapienza, R. S.; Spaulding, L. D.; Lynch, J. R.; Sansone, M. J. "Preprints of papers presented at the Symposium on New Tools in Catalysis" American Chemical Society: Washington, D. C. Meeting in Miami Beach, September, 1978, p. 1336.

119. Singh, K. J.; Grenga, H. E. J. Catal. 1977, 47, 328.

120. Rabo, J. A.; Risch, A. P.; Poutsma, M. L. J. Catal. 1978, 53, 295.

121. Anders, L. W.; Hansen, R. S. J. Chem. Phys. 1975, 62, 4652.

122. Arnoult, W. J.; McLellan, R. B. Scr. Metall. 1972, 6, 1013.

123. Hansen, M.; Anderko, K. "Constitution of Binary Alloys", 2nd ed.; McGraw Hill: New York, 1958.

124. Kempter, C. P. J. Chem. Phys. 1964, 41, 1515.

125. Kosolapova, T. "Carbides-Properties, Production and Applications" Plenum Press: New York, 1971.

126. Madey, T. E.; Yates, J. T. Chem. Phys. Lett. 1977, 51, 77.

127. Sarkany, A.; Matusek, K.; Tetenyi, P. J. Chem. Soc., Faraday Trans. 1 1977, 73, 1699.

128. Kraemer, K.; Menzel, D. Ber. Bunsenges. Phys. Chem. 1975, 79, 649.

129. Pichler, V. H.; Meir zu Kocker, H.; Gabler, W.; Gartner, R.; Kioussis, D. Brennst.-Chem. 1967, 48, 266.

130. Kaesz, H. D.; Saillant, R. B. Chem. Rev. 1972, 72, 231.

131. Trost, W. R. Can. J. Chem. 1959, 37, 469.

132. Bond, G. C. Discuss. Faraday Soc. 1966, 41, 200.

133. Weinberg, W. H.; Merrill, R. P. J. Catal. 1975, 40, 268.

134. van Dijk, W. L.; Groenewegen, J. A.; Ponec. V. J. Catal. 1976, 45, 277.

135. Ponec, V. Catal. Rev. 1978, 18, 151.

136. Wentrcek, P. R.; Wood, B. J.; Wise, H. J. Catal. 1976, 43, 363.

137. Sachtler, J. W. A.; Kool, J. M.; Ponec, V. J. Catal. 1979, 56, 284.

138. Fischer, F.; Tropsch, H. Chem. Ber. 1923, 56, 2423.

139. Hanisch, H. In "Die Methanol-und Isobutylolsynthese", Winnacker-Kuchlier, Ed.; Carl Hansel Verlag: Munchen, 1959, p. 386.

140. Fischer, F.; Meyer, K. Brennst.-Chem. 1931, 12, 225.

141. Fischer, F.; Koch, H. Brennst.-Chem. 1932, 13, 61.

142. Fischer, F.; Pichler, H. German Patent 731,295, 1936.

143. Fischer, F.; Pichler, H. German Patent 888,240, 1937.

144. Fischer, F.; Pichler, H. German Patent 888,841, 1937.

145. Roelen, O. German Patent 849,548, 1938.

146. Pichler, H.; Ziesecke, K. H. Brennst.-Chem. 1949, 30, 13.

147. Kolbel, H.; Engelhardt, F. German Patent 930,685, 1955.

148. Kolbel, H.; Engelhardt, F. Brennst.-Chem. 1951, 32, 150.

149. Pichler, H.; Firnhaber, B. Brennst.-Chem. 1963,44, 33.

150. Oil Gas J. March 12, 1973, p. 85.

151. Supp, E. Chem. Technol. 1973, 3, 430.

ACKNOWLEDGEMENTS

I would like to express my sincere gratitude to Dr. Robert S. Hansen for his support and guidance throughout this project. His encouragement during many informative discussions was invaluable. I also thank Dr. Hansen for the independence to develop this project and draw my own conclusions from the results.

I wish to thank Mr. Jim Andregg for his assistance in the ESCA work and Mr. Edward Quick for the use of his ruthenium ($10\bar{1}2$) crystal in the LEED work.

Particular thanks are due Mother, Mammie and Ba for their encouragement during my high school and undergraduate college years.

The gratitude that I owe my wonderful wife, Gayle, is immeasurable. It was Gayle's encouragment which was solely responsible for my decision to pursue this degree. The high goals that she has set for her life have challenged me to accomplish more in my own life. Without having Gayle to rely upon when things were not going right, I would never have completed this work. In addition to her own love and devotion, Gayle has given me the most wonderful gift ever-our son, Christopher. The love and happiness that they have provided have been my source of strength and joy.